ROLE OF CALCIUM-INDEPENDENT PHOSPHOLIPASE A$_2$ IN INSULIN-

STIMULATED GLUCOSE UPTAKE IN 3T3-L1 ADIPOCYTES

Except where reference is made to the work of others, the work described in this thesis is
my own or was done in collaboration with my advisory committee. This thesis does not
include proprietary or classified information.

_____
Juan Yang

Certificate of Approval:

_____   _____
Margaret C. Craig-Schmidt   Kevin W. Huggins, Chair
Professor   Assistant Professor
Nutrition & Food Science   Nutrition & Food Science

_____   _____
Suresh Mathews   Robert L. Judd
Assistant Professor   Associate Professor
Nutrition & Food Science   Anatomy, Physiology, Pharmacology

_____
George T. Flowers
Dean
Graduate School

ROLE OF CALCIUM-INDEPENDENT PHOSPHOLIPASE A$_2$ IN INSULIN-

STIMULATED GLUCOSE UPTAKE IN 3T3-L1 ADIPOCYTES

Juan Yang

A Dissertation

Submitted to

the Graduate Faculty of

Auburn University

in Partial Fulfillment of the

Requirements for the

Degree of

Doctor of Philosophy

Auburn, Alabama

December 18, 2009

ROLE OF CALCIUM-INDEPENDENT PHOSPHOLIPASE A_2 IN INSULIN-

STIMULATED GLUCOSE UPTAKE IN 3T3-L1 ADIPOCYTES

Juan Yang

_____
Signature of Author

_____
Date of Graduation

VITA

Juan Yang, daughter of Daizhang Yang and Shuyun Liu, was born in a small town named Shimen in southern China. After she graduated from a local high school in her hometown, she continued her study in the Life Science School of Wuhan University.

During her seven years in Wuhan University, she got her Bachelor of Science degree in Biology and then an M.S. degree in Microbiology. Before Juan enrolled as a graduate student in Auburn University in 2005, she had worked in the National Center For Gene Research in Shanghai, China for three years. At Auburn, she pursued a Ph.D. in Nutrition and a M.S. degree in Statistics.

DISSERTATION ABSTRACT

ROLE OF CALCIUM-INDEPENDENT PHOSPHOLIPASE A$_2$ IN INSULIN-

STIMULATED GLUCOSE UPTAKE IN 3T3-L1 ADIPOCYTES

Juan Yang

Doctor of Philosophy, December 18, 2009
(M.S., Wuhan University, 2001)
(B.S., Wuhan University, 1999)

156 Typed Pages

Directed by Kevin W. Huggins

Calcium-independent phospholipase A$_2$ (iPLA$_2$) is a member of the phospholipase A$_2$ family that catalyzes the hydrolysis of glycerophospholipid at the sn-2 position to liberate free fatty acid and lysophospholipid. Recent studies have suggested that iPLA$_2$ may be important for adipocyte biology. The purpose of this study was to determine the role of iPLA$_2$ in insulin-stimulated actions on glucose uptake in 3T3-L1 adipocytes.

The 3T3-L1 adipocytes were pretreated with bromoenol lactone (BEL, 10 or 50 μM), a chemical inhibitor of iPLA$_2$, for 30 minutes. After insulin (100 nM) stimulation, glucose uptake was determined by measuring intracellular incorporation of [^{3}H]-2-deoxyglucose. With 10 and 50 μM BEL treatment, insulin-stimulated glucose uptake was decreased by 30% and 45%, respectively, compared to DMSO vehicle-treated cells. Further investigations confirmed that iPLA$_2$ activity was responsive to the BEL

inhibitory effects, and that iPLA$_2\beta$ and iPLA$_2\gamma$ were both involved in this process. Additionally, exogenous arachidonic acid (AA, 100 μM) restored the reduction of insulin-stimulated glucose uptake induced by BEL treatment. Small interfering RNA (siRNA) technique was utilized to selectively inhibit iPLA$_2\beta$ and iPLA$_2\gamma$ gene expression in 3T3-L1 adipocytes. Consistent with the BEL treatment results, the 3T3-L1 adipocytes transfected with iPLA$_2\beta$ or iPLA$_2\gamma$ siRNA (50 nM) exhibited impaired glucose uptake upon insulin administration, showing approximate 40% inhibition compared to scrambled siRNA treated cells. To elucidate the underlying mechanism for the effects of iPLA$_2$ inhibition on insulin-stimulated glucose uptake, insulin-stimulated phosphorylation of insulin receptor (IR) and Akt was assessed by Western blot analysis. There was no significant difference between BEL-treated and vehicle-treated cells in the phosphorylation levels of IR and Akt. Fraction analysis of insulin-responsive GLUT4 translocation was also performed in adipocytes. Compared to vehicle control, BEL treatment noticeably inhibited the incorporation of GLUT4 into plasma membrane and lipid raft fractions in response to insulin.

These results demonstrate that insulin-stimulated glucose uptake was decreased by iPLA$_2$ inhibition, and that this effect was mediated via attenuation of the insulin-dependent GLUT4 translocation into plasma membrane. However, the early steps of insulin signaling were not affected by iPLA$_2$ inhibition. It is conclude that insulin-stimulated glucose uptake is mediated, at least in part, by iPLA$_2$, and that iPLA$_2$ may represent a novel therapeutic target for the treatment of insulin resistance related diseases, such as obesity, type 2 diabetes, and other metabolic diseases.

ACKNOWLEDGMENTS

Foremost, I would like to express my sincere gratitude to my advisor Dr. Kevin, Huggins. Without his guidance and encouragement, this work would not have been accomplished. He has been abundantly helpful in all the time of research and writing of this dissertation.

I am also indebted to Dr. Craig-Schmidt for her constant help and support for my research, study and life in Auburn. I equally wish to extend my appreciation and thanks to Dr. Mathews and Dr. Judd, the rest of my committee members, for their valuable help, support, interest and stimulating hints for my research.

I would like to thank the faculties in the Department of Nutrition and Food Science who have helped and inspired me during my doctoral study: Dr. White, Dr. Fellers, Dr. Kim, Dr. Keith, Dr. Huang, Dr. Gropper, Dr. Bell, and Dr. Zizza.

Many thanks go to the graduate students studying and working with me in Auburn. In particular, I am grateful to Yuan Kang and my former colleagues Kathryn Colbert and Carmen Teodorescu, for their friendship and help in my research, study and life.

I can not end the acknowledgements without my deepest appreciation to my family, my father Daizhang Yang, mother Shuyun Liu, and fiancée Xuan Li, on whose constant encouragement and love I have relied throughout my time at Auburn.

Style manual or journal used: The Journal of Nutrition

Computer software used: Microsoft Word, Microsoft PowerPoint, Microsoft Excel, Minitab, Adobe Acrobat Professional, LabWorks Image Acquisition Software v.4.6.

TABLE OF CONTENTS

LIST OF TABLES

LIST OF FIGURES

CHAPTER 1. INTRODUCTION

Over the past few decades, obesity has represented one of the most serious public health problems on a global scale. According to recent reports, there are at least 400 million obese adults around the world, and the incidence of obesity keeps rising at an alarming rate (1-3). In correlation with the rise in obesity, the prevalence of type 2 diabetes, cardiovascular diseases and other pathological consequences is also increasing (4, 5). Numerous studies have demonstrated that obesity, and obesity-related metabolic diseases are characterized with abnormal energy storage and utilization, which is closely linked to adipose tissue dysfunction (6-8). As a central place for calorie storage, as well as an important secretory organ, adipose tissue plays critical roles in modulating whole body lipid and glucose homeostasis. A better comprehension of the physiological functions of adipocytes is essential for dissecting the pathophysiological origin and exploring possible therapies for obesity and associated diseases.

Phospholipase A_2 (PLA_2) is a diverse group of acyl-hydrolases that catalyze the cleavage of the sn-2 fatty acyl bond of glycerophospholipids, resulting in the liberation of free fatty acid and lysophospholipid. These two products are both precursors for signaling molecules, which are particularly important for various physiological processes. Based on the activity dependence on calcium ion and sequence homology, the mammalian PLA_2

superfamily are categorized into five principal types, namely the secreted PLA$_2$ (sPLA$_2$), the cytosolic Ca^{2+}-dependent PLA$_2$ (cPLA$_2$), the platelet-activating factor acetylhydrolase (PAF-AH), lysosomal PLA$_2$ (LPLA$_2$), and the cytosolic Ca^{2+}-independent PLA$_2$ (iPLA$_2$) (9). Most recently, a calcium-dependent intracellular PLA$_2$ was identified in white adipose tissue, and denoted as adipose PLA$_2$ (AdPLA) (10).

In the PLA$_2$ superfamily, iPLA$_2$ enzymes are among the most recently described and least well-characterized lipases. It is generally accepted that the iPLA$_2$ enzymes have multiple biological functions in homeostatic glycerophospholipids membrane remodeling, cell growth and proliferation, eicosanoid metabolism, apoptosis, gene expression, chemotaxis, signaling transduction and calcium entry (11-14). Importantly, there is an increasing body of evidence indicating the important roles of iPLA$_2$ in whole body metabolism, including adipocytes differentiation (15), insulin secretion (16-21), glucose homeostasis (22, 23), hepatic adipogenesis (24, 25), and mitochondrial functioning (26, 27). Based on these data, various investigations have postulated the connections between iPLA$_2$ and obesity, type 2 diabetes, fatty liver disease and other manifestations of the metabolic syndrome (25).

It is noteworthy that as 3T3-L1 fibroblasts differentiate into adipocytes, dramatically increased gene expression occurs in two members of iPLA$_2$ family: iPLA$_2\xi$ (iPLA$_2$-GVIE) and iPLA$_2\varepsilon$ (iPLA$_2$-GVID) (28). Similar results have also been found in other iPLA$_2$ members: iPLA$_2\beta$ (iPLA$_2$-GVIA) and iPLA$_2\gamma$ (iPLA$_2$-GVIB) (15). More interesting, Su and coworkers have demonstrated that the gene knockdown of iPLA$_2\beta$ and iPLA$_2\gamma$ inhibits hormone-induced adipocyte differentiation by preventing peroxisome

proliferator-activated receptor γ (PPARγ) and the CCAAT/enhancer-binding protein α (C/EBPα) expression (15). In addition, the protein levels of iPLA$_2$β and iPLA$_2$γ were found both significantly increased in white adipose tissue of genetically obese *fa/fa* rats, compared to the lean controls (15). All of these results have underlined the importance of iPLA$_2$ in adipocyte metabolism. However, the roles of iPLA$_2$ in adipocyte biology, particularly the response to insulin, are currently unknown.

The objective of this study was to investigate the possible cellular functions of iPLA$_2$ in insulin-stimulated adipocytes. In this study, we demonstrate a role for iPLA$_2$ in glucose transport in the presence of insulin. To elucidate the iPLA$_2$ function in insulin-stimulated glucose uptake, we utilized a specific inhibitor of iPLA$_2$, Bromoenol lactone (BEL) and small interfering RNA (siRNA) technique to selectively inhibit iPLA$_2$ in 3T3-L1 adipocytes. We further examined the effects of BEL-induced iPLA$_2$ inhibition in GLUT4 translocation and insulin signaling. Our studies are the first to demonstrate the significance of iPLA$_2$ in insulin action of fully differentiated adipocytes.

CHAPTER 2. REVIEW OF LITERATURE

2.1. PHOSPHOLIPASE A$_2$

The superfamily of phospholipase A$_2$ (PLA$_2$) is composed of a group of enzymes catalyzing the cleavage at the sn-2 position of glycerophospholipids. This hydrolysis reaction results in the release of free fatty acids and lysophospholipids (lyso PL), and both products serve as important precursors for bioactive molecules that can exert a multitude of biological functions (9). As a typical PLA$_2$-derived free fatty acid, arachidonic acid (AA) is particularly important, because it can be converted by varied downstream metabolic enzymes, such as prostaglandin synthases, cytochrome P450 proteins, and lipoxygenases, into numerous biologically active lipophilic compounds called eicosanoids, including prostaglandins (PGs), leukotrienes (LTs) and lipoxins (29). Through binding to specific G-protein receptors, these eicosanoids play critical roles in a wide range of physiological and pathological processes such as sleep regulation, immune responses, inflammation, and pain perception (30, 31). Lysophospholipids lysophosphatidic acid (LPA) and lysophosphatidylcholine (LPC), or their metabolites such as platelet activating factor (PAF), are lipid mediators that are essential for cell proliferation, survival and migration (32, 33). Since all metabolites mentioned above are

greatly modulated by a variety of extracellular stimuli, and highly involved in the stimuli-mediated signaling pathways, the enzymes catalyzing the initial step, PLA_2s, are important for these signaling processes. As well, PLA_2s often play vital roles in cell membrane homeostasis by contributing to the recycling of fatty acids moieties within membrane phospholipids and assisting phospholipid mass regulation (11).

2.1.1. Classification of Phospholipase A_2

There are more than 27 different proteins exerting PLA_2 enzymatic activities that have been identified and cloned in mammalian systems. Initially, these proteins are grouped by a numbering system which is based on the nucleotide and amino acid sequence criteria (13, 34-36). However, the most commonly used classification of PLA_2 is based on the biochemical commonalities. Regarding the disparities of catalytic mechanism, as well as the difference in functional and structural features, the superfamily of PLA_2 are traditionally grouped into five primary types, named the secreted PLA_2s ($sPLA_2$), the cytosolic calcium-dependent PLA_2s ($cPLA_2$), the platelet-activating factor acetylhydrolases (PAF-AH), the lysosomal PLA_2, and cytosolic calcium-independent PLA_2s ($iPLA_2$) (37). Most recently, a new group of PLA_2s has been identified and characterized in white adipose tissue (10). Because of its unique expression in adipose tissue, this 18 kDa protein was termed as Adipose PLA_2 (AdPLA) (10).

2.1.2. Secreted Phospholipase A_2

The secreted PLA_2s ($sPLA_2$s) group is the largest and first discovered PLA_2 type, which have been isolated from a variety of sources such as bacteria, plants, insects,

reptiles and mammals (38). In mammalian system, there are 10 sPLA$_2$ member proteins, which are ubiquitously expressed in all studied tissues with group specificities (13). They are proteins with small molecular weights around 14–18 kDa, and structurally characterized with multiple disulfide bonds, highly conserved Ca^{2+}-binding loop, as well as catalytic histidine sites (9, 13). The sPLA$_2$s require comparably high concentrations of Ca^{2+} (μM levels) for their catalytic activities (9, 38). One of the primary functions of sPLA$_2$s is to release AA from cellular membrane. The generated AA subsequently enters the eicosanoids synthesis cascades (39, 40); therefore, the sPLA$_2$s appear to be involved play a role in several inflammatory diseases, such as rheumatoid arthritis, adult respiratory distress syndrome (ARDS), inflammatory bowel disease, pancreatitis and sepsis (41, 42). Furthermore, sPLA$_2$s were suggested to play a role in the hydrolysis of low-density lipoprotein (LDL) and thus, may contribute to the development of atherosclerosis (9, 42). Other biological functions of sPLA$_2$s, as reviewed by Kudo (13), include digestion, exocytosis, antibacterial action, and anticoagulation.

2.1.3. Cytosolic Calcium-Dependent Phospholipase A$_2$

Cytosolic calcium-dependent PLA$_2$ (cPLA$_2$) are a group of large cytosolic proteins having variable protein masses which range from 61 to 114 kDa. At present, 6 intracellular PLA$_2$s are assigned to this group based on the sequence similarity. Generally, the cPLA$_2$s contain an active serine site and a Ca^{2+} dependent lipid binding C2 domain, and both domains are important for a full activation of these enzymes (37). Among those serine acylhydrolases, cPLA$_2$α (GIVA-PLA$_2$) is the most extensively studied enzyme, and it is widely expressed in mammalian cells (43). The cPLA2α is the key enzyme that

6

mediates the release of arachidonic acid for the production of eicosanoids in response to extracellular stimuli. Thus its activation is important in physiological processes under various conditions in both health and disease (44). Numerous lines of evidence have demonstrated that cPLA2α contributes to the pathogenesis of a variety of inflammation diseases such as allergic reactions, acute lung injury, pulmonary fibrosis, brain injury, arthritis, bone resorption (44). This enzyme is also involved in the regulation of apoptosis, ulceration, tumorgenesis, pregnancy and labor (13).

2.1.4. Platelet-Activating Factor Acetylhydrolase

Platelet-activating factor acetylhydrolases (PAF-AHs) catalyze the acylhydrolysis at the sn-2 position of PAF (13). This group is composed of four serine enzyme assigned to two numbering groups GVII and GVIII (9). Lipoprotein-associated PLA_2 is known to be one of GVII PLA_2s, and it is the only secretory member in this group; the other three are all cytosolic proteins (9). PAF-AHs are showed to have effects in inhibiting the progression of atherogenesis, protecting cells against oxidative stress, and regulating brain development (9).

2.1.5. Other Phospholipase A_2

The last two groups of PLA_2s, lysosomal GXV phosphoslipase A_2 ($LPLA_2$) and adipose GXVI phosphoslipase A_2 (AdPLA) are recently identified, and their biological functions remain unclear. $LPLA_2$ is a protein localized to lysosome with Ca^{2+}-independent PLA_2 and transacylase activities (45, 46). AdPLA contains a histidine lipase motif and possesses a Ca^{2+}-dependent PLA_2 activity (10).

7

2.2. CALCIUM-INDEPENDENT PHOSPHOLIPASE A$_2$

Calcium-independent PLA$_2$s (iPLA$_2$) are high-molecular weight cytosolic proteins utilizing a serine active site. They do not require Ca^{2+} for catalysis. At present, up to 6 proteins from different mammalian sources have been recognized as iPLA$_2$ family members.

2.2.1. Identification and Characterization of Calcium-Independent Phospholipase A$_2$

The first iPLA$_2$ from a mammalian source was identified as a protein with a molecular weight about 85 kDa in P388D1 macrophages (47, 48), then purified, characterized and further cloned from Chinese hamster ovary (CHO) cells (47, 49, 50). It is the most extensively studied enzyme of this group, designated as group VIA PLA$_2$ (iPLA$_2$-VIA) (47, 50, 51). iPLA$_2$-VIA includes at least 5 splice variants with similar structural features with ankyrin repeats (13, 25, 50). Due to exon-skipping and intron-insertion in gene translation process, three of the variants, iPLA$_2$-VIA-1, -2, -3, possess both eight ankyrin repeated domains and the N-terminal catalytic serine, while other two, iPLA$_2$-VIA-Ankyrin-1, and -Ankrin-2 are enzymatically inactive because of the lack of catalytic serine (52, 53). It is reported that each splice variant of iPLA$_2$-VIA exhibits specific tissue distribution, and that this enzyme is ubiquitously expressed in a wide range of cells and tissues (52, 53).

In 2000, another mammalian protein possessing iPLA$_2$ enzymatic activity was identified, and named as iPLA$_2$-VIB by searching nucleic acid data base (54). Compared

to iPLA$_2$-VIA, this enzyme has several highly conserved sequences in the C-terminal, but little homology at the N-terminal (54). It is also ubiquitously distributed in all tissues examined, and presumably membrane-bound, since it is predominantly presented in the membrane fraction when transfected into cells (54, 55). Besides the serine catalytic site, iPLA$_2$-VIB is rich in serine and threonine residues, providing many potential phosphorylation sites for protein kinases A and C, proline-directed kinases, and mitogen-activated protein kinase (MAPK) (54). These putative phosphorylation sites suggest possible mechanisms for regulatory controls on the activities of iPLA$_2$-VIB enzyme (13). There are 4 methionine residues acting as potential translation initiation sites in iPLA$_2$-VIB, which produce distinct sizes of its protein (56); the expression of the individual splice variant of iPLA$_2$-VIB is unique in different cell types, as well as different cellular compartments (56, 57).

Recently, there are four novel iPLA$_2$ family members identified and termed as iPLA$_2$-VIC, -VID, -VIE, and-VIF, respectively with the terminology of group numbering system (9). The iPLA$_2$-VIC is an integral membrane protein expressed in neurons of human and mice, sharing some sequence similarity to iPLA$_2$-VIA. It was previously reported to act as a neuropathy target esterase (NTE) (58, 59). In addition to the esterase role in brain development, iPLA$_2$-VIC can first hydrolyze the sn-2 fatty acid from phosphatidylcholine (PC), and then release the fatty acid at the sn-1 site, which might be important for membranes homeostasis in neurons (60). Other three novel iPLA$_2$s had been found in adipose tissue with activities other than phospholipase (28). Jenkins and coworkers have shown that these iPLA$_2$s are capable of catalyzing the hydrolysis of both

linoleic acid (LA) and AA at the sn-2 position in the absence of free Ca^{2+} (28). In addition to the phospholipase activity, they also possess enzymatic activities such as triacylglycerol lipase and acylglycerol transacylase (28). It is interesting that, in some papers, $cPLA_2$-IVC ($cPLA_2\gamma$) is also classified as one $iPLA_2$ family member, since its PLA_2 activity is not dependent on free Ca^{2+} (61).

In literature, these enzymes are also referred to as $iPLA_2\beta$, $-\gamma$, $-\delta$, $-\varepsilon$, $-\zeta$, and $-\eta$ ($iPLA_2$-α being used for paratin, a non-mammalian enzyme structurally similar to $cPLA_2$-α) (13). Table 1 provides a brief summary for the classification of $iPLA_2$ family. Due to the simplicity of this name system, these notations will be used in the following parts of this dissertation.

Table 1. Calcium-Independent Group VI phospholipase A$_2$

Group	Molecular Mass (kDa)	Features	Alternative Names
iPLA$_2$-VIA	47-90	Ankyrin repeats	iPLA$_2\beta$
iPLA$_2$-VIB	60-91	Membrane-bound	iPLA$_2\gamma$
iPLA$_2$-VIC	146	Integral membrane protein	iPLA$_2\delta$, neuropathy target esterase (NTE)
iPLA$_2$-VID	53	Acylglycerol Transacylase, triacylglycerol lipase	iPLA$_2\varepsilon$, adiponutrin
iPLA$_2$-VIE	57	Acylglycerol Transacylase, triacylglycerol lipase	iPLA$_2\xi$, transport secretion protein-2.2 (TTS-2.2)
iPLA$_2$-VIF	28	Acylglycerol Transacylase, triacylglycerol lipase	iPLA$_2\eta$, gene sequence 2 (GS2)

The table has been adapted from (9) and modified based on (13, 28).

2.2.2. Regulations of Calcium-Independent Phospholipase A$_2$ Activation

Although the activity of iPLA$_2$ is calcium independent, it is showed that Ca^{2+} is still highly involved in the regulation of iPLA$_2$ activities (11, 14). The iPLA$_2\beta$ is reported to be activated with the depletion of intracellular Ca^{2+} concentration or the suppression of interaction of calmodulin with target binding proteins, resulting in AA release in resting smooth muscle cells (62). Similar results can be also found in research on pancreatic islets (63). Recently, Jenkins and coworkers identified the calmodulin binding site in iPLA$_2\beta$ and verified this physically interaction: the activity of this enzyme can be inhibited or activated via the binding or separation of calmodulin, respectively (64). Several studies have also suggested the involvement of protein kinase C α (PKCα) in the regulation of iPLA$_2\beta$ activity (65-67). There are several possible underlying mechanisms: 1.) The regulatory effects on iPLA$_2$ are realized via the phosphorylation of an associated regulatory protein. 2.) The protein kinases may serve as a co-factor for iPLA$_2$ activation without direct phosphorylation (68). Other lines of evidence have suggested that PKC affects the association of iPLA$_2$ to membrane compartments, resulting in the activation of iPLA$_2$ (65, 69). Other kinases, such as p38 MAPK is showed to be implicated in the thrombin-stimulated cellular regulation on iPLA$_2$ activity (70).

Under certain experimental circumstances, adenosine triphosphate (ATP) is reported to activate iPLA$_2$ using in vitro assays, or to protect the enzyme from losing activity (53, 71). Moreover, reactive oxygen species (ROS), including superoxide anion, hydroxyl radical and hydrogen peroxide have been known to potentiate iPLA$_2$ activity (72-74). When the uterine stromal cells were stimulated by hydrogen peroxide, a

significant increase in iPLA$_2$ was detected via the increased calcium-independent AA release (73). Similarly, in RAW 264.7 cells or mouse peritoneal macrophages, both hydrogen peroxide and superoxide anion treatments led to increases in iPLA$_2$ activity (75). The underlying mechanism was proposed by Balboa and Balsinde: the oxidative stress or damage induced lipid peroxide accumulation, subsequently changed the physical state of membrane substrate for iPLA$_2$, leading to the enzyme activation (76).

Furthermore, other regulatory factors influencing iPLA$_2$ activities include proteolytic processing (50, 77, 78), and translational/posttranslational modifications (26, 54, 79).

2.2.3. Inhibition of Calcium-Independent Phospholipase A$_2$

As indicated above, the presence of catalytic serine in iPLA$_2$ indicates that it is readily inhibited by hydrophobic serine site-directed inhibitors. At present, several chemical inhibitors are available, including methyl arachidonyl fluorophosphonate (MAFP) (51, 80), fatty acyl trifluoromethyl ketones and tricarbonyls (e.g. arachidonyl trifluoromethyl ketone (AACOCF$_3$)) (49), and bromoenol lactone (BEL) (49, 81, 82). As shown as Table 2, MAFP and AACOCF3 share a common chemical structure as an arachidonyl tail, which can be coupled to a Ser-reactive group. Because of the similarity in reactive-site of iPLA$_2$ and cPLA$_2$, the inhibitors MAFP and AACOCF3 fail to distinguish iPLA$_2$ and cPLA$_2$. Additionally, recent study has shown that different iPLA$_2$ isoforms have distinct inhibition profiles across specifies and tissues, and the inhibitory effects of MAFP on iPLA$_2\gamma$ and membrane-associated iPLA$_2\beta$ are limited to the specific

species and tissues: the microsomal iPLA$_2$s are not inhibited by MAFP in rabbit kidney and heart, and rat kidney, nevertheless, these enzymes are significantly inhibited by MAFP in rat heart and brain tissues (61).

Among inhibitors mentioned above, BEL is the only one which selectively targets iPLA$_2$ over other calcium-dependent PLA$_2$s (49, 81, 82). BEL serves as a mechanism-based suicide inhibitor, which means that the compound has to first react with iPLA$_2$ enzyme to produce the inhibitory derivatives. The inhibitory BEL derivative results from an enzymatic rupture of the lactone ring present in the molecule (as shown in Table 2), which covalently binds at or near the active site of iPLA$_2$ immediately after hydrolysis and prior to diffusion from the catalytic cleft, leading to an irreversible inactivation (81, 83). Furthermore, all known iPLA$_2$s have been shown to be inhibited by BEL (28, 84-86). It has also been demonstrated that BEL inhibits the triglyceride lipase activity of iPLA$_2\delta$, -ϵ and -ζ (28). Therefore, BEL is the most prominent inhibitor used to investigate the cellular functions of iPLA$_2$.
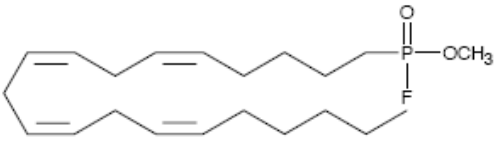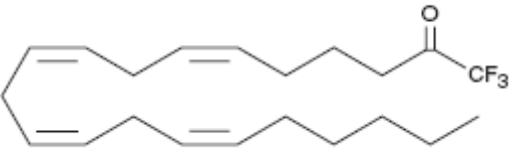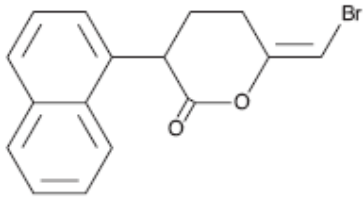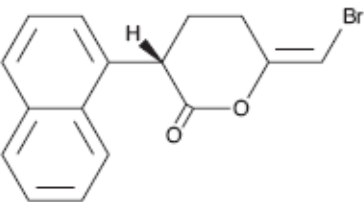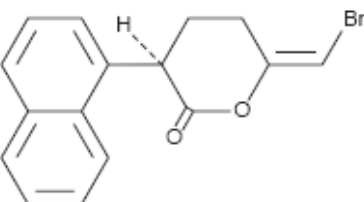
Unfortunately, BEL is also reported to react with other enzymes, such as the Mg^{2+}-dependent phosphatidic acid phosphohydrolase (PAP-1, lipin) (84). So, it is necessary to rule out the roles of PAP-1 by using PAP-1 inhibitor propranolol at high concentrations (greater than 150 μM) when BEL is utilized in iPLA$_2$ studies (87-89).

More recently, Jenkins et al. (54) identified two chiral specific enantiomers for BEL, (S)-BEL and (R)-BEL. They also found that the inhibiting preference of these two isomers is different: (S)-BEL was considerably more selective for iPLA$_2\beta$ in comparison

to iPLA$_2$γ whereas (R)-BEL inhibited iPLA$_2$γ much better than iPLA$_2$β (54). These results make BEL a more powerful compound to distinguish between these two iPLA$_2$ enzymes.

Besides the application of chemical inhibitors, selective inhibition on iPLA$_2$s can be performed through targeted gene silencing strategies. Those studies using antisense oligonucleotide or small interfering RNA (siRNA) provide more compelling evidence for the involvement of iPLA$_2$ in interested cellular process in vitro (15, 57, 90). The iPLA$_2$ knockout animal models are also available for investigators to more accurately determine the physiological roles of iPLA$_2$ in vivo (18, 91).

Table 2. Calcium-Independent Phospholipase A$_2$ Inhibitors

Inhibitor	Chemical Structure/Molecular Formula	PLA$_2$s inhibited
MAFP, Methyl Arachidonyl Fluorophosphonate	$C_{21}H_{36}FO_2P$	cPLA$_2$, AdPLA, iPLA$_2$
AACOCF$_3$, Fatty Acyl Trifluoromethyl Ketone	$C_{21}H_{31}F_3O$	cPLA$_2$, AdPLA, iPLA$_2$
BEL, Bromoenol Lactone	$C_{16}H_{13}BrO_2$	iPLA$_2$ β, γ
(S)-BEL, (S)-Bromoenol Lactone	$C_{16}H_{13}BrO_2$	iPLA$_2$ β
(R)-BEL, (R)-Bromoenol Lactone	$C_{16}H_{13}BrO_2$	iPLA$_2$ γ

2.2.4. Cellular Functions of Calcium-Independent Phospholipase A$_2$

Of the iPLA$_2$ family, iPLA$_2\beta$ and iPLA$_2\gamma$ are predominantly responsive for the PLA$_2$ activity, whereas other four members show lipase or transacylase in marked preference to PLA$_2$ activity. Moreover, iPLA$_2\beta$ and iPLA$_2\gamma$ are two iPLA$_2$s that have been earlier identified and more extensively studied. For these reasons, the cellular functions of iPLA$_2$ discussed in this section are based on studies about iPLA$_2\beta$ and iPLA$_2\gamma$.

2.2.4.1. Phospholipid Remodeling

As mentioned above, intracellular PLA$_2$s promote the cleavage of pre-existing membrane PL, leading to the production of free fatty acids and 2-lyso PL. The generated free fatty acid may be reincorporated into different membrane PL molecules, and the lyso PL may be reacylated with a different fatty acid as well. In this case, PLA$_2$s are highly involved in the ongoing deacylation/reacylation cycle essential for the maintenance of membrane homeostasis (12). As a major group of PLA$_2$ ubiquitously expressed in mammalian system, iPLA$_2$s across different tissue sources have been reported to play roles in phospholipids remodeling, especially function on the incorporation of long chain polyunsaturated fatty acids (LCPUFA) into the glycerophospholipids (92-96). The LCPUFA incorporation process is particularly important for inflammatory cells such as macrophages and neutrophiles. Macrophages present a high capacity in membrane AA incorporation, which is mostly maintained by iPLA$_2$ activity. Inhibition on iPLA$_2\beta$ via BEL treatment or antisense oligonucleotide both lead to reduced AA incorporation into

PLs and cellular LPC levels in P388D1 macrophages (82). Similar results are also found in brain cell studies: it is showed that BEL treatment inhibits the release of docosahexaenoic acid from the membrane phospholipids of astrocytes upon ATP stimulation (96). In contrast, overexpression of iPLA$_2$ β and iPLA$_2$γ in HEK293 cells results in the accumulation of free fatty acid and LPC, and this event can be blunted by BEL (57). Taken together, these findings highlight the importance of iPLA$_2$β in membrane housekeeping.

2.2.4.2. Arachidonic Acid Metabolism

Given that AA and lyso PL can be both metabolized into a range of biologically active compounds, PLA$_2$ activity are essential for many cell signaling functions. Released AA can be directed to the cyclooxygenase (COX) and lipoxygenase pathways for eicosanoid synthesis (97). Previous studies have demonstrated that cPLA$_2$ and sPLA$_2$ are the most contributors to AA release in response to a variety of stimuli (34, 98). Recently, iPLA$_2$ has been found to play a role in cellular signaling initiated by AA release and sequential metabolism under certain conditions (66, 99, 100). For example, in RAW261.7 macrophages, BEL markedly restricted the nitric-oxide-induced AA mobilization (99). In zymosan-stimulated P388D1 macrophages, prostaglandin E$_2$ (PGE$_2$) generation is significantly attenuated by BEL treatment or iPLA$_2$β antisense (67). Similar results can also be found in calcium-ionophore-treated neutrophiles and pancreatic β cells exposed to glucose (89, 101). These effects appear to be iPLA$_2$β dependent. In these cells, the cytosolic enzyme iPLA$_2$β is translocated to the membrane fractions in response to the stimuli, and iPLA$_2$β movement appears to be regulated by protein kinase C (102). Even

though iPLA$_2\gamma$ is less well investigated, there is strong evidence showing that this enzyme is also involved in AA release that ultimately results in the formation and metabolism of eicosanoids in HEK 293 cells (57).

2.2.4.3. Control of Calcium Entry

Agonist-induced depletion of intracellular Ca^{2+} store is known to activate channels and capacitative Ca^{2+} entry (103). Although the mechanisms underlying this replenishment remain unclear, two major models are proposed: "conformational coupling" and "Calcium Influx Factor" (CIF) (98). In the CIF model, a diffusible molecule is generated with the diminution of calcium stores, which interacts with the store-operated channels sitting in plasma membrane and induces Ca^{2+} flux (98). Increasing evidence shows that iPLA$_2$ is involved in this process. A possible link between iPLA$_2$ and calcium signaling was first discovered in 1990's by two research groups (63, 104), who reported that the depletion of intracellular Ca^{2+} stores resulted in an increased iPLA$_2$ enzymatic activity, leading to phospholipid hydrolysis and free fatty acids accumulation in rat smooth muscle cells (104) and pancreatic islets (63). More recently, several investigations have shown similar results that iPLA$_2$ is activated when intracellular Ca^{2+} stores are depleted (64, 69, 105). Also, iPLA$_2$ appears to serve as a regulator of Ca^{2+} replenishment. In a variety of cells and tissues, such as smooth muscle cells (105), rat basophilic leukemia (RBL) cells (106), platelets (107), prostate cancer cells (108), inhibition of iPLA$_2\beta$ by (S)-BEL or antisence oligonucleotides blocks calcium release-activated channels (CRAC) calcium influx. More importantly, LPC can reverse the inhibitory effects of (S)-BEL on store-operated channels and restore the Ca^{2+}

influx, indicating that the iPLA$_2$ activity-dependent LPC generation is required for the activation of store-operated channels. According to these observations, intracellular Ca^{2+} store exhaustion induces the production of calcium influx factor, which interferes with the combination of calmodulin and iPLA$_2\beta$. This dissociation with calmodulin triggers the enzymatic activity of iPLA$_2\beta$ leading to the production of lysophospholipids, which sequentially activate the store-operated channels and capacitative Ca^{2+} influx. Upon refilling of the stores and cessation of calcium-influx factor production, calmodulin would reassociate with iPLA$_2\beta$, and terminate repletion of Ca^{2+} (105). Additionally, some other investigations propose another target regulated by iPLA$_2$ activity affecting the Ca^{2+} homeostasis, transient receptor potential (TRP) channels (108, 109). For example, in the Chinese hamster ovary cells, the response of cold-sensitive channel transient receptor potential (melastatin)-8 (TRPM8) to exogenous stimuli were abolished by inhibition of the iPLA$_2$. Both lysophospholipids and polyunsaturated fatty acids (PUFAs) are involved in regulating the activity of these channels (109).

2.2.4.4. Secretion and Exocytosis

Upon activation of PLA$_2$, the accumulation of lysophospholipids and free fatty acids may occur in local areas of membrane, and consequently change the membrane fluidity or promote non-bilayer structures, which eventually encourage the fusion of biological membranes. An accumulating body of evidence has confirmed the linkage of iPLA$_2$ activity and secretion functions. For example, the lysozyme secretory responses to stimuli was diminished by iPLA$_2\beta$ antisense oligonucleotide treatment in U937 cells, and reduced levels of LPC were also observed (110). However, reconstitution of LPC

ultimately restored the lysozyme secretion, indicating that iPLA$_2$β -mediated generation of LPC is important for full secretion to take place (110). Similar effects of iPLA$_2$ inhibition in secretion can be also established in other studies, including glucose-stimulated insulin secretion in pancreatic β cells (89, 111, 112), exocytosis of amylase from parotid acinar cells (113), and lysosome-mediated interleukin-1β (IL-1β) secretion (114). In many exocytosis processes, increased cytosolic calcium is known to be required. BEL treatment has been shown to inhibit such processes, including release of neurotransmitter (115) and mast cell granule (116). Therefore, the regulatory roles of iPLA$_2$ on calcium entry mentioned above may explain some aspects of its importance in secretion.

2.2.4.5. Other Cell Signaling Functions

Other cellular signaling functions of iPLA$_2$ consist of cell growth and proliferation (117, 118), apoptosis (119-121), chemotaxis (122, 123), gene expression (35, 124, 125), endothelium-dependent vascular relaxation (126), and development of cardiac ischemia (127, 128), none of these will be discussed in detail in this review.

2.2.5. Calcium-Independent Phospholipase A$_2$ in Metabolism

Recently, several studies established the emerging roles of iPLA$_2$ in whole body metabolism, including the adipocytes differentiation (15), glucose-stimulated insulin secretion (16-21), hepatic adipogenesis (24, 25), glucose homeostasis (22, 23), and cardiac myocytes mitochondrial functioning (26, 27). These findings spotlight iPLA$_2$ as a

possible therapeutic target for obesity, type II diabetes, fatty liver disease and other manifestations of the metabolic syndrome (25).

2.2.5.1. Glucose-Stimulated Insulin Secretion

Pancreas dysfunction is a typical pathological characteristic of diabetes mellitus; thus, proper pancreatic β cell function is essential for the whole body homeostasis. It is well understood that glucose-stimulated insulin secretion in pancreatic β-cells and related cell lines is associated with increased hydrolysis of phospholipids (89, 111): glucose stimulation results in both insulin secretion and AA release, and inhibitors of phospholipase suppress the secretion of insulin. Involvement of iPLA$_2$ in such a process was initially suggested by Ramanadham et al. in 1993. BEL, the selective inhibitor of iPLA$_2$ completely suppressed insulin secretion, as well as phospholipid hydrolysis (111). More recent studies extend these findings by using the INS-1 cells (rat insulinoma cell) transfected with iPLA$_2$β. In the iPLA$_2$β overexpressed cells, improvement was observed in both glucose responsiveness and insulin secretion in response to cyclic adenosine monophosphate (cAMP)-elevating agents (112, 129), which induce the translocation of iPLA$_2$β to a perinuclear region facilitating the phospholipid hydrolysis in endoplasmic reticulum (ER) membrane. Released AA is postulated to serve as a signaling molecule for insulin secretion. Consistent with this hypothesis, inhibition of the insulin secretion was restored by exogenous AA (15). Studies in vivo provide supplementary proof for the roles of iPLA$_2$β in this process. The iPLA$_2$β knockout mice showed insufficient insulin secretion in response to glucose, developed severe glucose intolerance response to high-fat diet, and exhibited more sensitivity to the streptozotocin (STZ) treatment (22, 23). On

22

the contrary, iPLA$_2\beta$ transgenic mice have a lower fasting glucose and higher insulin levels compared to wild type controls (23).

2.2.5.2. Adipocyte Differentiation

The hormone-stimulated differentiation of pre-adipocytes into mature adipocytes is effectively controlled by CCAAT/enhancer-binding protein (C/EBP) family and peroxisome proliferator-activated receptor γ (PPARγ), which are also important for glucose and lipid metabolism (130, 131). Recently, Su *et al*. (15) reported the indispensable roles of iPLA$_2$ in 3T3-L1 adipocyte differentiation, as well as the relationship between iPLA$_2$ activity and PPARγ regulation. In this study, iPLA$_2\beta$ and iPLA$_2\gamma$ were upregulated during the differentiation procedure, while cPLA$_2$ was reduced to background level in mature adipocytes. Loss of iPLA$_2$ β and iPLA$_2\gamma$ by BEL treatment or small interfering RNA inhibited the hormone-induced adipocyte differentiation via preventing PPARγ and C/EBPα gene expression. However, when the cells were treated by a PPARγ agonist, trigolitazone, the adipogenesis was restored. The authors speculated that LPC generated from iPLA$_2$-catalyzed phospholipid hydrolysis, derivate LPA or other bioactive metabolites may serve as activators of PPARγ (15). In addition, the protein levels of iPLA$_2\beta$ and iPLA$_2\gamma$ were found both significantly increased in white adipose tissue of genetically obese *fa/fa* rats, compared to the lean controls (15). Another study also reported that during the differentiation of 3T3-L1 cells into adipocytes, there was dramatically upregulated gene expression in two other members of iPLA$_2$ family: iPLA$_2\xi$ and iPLA$_2\varepsilon$ (132). All these results suggest that iPLA$_2$ may play important roles in the energy homeostasis in adipocytes.

2.2.5.3. Hepatic Lipogenesis

Besides PPARγ and C/EBPα, sterol regulatory element binding proteins (SREBPs) are other key modulators for lipogenesis (133, 134). Calcium-independent PLA_2 is also shown to be associated with the regulation of SREBP. It is well-established that PUFAs are capable of influencing SREBPs processing and translocation, resulting in the inhibition on fatty acid synthase, acetyl CoA carboxylase, and other lipogenic genes associated with triglyceride synthesis (135, 136). Based on these observations, Wilkins research group initiated a study on the regulatory effects of $iPLA_2$ in SREBP (98). In this study, $iPLA_2$ inhibition and overexpression in HepG2 cells resulted in the increases and decreases of the transcriptional activity of SREBP expression, respectively. These results indicate a potential role of $iPLA_2$ in hepatic adipogenesis.

2.2.5.4. Mitochondrial Functions

It has been demonstrated that $iPLA_2\gamma$ is a membrane-associated protein which is localized to mitochondria (137-139). In recent studies, $iPLA_2\gamma$ has been reported to play an essential role in maintaining proper mitochondrial functions (26, 27). In isolated rabbit renal cortex mitochondria, inhibition of $iPLA_2\gamma$ by (R)-BEL accelerates lipid peroxidation and swelling, and blocks mitochondrial permeability transition, which is critical for cell apoptosis (140, 141). More importantly, the $iPLA_2$ knockout mice perform reduced Complex IV-mediated oxygen consumption, decreased cold tolerance, diminished exercise capacity but low capacity to gain weight (26, 27). Taken together, these findings suggest that the loss $iPLA_2 \gamma$ induced whole body energy unbalance. It is intriguing that

in iPLA$_2\gamma$-overexpressed myocytes or iPLA$_2\gamma$ transgenic animals, however, the mitochondria exhibit reduced respiratory control quotient (26). Although future studies are necessary for better understanding of the regulatory effects of iPLA$_2\gamma$ in these procedures, these findings underscore the significance iPLA$_2\gamma$ in energy homeostasis.

2.3. INSULIN SIGNALING

Insulin is the most influential hormone secreted by pancreas. This hormone lowers the blood glucose level by stimulating glucose influx into peripheral tissues, and promoting the fat deposition in adipocytes, glycogen synthesis in muscle and liver, as well as inhibiting the production and release of glucose from the liver (142). As a result, the key actions of insulin include modulating the whole body energy homeostasis, promoting proper metabolism, and helping body to keep normal body weight (143). Those actions are performed through a series of intracellular signal transduction.

When insulin is bond to the alpha-subunit of the insulin receptor (IR) residing on cell membrane, a transmembrane conformational change occurs, and the beta-subunit of IR undergoes a rapid autophosphorylation (addition of a PO4 group from adenosine triphosphate) reaction, leading to the phosphorylation at multiple tyrosine (Tyr) residues, which is necessary for the appropriate recognition of IR substrates and the activation of IR tyrosine kinase (IRK) activity. Subsequently, the downstream cytosolic moieties are tyrosine phosphorylated by, which include insulin receptor substrate family proteins (IRS-1, to -6), growth factor receptor bound 2 (Grb2)-associated binder-1 (Gab 1), Src homologous and collagen (Shc) proteins, signal-regulated proteins (SIRPs), Cbl, and

25

adapter protein with pleckstrin homology and Src homology domains (APS) (144). These proximal intracellular phosphorylation targets serve as docking sites for downstream effector proteins containing Src homology 2 (SH2) and phosphotyrosine binding (PTB) domains (145). Three major signaling pathways are propagated (Figure 1): phosphatidylinositol 3-kinase (PI3K) pathway, Cbl/CAP pathway and the mitogen-activated protein kinase (MAPK) pathway (144, 146).

2.3.1. Phosphatidylinositol 3-Kinase Pathway

Among those three pathways activated by insulin, PI3K cascade is the best established. In addition to glucose transport, it also mediates other metabolic functions of insulin. The IRS family in the PI3K cascade has attracted considerable attention due to their key roles in triggering insulin signaling (147). Upon tyrosine phosphorylation, the IRS proteins are associated with the 85-Kda regulatory subunit of phosphoinositide-3-kinase (PI3K) thereby activate PI3K. Analogous to p85 PI3K subunit, other SH2 domain-containing proteins, such as Nck, Fyn, Grb-2, and SHP2, also bind to IRS proteins and mediate the various aspects of insulin action (142, 148). PI3K regulates several signaling pathways through the generated lipid messenger, phosphotidyl-3, 4, 5-triphosphophate (PIP3), which stimulates phosphoinositide-dependent kinase (PDK-1) activity and initiates the activation of its downstream effectors, such as protein kinase B(Akt/PKB), mammalian target of rapamycin (mTOR), p70 S6 kinase (S6K1), and atypical protein kinase C isoforms (aPKCλ/ζ) (149-153). Akt is one of the critical targets playing pivotal roles in mediating the insulin-responsive metabolic actions (154).The full activation of Akt can only be achieved via a dual phosphorylation on the both serine (Ser) and

26

threonine (Thr) residues. It is showed that PDK1 phosphorylats Thr^{308} (155), while the kinase for Ser^{473} phosphorylation is referred to as either PDK2 (156) or DNA-dependent protein kinase (156, 157). It appears that Ser^{473} phosphorylation is required for the phosphorylation of Thr^{308} (155). Once activated, Akt detaches from the plasma membrane and promotes the translocation of GLUT4 from intracellular compartments to cell surface, facilitating the glucose uptake into adipocytes or skeletal muscle cells (154). Another target of Akt is glycogen synthase kinase-3β (GSK-3β), which is a negative regulator of glycogen synthesis. Ser-phosphorylation of GSK-3β by Akt activates glycogen synthase and boosts the glucose anabolism in skeletal muscle cells (158, 159). Akt- GSK-3β pathway has also been proposed to mediate the anti-inflammatory effects of insulin (158, 159). Some other actions of the activation of Akt include promoting lipid deposition and protein anabolism, and regulating cell survival and growth (160-162).

2.3.2. Cbl/CAP Pathway

The Cbl/CAP pathway is another pathway mediating glucose uptake upon insulin administration. Research evidence for Cbl/CAP cascade remains controversial; however, increasing numbers of key effectors in this pathway have been identified in recent studies. As a substrate for IR phosphorylation, Cbl undergoes a tyrosine phosphorylation assisted by the associated protein substrate, APS (163). And then Cbl-associated protein (CAP) targets Cbl to recruit with IR in lipid raft domains, making the tyrosine phosphorylated Cbl serve as docking sites for the CrkII/C3G complex (164-166). CrkII (chicken tumor virus no.10 (CT10) regulator of kinase II) is an adaptor protein assisting the binding of Cbl to Crk SH3-binding guanine nucleotide-releasing factor (C3G), and C3G functions as

27

a guanine nucleotide exchange factor for the small GTP binding protein TC10, a protein essential for GLUT4 translocation (167), which is also thought to contribute to the maintenance of actin structure in 3T3-L1 adipocytes (167, 168). It is proposed that the last step of this pathway is associated with actin dynamics and linked to GLUT4 translocation (169-171). Interestingly, in contrast to the original idea that Cbl/CAP and PI3K pathways are independent, some investigations have demonstrated that Cbl can also activate PKCλ/ζ in a way paralleled to PI3K pathway (172, 173), and TC10 activation was linked to PI3P production, which may affect the GLUT4 translocation independent of Cbl/CAP cascade (174).

2.3.3. Mitogen-Activated Protein Kinase Pathway

The mitogen-activated protein kinase cascade mediates the insulin receptor signaling and triggers the mitogen-activated protein kinase (MAPK) isoform p42MAPK/p44MAPK (ERK1/ERK2) cascade, which is not required for insulin's metabolic effects but essential for mitogenic signaling manipulating gene expression in various cellular processes, like proliferation, differentiation and apoptosis (175). Upon the autophosphorylation on tyrosine residues of the insulin receptor, a Shc-Grb2 complex is formed, and recruited to the plasma membrane, where it binds to son-of-sevenless (Sos), a nucleotide exchange protein that increases the rate of exchange of GTP for GDP on Ras (a family of small GTP binding proteins), in turn activates Raf /MAP/ERK kinase cascade (176). This leads to activation of a serine/threonine-tyrosine kinase, MEK, which phosphorylates and activates extracellular signal-related kinase ERK1/2. One important downstream element phosphorylated by ERKs is p90 ribosomal S6 kinase

(RSK2) (177)**.** The proposed cellular functions of RSK include regulating gene expression via interaction with transcriptional regulators including c-Fos (a cellular proto-oncogene belonging to the immediate early gene family of transcription factors), estrogen receptor, nuclear factor-κB (NFκB) /inhibitor of NFκB (IκBα), cAMP-response element-binding protein (CREBP), controlling cell cycle, modulating protein synthesis, and phosphorylating the Ras GTP/GDP-exchange factor, Sos leading to feedback inhibition of the Ras-ERK pathway (178).
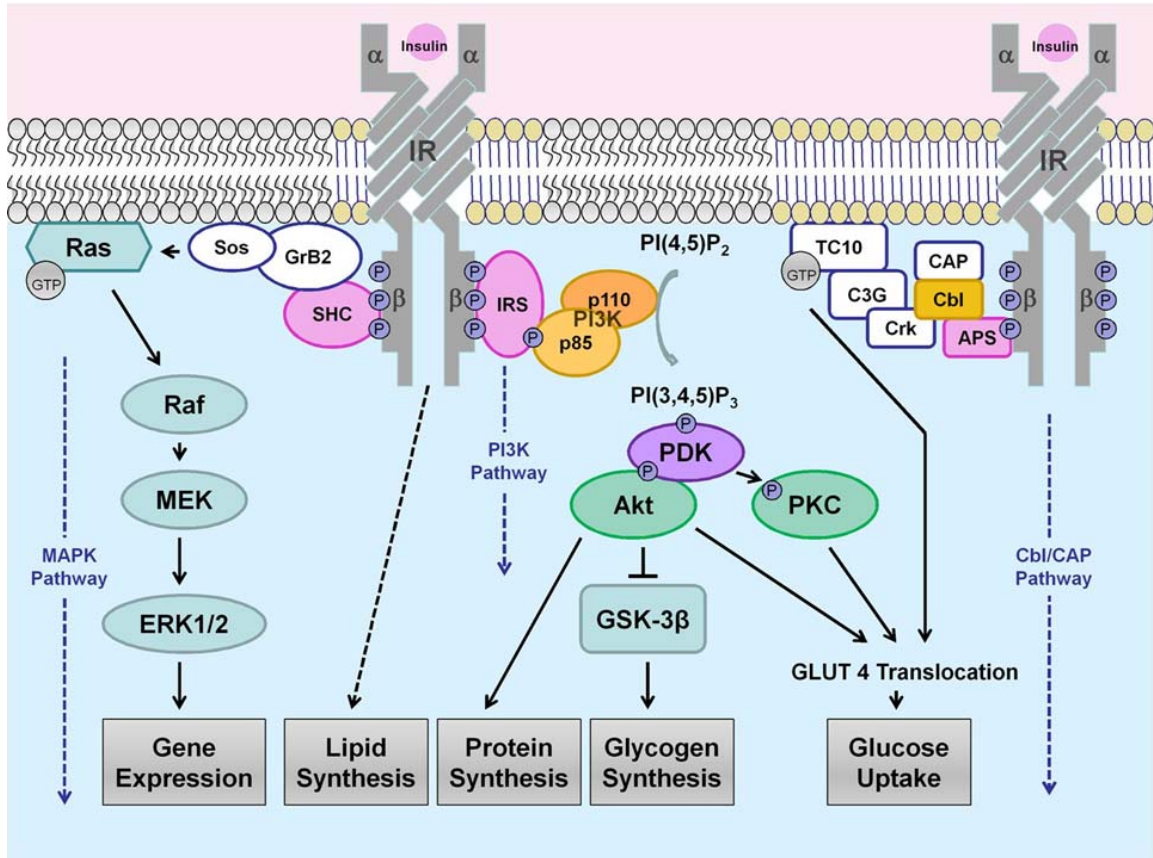
Figure 1. Three pathways initiated by insulin signaling. Insulin binding to alpha-subunit of the insulin receptor (IR) results in a rapid autophosphorylation in beta-subunit of IR, leading to the phosphorylation and activation of IR substrates. Subsequently, three downstream signaling cascades are propagated to mediate the insulin actions.

2.4. INSULIN-STIMULATED GLUT4 TRANSPORT

The ability of insulin in clearing the blood glucose is mainly achieved by the regulation of glucose transporters in insulin-sensitive cells. Under basal conditions, these transporters are impounded in an intracellular compartment, while under the stimulation of insulin, they are rapidly driven to translocate into the plasma membrane, resulting in the glucose uptake of the cells from the plasma (179, 180). Currently there are 13 members of this family identified including glucose transporter GLUT-1-12, and the H^+-myo-inositol transporter HMIT1 (181). Each of them exhibits different tissue distributions, kinetic properties and sugar specificity. GLUT-1 to 4, the class I glucose transporters, are the best-characterized members of this family (142). Among them, glucose transporter 4 (GLUT4) is the predominant one responding to the insulin signaling in the fat or muscle cells.

In the resting state, GLUT4 cycles slowly between the vesicles compartments and cell surface, with the vast majority of the transporters localized in the intracellular pool. Upon insulin stimulation, the activation of signaling cascades substantially increases the rate of GLUT4 exocytosis. Simultaneously, the endocytosis of GLUT4 is attenuated. Collectively, the net effect of these steps leads to a dramatic redistribution of GLUT4 to the plasma membrane (PM) (179, 182, 183).

Despite intensive investigation for several years, the insulin-responsive shift of GLUT4 in the distribution from intracellular compartments to the PM has not been fully deciphered. According to the basic trafficking process of GLUT4 in response to insulin,

31

posttranslational regulatory modalities are mainly identified in two biological systems —
signal transduction and vesicular transport.

2.4.1. Insulin Signaling Regulators

PI3K pathway and Cbl/CAP pathway represent two distinct branches contributing
to glucose uptake response to insulin stimulation. Therefore, the signaling molecules
participating in these two cascades must intensively impact the initiation of GLUT4
translocation.

As the key factor for the initiation of PI3K cascade, IRS proteins are required for
insulin-dependent GLUT 4 translocation, which is supported by siRNA and gene
knockout studies (172, 184). There are also extensive results proving that the activation
of PI3K and consequent generation of PIP3 are indispensable for GLUT4 translocation.
Overexpression of p110α subunit of PI3K in 3T3-L1 adipocytes induced an
approximately 14-fold increase in the basal glucose transport rate, even greater than that
observed in the stimulated control (185). Similar results were found in study with rat
adipose cells (186). In opposition, inhibition of PI3K by pharmacological inhibitors (187,
188), dominant-interfering mutants (187), endogenous inhibitory kinase (189), prevented
the GLUT4 translocation to the PM, while exogenous PIP3 rescued the GLUT4 fusion
with PM (188). However, the exogenous PIP3 dependent GLUT4 translocation was
inadequate to fulfill the glucose uptake (188). Further investigation showed that an
unmasked GLUT4 COOH terminus was needed to achieve the full function of the
transporter, and the unmasking process was proposed to be controlled by PI3K activity

32

(188) (190), indicating a potential molecular mechanism for regulation on GLUT4 activity(191). As the key downstream mediator of the PI3K pathway, Akt is directly correlated with GLUT4 translocation. The overexpression of a constitutively active, membrane-bound form of Akt in NIH3T3 adipocytes promoted GLUT4 translation (192). In contrast, downregulation on Akt by dominant-negative mutant (150), competing peptides (193), or gene silencing (194-196) inhibited GLUT4 translocation. PKCλ/ζ is another downstream effector also involved in GLUT4-mediated glucose transport. The activation of PKCλ/ζ has shown to contribute significantly to insulin-stimulated glucose uptake (173, 197, 198). For example, PKCζ transgenic skeletal cells exhibited an enhanced glucose uptake (199), whereas aPKC selective inhibitory peptide significantly reduced the glucose transport in insulin-stimulated L6 cells (173), without affecting Akt (200, 201). However, the dependence of insulin-stimulated GLUT4 translocation on aPKCλ/ζ remains controversial (196), and requires further investigation excluding the lurking factors (191).

In spite of intensive exploration, downstream effectors of Cbl/CAP pathway exhibit controversial effects. Overexpressing mutants of CAP and TC10 impede the GLUT4 translocation, documenting their significance in this process (167). However, gene silencing of CAP, Cbl isoforms, and CrkII fail to impact in the insulin-dependent GLUT4 translocation in 3T3L1 adipocytes (202), indicating that they are not required components of insulin signaling to GLUT4 transporters. In addition, APS knockout mice exhibit increased insulin sensitivity and hypoinsulinemia compared to wild type control or APS overexpressed mice, though the transgenic model did not show any negative

33

alterations in insulin signaling and glucose uptake (203). Further studies are required to explain these observed discrepancies.

In contrast to insulin-induced "turning on" actions, GLUT4 translocation can be turned off by negative regulation on insulin signaling. For example, serine/threonine phosphorylation of the IRS results into the dissociation of IR:IRS and IRS:PI3K complex, eventually blocks the insulin activated GLUT4 translocation (152, 162, 204). On the other hand, dephosphorylation of specific kinases by corresponding phosphatases also diminishes the insulin signaling. IRS-1 or Akt/ PKC have shown to be the inactivated by protein tyrosine phosphatase 1B (PTP1B) (205, 206) or serine/threonine protein phosphatase 2A (PP2A) (207), respectively, resulting in the negative control toward GLUT4. In addition, lipid phosphatases, such as tumor suppressor gene phosphatase and tensin homolog deleted on chromosome 10 (PTEN) (208, 209) and SH2-containing inositol phosphatase 2(SHIP2) (210-212), are thought to negatively modulate insulin signaling controlling the duration of signaling. Overexpression of these proteins in 3T3-L1 adipocytes leads to reduced PIP3 levels, inactivated Akt/PKC, and subsequently inhibits GLUT4 translocation (210-212).

2.4.2. Newly Identified Akt Substrates Involved in GLUT4 Exocytosis

More recently, a 160 KDa protein was identified in both adipocyte and skeletal muscle cells as an Akt substrate and denoted as AS160 (213). AS160 contains six consensus Akt phosphorylation domains as well as a Rab GTPase activating protein (GAP) domain (214). Since Rab proteins represent the largest branch of the Ras

superfamily of small GTP-binding proteins, and they regulate several steps of membrane transport, including vesicle budding, motility, tethering and fusion (215, 216). It is supposed that AS160 could serve as an mediator connecting insulin signaling transduction to GLUT4 translocation. Based on current data from AS160 studies, a working model has been postulated (217, 218): in the rest cells, AS160 maintains a GAP activity and inhibits the downstream Rab protein; after being phosphorylated on multiple Akt phosphomotifs in response to insulin signaling, the GAP activity of AS160 is blunted by phosphorylation or dissociation, leading to the transition of downstream Rab protein from GDP-bound form to a GTP-bound activate form, eventually facilitating GLUT4 translocation (217, 218).

SNAREs are membrane-bound partners for the soluble NSF attachment proteins (SNPs), and highly involved in the vesicle fusion machinery. Two potential SNAREs are demonstrated to be correlated with GLUT4 vesicle fusion: Vesicle-associated membrane proteins 2 and 3 (VAMP2 and VAMP3) (145). As a SNAER-associated protein, synip is another recent identified Akt substrate, which is supposed to bind syntaxin 4, a target-SNARE (t-SNARE) localized to the cell surface and VAMP2, a v-SNARE on vesicle, and then regulate the docking and fusion of GLUT4 vesicles (219).

2.4.3. Actin Remodeling

With regard to insulin action and glucose transport, an increasing body of data demonstrates that actin plays a critical role in GLUT4 translocation (220-226). It is observed that under insulin stimulation, actin cytoskeleton perform a PI3K-dependent

remodeling in both adipocytes (225) and muscle cells (226). Additionally, the PI3K products, such as PIP3 or PIP2 (phosphotidyl-4, 5-biphosphophate) have been shown to bind to the cytoskeletal protein profilin, serving as an organizational site for actin remodeling (227). It has been reported that disruption of cortical actin filament formation by pharmaceutical inhibitors, inhibits insulin-stimulated GLUT4 translocation (220, 224, 228). There are also some actin binding proteins indentified to mediate the insulin regulator effects, such as actin regulatory protein N-WASP (Neuronal Wiskott-Aldrich syndrome protein) (229). Moreover, TC10 is associated with actin dynamics and linked to GLUT4 translocation (142, 170). Taken together, it has been postulated that actin remodeling may provide a scaffold that coordinates the production of PIP3, recruits other signaling molecules, or offers a platform directing the GLUT4 compartments to the plasma membrane (PM) (191).

2.4.4. Calcium Influx

At the plasma membrane, activated GLUT4 vesicles undergo docking and fusion through a process assisted by several SNARE proteins, including VAMP-2, Synip, and Syntaxin-4 (230). Such an exocytosis process is very similar to the release of neurotransmitter, a process that is generally induced by transient increases in the Ca^{2+} concentration at the release sites (231-233). Additionally, previous studies have shown that molecules chelating Ca^{2+} calmodulin antagonists attenuate the insulin-stimulated glucose uptake, along with the reduced GLUT4 translocation in adipocytes (234) or skeletal muscle cells (235, 236). Furthermore, other studies have demonstrated that insulin stimulation activates the Ca^{2+} influx in a PI3K dependent manner, leading to

significantly increased calcium concentration close to the plasma membrane (237, 238).

Collectively, the fact that increase or decrease Ca^{2+} influx also increase or decrease insulin-mediated glucose uptake makes Ca^{2+} influx a potential regulator for insulin-stimulated GLUT4 translocation (239), and it mainly acts on late steps in the insulin-signaling pathway (234, 240). In the skeletal muscle cell, it was observed that inhibition of Ca^{2+} influx with 2-aminoethoxydiphenyl borate (2-APB) reduced the glucose uptake but had no influence the phosphorylation state of PKB or the MAP kinases ERK1/2 was not affected by (240). Whitehead, et al. also reported that in the 3T3-L1 adipocytes, Ca^{2+}/calmodulin plays a fundamental role in eukaryotic vesicle docking and fusion (234). Thus, it is proposed that the late steps in insulin signaling might involve an intracellular microdomain with increased Ca^{2+} and Ca^{2+} sensing proteins, which directly or indirectly modulate GLUT4 exocytosis (230).

This emerging role of Ca^{2+} influx has been further supported by several potential Ca^{2+} censored proteins correlated with this process. Synaptotagmin-VII, a membrane protein in the synaptotagmin family recognized as Ca^{2+} sensors in exocytosis (232, 233), is proven to play roles in insulin-mediated glucose uptake and GLUT4 trafficking in adipocytes by a study using synaptotagmin VII-deficient mice, which performed impaired insulin response (241). Ca^{2+}-calmodulin-regulated actin-filament-attached motor protein, Myo1c is also demonstrated to join in this process. Several research groups observed that genetic knockdown of Myo1c in 3T3-L1 adipocytes inhibited insulin-stimulated GLUT4 translocation and glucose uptake (242, 243). It is assumed that in insulin-stimulated adipocytes, Myo1c translocates to the plasma membrane and

interacts with GLUT4 in a Ca^{2+}-dependent manner. Chen et al. showed that the interaction between the motor protein Myo1c and the small GTPase RaIA was required for GLUT4 vesicles docking, and the association between Myo1c and RaIA is modulated by calmodulin in a Ca^{2+}-dependent manner (243).

2.5. OBESITY, TYPE 2 DIABETES AND INSULIN RESISTANCE

2.5.1. Epidemic of Obesity and Type 2 Diabetes

Obesity, defined by a body mass index (BMI) greater than $30kg/m^2$, was introduced to the international classification of diseases more than half a century ago. In the current 21st century, obesity represents an expanding problem that has reached epidemic proportions in the worldwide scale. As conservatively estimated by the International Obesity Taskforce and World Health Organization (WHO), at least 9.8% adults around the world are obese (1, 3, 244). In some western countries, the percentage is even greater: for example, in the United States, 32.2% adults are obese (245). In addition, near 2.3 billion of people in the world may be at a risk for diseases associated with being overweight. Current mortality rates due to the high BMI could double to 5 million deaths per year by the year 2030 - unless urgent action is taken now (1, 3, 244).

This global pandemic disease is polygenic, and it is mostly induced by malfunctions in energy homeostasis due to specific congenital or hereditary defects. The recent rapid increase in obesity occurrence is thought to be a result of the unbalance in energy homeostasis: when energy storage exceeds energy expenditure, accumulated fat leads to weight gain and eventually results into obesity (246-248). The commonly cited

factors include the large quantities of calorie-rich food that are readily accessible in modern society; eating habits adapted to fast-paced lifestyles; low levels of physical activity; and genetic programs that have evolved, especially in populations prone to famine, to favor the storage of excess calories (244).

As a result of metabolic overload, obesity, along with insulin resistance, hyperglycemia, dyslipidemia, hypertension, and atherosclerosis developing together make up the metabolic syndrome (249, 250). Obesity has been identified as a major causative factor for the insulin resistance and hyperglycemia associated with type 2 diabetes (251). A growing body of evidence has also suggested the links of overweight and obesity to a range of other serious diseases from heart disease to cancer (3, 252). The high rates of obesity occurrence have led to dramatic increases in the obesity-associated diseases. For instance, the increasing prevalence of type 2 diabetes in the United States has doubled and closely paralleled the rising rate of obesity that has been observed over the past decade (5).

Diabetes mellitus type 2 or type 2 diabetes is a clinical disorder that is characterized with hyperglycemia in the context of insulin resistance and relative insulin deficiency. According to the reports of WHO, the global incidence of diabetes is surmounting 180 million, and type 2 diabetes comprises 90% of the people with diabetes around the world (253). Furthermore, this huge number will be doubled to 350 million cases by the year 2030 (254).

As blood sugar levels remain persistently high over time, diabetes in the long run can induce the damages in the heart, blood vessels, eyes, kidneys, and nerves (253). The associated clinical complications consist of retinopathy, nephropathy, neuropathy and cardiovascular disease development, which increase the patient's morbidity and mortality. The overall risk of dying among patients with diabetes is at least double the risk of their peers without diabetes (253). Besides the severe health compromising effects, type 2 diabetes and its complications impose significant economic consequences on individuals, families, health systems and countries. Over the next 30 years, the expenditure attributed to diabetes is estimated to reach $132 billion in United States alone (5, 245).

Obesity, type 2 diabetes and other metabolic syndrome diseases are strongly associated with insulin resistance, which is a pathophysiological state exhibiting combined inability of muscle and adipose tissue to facilitate glucose uptake and of the liver to suppress glucose output in response to increasing amounts of insulin. The high incidence of obesity, type 2 diabetes and the seriousness of their clinic consequences make it imperative to understand the molecular basis of insulin signaling and insulin resistance.

2.5.2. Molecular Mechanism of Insulin Resistance

Insulin resistance is defined as the failure of nominal levels of insulin to trigger its downstream metabolic actions, and it is a hallmark characteristic for the development of type 2 diabetes, obesity, and other metabolic syndromes (255). Various studies have proved that insulin resistance is tightly correlated to the impairment of insulin signaling

resulting from negative modulation on downstream effector activities (256). It is also becoming clear that obesity promotes a chronic inflammation state and eventually develops insulin resistance, which is due to changes in functions of adipocytes and macrophages (7).

Control over insulin signaling can be accomplished by autoregulation (feedback controls from downstream signaling effectors) or signals from other paralleled signaling pathways. IR and IRS are the primary targets for those control mechanisms. Many insulin resistance inducers are observed to activate IRS kinases that negatively regulate IRS mediated insulin action. The activation of these IRS kinases induces the serine/threonine phosphorylation of the IRS, resulting in the dissociation of IR:IRS and IRS:PI3K complex, eventually block the insulin action (152, 204, 257). During the studies searching the candidate IRS kinases, several unrelated signaling pathways are found to contribute to the development of insulin resistance. Desensitization of insulin signaling can be elicited by two major cascades in response to inflammatory signals. One is JNK (c-Jun N-terminal kinase 1) mediated pathway, another is mediated by IKKβ (IκB kinase β) (258). In response to tumor necrosis factor-α (TNF-α), JNK phosphorylates IRS-1 at a serine residue (Ser^{307} in rodents; Ser^{312} in humans). These residues are generally adjacent to the PTB domain (259, 260). Therefore, serine phosphorylation impedes the tyrosine phosphorylation of IRS-1, impairing the following insulin signals (259, 261). Support for this conclusion is derived from studies with JNK-deficient animal models; decreased adipocity and significantly improved insulin response were observed in these animals (262). On the contrary, in both genetic and dietary-induced obese animal models, an

41

increased JNK activity was detected in the liver, muscle, and adipose tissue (262). More interestingly, JNK activation in pancreatic β cells rendered transcriptional inhibition in pivotal genes, including insulin gene (263). This negative modulating effect was mainly caused by a phosphorylation of both IRS-1 and IRS-2 (263).

Similar to JNK, IKKβ is a Ser/Thr protein kinase. It, however, works at a slightly different manner. There are two possible mechanisms for IKKβ to affect insulin signaling. As a part of the IKK complex, IKKβ phosphorylats the inhibitor of NF-κB (nuclear factor-κB), IκB, resulting in the degradation of IκB, hence activating NF-κB (264) that stimulates the synthesis of pro-inflammatory molecules such as TNF-α and interleukin-6 (IL-6), (265, 266). In genetic obese model ob/ob mice, heterozygous deletion of IKKβ prevented the development of insulin resistance during the high fat diet (258, 267). Similar results were also derived from studies in mice with selectively IKKβ – deficiency in myeloid cells (268). Conversely, over-expression of IKKβ in cultured 3T3-L1 adipocytes was observed to attenuate insulin signaling, whereas its inhibition reversed insulin resistance (258). These findings support that IKKβ exerts its effects both in globally and locally and has a central role in the induction of insulin resistance. Besides the effects through IκB, IKKβ also have been observed to interact with IRS-1 through phosphorylation at the serine residue. Nakmori et al. demonstrated the formation IRS-1–IKKβ complex, which was assisted by NEMO (nuclear factor κB essential modulator) and motor protein Myo1c promoted the TNF-α–induced Ser^{307} phosphorylation of IRS-1, resulting in the attenuation of insulin signaling and glucose transport (269).

Impaired insulin signaling transduction can be also triggered by activation of PKCθ, which is induced by the content of long-chain fatty acyl-CoA. The upregulated activity of PKCθ leads to a decrease of IR tyrosine phosphorylation and reduced insulin sensitivity (270, 271); whereas the PKCθ deletion enhanced insulin sensitivity in high fat diet fed mice (272). It is most likely that PKCθ plays essential roles in the fatty-acid induced insulin resistance. At the molecular level, PKCθ can also work as the activator of JNK and IKKβ and indirectly inactivate IRS (272, 273).

2.5.3. Adipose Tissue and Insulin Resistance

In classical perception, adipose tissue is considered as an energy-storing depot. Nevertheless, work over the past several years has fundamentally replaced our understanding of the physiological functions of adipose tissue. Besides storing free fatty acids after food intake, adipose tissue serves as a key endocrine and secretory organ, releasing non-esterified fatty acids (NEFAs), glycerol, hormones (e.g. leptin, adiponectin, resistin, endothelin-1, retinol binding protein 4 (RBP4)), and proinflammatory cytokines (e.g. TNF-α, IL-6, IL-1β) (7, 255). With the intensive investigation, more and more adipokines have been discovered and indentified in this rapidly expanding family, including chemerin, omentin, and vaspin (274). These bioactive molecules play a pivotal role in lipid and glucose metabolism in both normal and disease situations (8). As adipocity increases in obesity, the ability of adipocytes to function as endocrine cells is altered. The term "adipocyte dysfunction" is denoted for this state of hypersecretion of pro-atherogenic, pro-inflammatory, and pro-diabetic bioactive molecules (e.g. TNF-α, IL-6, resistin, and RBP4) accompanied with hyposecretion of anti-atherogenic, anti-

inflammatory, and anti-diabetic adipocytokines (i.e. adiponectin, chemerin, omentin and vaspin) (7, 255, 274, 275). The abnormal secretion profile ensues to a pathological state, i.e. insulin resistance. Below is a summary for several of the most studied adipokines associated with insulin resistance.

High circulating free fatty acids (FFAs) has been identified as a key mediator for insulin resistance in skeletal muscle and adipose tissue. This conclusion is supported by studies where elevated FFAs in circulation caused peripheral insulin insensitivity in both animals and humans (276, 277), as well as studies where pharmacologically lowering of FFAs enhanced insulin-stimulated glucose uptake in the periphery (278). They also affect downstream targets of the insulin receptor such as PI3-K activity in the skeletal muscle (115) or insulin signaling regulator PKCθ as discussed above.

Inflammatory cytokines, TNF-α, and interleukin-6 (IL-6), are the most widely studied cytokines, playing essential roles in the development of insulin resistance. In humans, adipose tissue TNF-α expression was shown to be correlated with BMI, percentage of body fat, and hyperinsulinemia, whereas weight loss decreased TNF-α level (279). In addition, targeted null mutation in the TNF-α and TNF-α receptors resulted in significantly improved insulin sensitivity in both diet-induced obese and ob/ob mice models (280). These results indicate that TNF-alpha is an important mediator of insulin resistance in obesity through its effects on several important sites of insulin action. Similarly, increased circulating IL-6 levels were observed in obese and insulin resistant subjects (281, 282). However, there are conflicting data regarding the role of IL-6 in insulin resistance. IL-6 was reported to impair insulin response by reducing insulin-

44

dependent hepatic glycogen synthesis (283, 284) and glucose uptake in adipocytes (285), whereas enhance insulin signaling in myotubes by increasing insulin-dependent glucose uptake and glycogen synthesis, concomitant with lipid oxidation (286). Nevertheless, both TNF-α and IL-6 are capable of activating the inflammation pathways JNK and IKKβ pathways and demolishing insulin signaling (285).

Unlike most other adipokines, plasma adiponectin levels were reduced in animal models of obesity and insulin resistance (287, 288), while the administration of adiponectin to obese and insulin resistant mice improves insulin sensitivity (289-291). The anti-diabetic metabolic effects of adiponectin are dependent on two distinct receptors termed adiponectin receptor 1 (AdipoR1) and adiponectin receptor 2 (AdipoR2) (292), and the expression of both receptors was also decreased in mouse models with insulin resistance (293, 294). Studies with transgenic or disrupted expression of AdipoR1 or AdipoR2 indicated that adiponectin exerted a potent insulin-sensitizing effect through binding to its receptors AdipoR1 and AdipoR2, leading to activation of AMPK, peroxisome proliferator-activated receptor α (PPARα), and presumably other yet-unknown signaling pathways (294-297) .

CHAPTER 3. CALCIUM-INDEPENDENT PHOSPHOLIPASE A$_2$ IS INVOLVED IN INSULIN-STIMULATED GLUCOSE UPTAKE IN 3T3-L1 ADIPOCYTES

3.1. ABSTRACT

Calcium-independent phospholipase A$_2$ (iPLA$_2$) is a type of hydrolase that catalyzes the release of free fatty acid from the sn-2 position of glycerophospholipids. Recent studies have shown that iPLA$_2$ expression is upregulated during the differentiation of 3T3-L1 fibroblast into adipocytes, and that its activity is required for hormone-stimulated differentiation of 3T3-L1 adipocytes. The purpose of the present study was to determine the role of iPLA$_2$ in insulin-stimulated glucose uptake in 3T3-L1 adipocytes.

Bromoenol lactone (BEL), a selective inhibitor of iPLA$_2$ was utilized to treat 3T3-L1 adipocytes. In pretreated adipocytes, insulin-stimulated glucose uptake was determined by measuring intracellular incorporation of [^{3}H]-2-deoxyglucose. With 10 and 50 μM BEL treatment, insulin-stimulated glucose uptake was decreased by 30% and 45%, respectively, compared to vehicle-treated cells. BEL is also reported to inhibit Mg^{2+}-dependent phosphatidate phosphohydrolase-1 (PAP-1). Propranolol, the specific inhibitor of PAP-1, failed to inhibit insulin-stimulated glucose uptake in 3T3-L1 adipocytes, ruling out the involvement of PAP-1 in this process. Additionally, methyl

46

arachidonyl fluorophosphonate (MAFP), a non-specific inhibitor for PLA$_2$, exhibited similar inhibitory effects as BEL on insulin-stimulated glucose uptake in 3T3-L1 adipocytes, indicating that the BEL inhibitory effects resulted from iPLA$_2$ inhibition. Furthermore, BEL treatment also dramatically impaired the insulin-stimulated glucose uptake in L6-GLUT4 myotubes.

To evaluate the effects of iPLA$_2$ inhibition on insulin signaling, insulin-stimulated phosphorylation of insulin receptor (IR) and Akt was assessed by western blot analysis, and GLUT4 translocation was analyzed by subcellular fraction analysis in BEL-pretreated cells. There was no significant difference between BEL-treated and vehicle-treated cells in the phosphorylation levels of IR and Akt response to insulin. However, there was a reduced level of insulin-responsive GLUT4 incorporated in plasma membrane and lipid raft fractions of BEL-treated cells versus vehicle-treated controls.

These results demonstrate that insulin-stimulated glucose uptake is decreased by BEL-induced iPLA$_2$ inhibition, and that this effect is mediated via decreased incorporation of GLUT4 into plasma membrane, without affecting insulin signaling up to Akt phosphorylation.

3.2. INTRODUCTION

Phospholipase A$_2$ is a diverse group of acyl-hydrolases that catalyze the cleavage of the sn-2 fatty acyl bond of glycerophospholipids, resulting in the liberation of free fatty acid and lysophospholipids. Both products of this reaction are precursors for signaling molecules, which are particularly important for various physiological processes

47

(9). Based on the activity dependence on calcium ion as well as sequence homology, mammalian PLA_2s are categorized into five principle types, namely the secreted PLA_2s ($sPLA_2$), the cytosolic Ca^{2+}-dependent PLA_2s ($cPLA_2$s), the platelet-activating factor (PAF) acetylhydrolases, the lysosome PLA_2s, and the cytosolic Ca^{2+}-independent PLA_2s ($iPLA_2$) (9).

Compared to other types of PLA_2s, $iPLA_2$s are unique in that they do not require Ca^{2+} for their enzymatic activity (298). It is generally accepted that the $iPLA_2$s have multiple biological functions in homeostatic phospholipid (PL) remodeling, cell growth, eicosanoid metabolism, apoptosis, gene expression, chemotaxis, and calcium entry (11). In addition, accumulating evidence indicates that these special enzymes also play roles in signal transduction. The inhibition of $iPLA_2$ with the inhibitor BEL suppresses diverse signaling pathways, such as parathyroid-induced generation of AA in rat proximal tubules (299), superoxide generation in neutrophiles (300, 301), stimulated production of inducible nitric oxide synthase (iNOS) protein and nitric oxide in cardiac myocytes (302), and glucose induced insulin secretion in β-pancreatic cells (303).

Recently, it was reported that when 3T3-L1 cells differentiate into adipocytes, $iPLA_2\beta$ ($iPLA_2$-GVIA) and $iPLA_2\gamma$ gene expression was dramatically upregulated ($iPLA_2$-GVIB) (15). In addition, Su and coworkers have demonstrated that the gene knockdown of $iPLA_2\beta$ and $iPLA_2\gamma$ inhibits hormone-induced adipocyte differentiation by preventing PPARγ and C/EBPα expression. Also, the protein levels of $iPLA_2\beta$ and $iPLA_2\gamma$ were both found significantly increased in white adipose tissue of genetically

obese *fa/fa* Zucker rats, compared to the lean controls (15). All these findings have underlined the significance of iPLA$_2$ in adipocyte metabolism.

In addition to be a place for fatty acid storage, adipocytes serve as important secretory cells and release various bioactive adipokines, which are essential for whole body homeostasis (7, 255). The pivotal role of adipose tissue is fulfilled through the high responsiveness of adipocytes to insulin. Previous studies have confirmed that insulin action enhance the activity of PLA$_2$ in adipocytes (304). However, the potential role of adipocytes iPLA$_2$ in insulin signaling is still unclear. The goal of this study was to elucidate the role of iPLA$_2$ in adipocytes response to insulin treatment.

3.3. MATERIALS AND METHODS

3.3.1. Materials

3T3-L1 cells were purchased from ATCC (Manassas, VA). Fetal calf serum (FCS), fetal bovine serum (FBS), glutamine, penicillin streptomycin and Dulbecco's modified Eagle's medium (DMEM) were obtained from Invitrogen, Inc. (Carlsbad, CA). Phosphate-buffered saline (PBS) was purchased from Mediatech, Inc. (Manassas, VA). Reagents for RNA extraction, reverse transcription and quantitative polymerase chain reaction (PCR) were obtained from Bio-Rad (Hercules, CA). Oligonucleotide primer pairs were ordered from Integrated DNA Technologies, Inc (Coralville, IA). Radiolabeled 2-deoxyglucose was obtained from Perkin Elmer (Waltham, MA). BEL, (S) or (R)-BEL, MAFP were purchased from Cayman (Ann Arbor, MI). Anti-GLUT4 antibody, anti-phospho-Akt (Thr[308]) antibody, and anti-Akt antibody were obtained from

Cell signaling (Boston, MA). Anti-insulin receptor antibody (C-19) was obtained from Santa Cruz Biotechonology, Inc. (Santa Cruz, CA), and anti-phosphotyrosine antibody was obtained from Upstate (Millipore, Billerica, MA). Anti-flotillin-1 antibody and anti-caveolin-1 were obtained from BD Biosciences (San Jose, CA). Anti-β-actin antibody was purchased from Sigma (St. Louis, MO). Horseradish peroxidase linked anti-rabbit and anti-mouse IgG and western blotting detection reagents were obtained from GE Healthcare (Piscataway, NJ). All other chemicals were obtained from Sigma except those as indicated.

3.3.2. Cell Culture of 3T3-L1 Fibroblasts and Adipocytes

3T3-L1 fibroblasts were grown in DMEM containing 4.5 g/L D-glucose, 10% FCS, 1% L-glutamine, and 1% penicillin streptomycin at 37 °C and 5% CO_2. The medium was changed every other day until 100% confluent. Two days after confluence (Day 0), cell differentiation into adipocytes was introduced by changing the medium to DMEM containing 5% D-glucose, 10% FBS, 1% L-glutamine, 1% penicillin streptomycin, 4 µg/ml insulin, 0.5 mM 3-isobutyl-1-methylxanthine (IBMX), and 0.25 mM dexamethasone. Subsequent medium changes contained 4 µg/mL insulin and occurred every three days until the cells were fully differentiated and harvested for succeeding experiments. Prior to use, cells were washed three times in sterile PBS buffer and serum-starved in serum free DMEM with 0.1% bovine serum albumin (BSA) (Fisher, Waltham, MA) for 2 hours.

3.3.3. Reverse Transcription and Quantitative PCR

Following the protocol provided by the manufacturer of RNA extraction kit from Qiagen (Valencia, CA), total RNA was extracted from 3T3-L1 fibroblasts (Day 0), preadipocytes (Day 2,4, and 6) and adipocytes (Day 8), and the RNA concentration and purity were assayed by determining the absorbency of the RNA sample at 260 nm and 280 nm using DV® 530 Life Science UV/Vis spectrophotometer (Beckman, Fullerton, CA).Complementary DNA (cDNA) was synthesized from 1μg of the total RNA of each sample according to the manufacturer's protocol using an iScript^{TM} cDNA Synthesis Kit (Bio-Rad). The cDNA synthesis was initiated by incubating the reaction mixture in 25°C for 5 minutes, extended by 42°C incubation for 30 minutes and then inactivated by 85°C incubation for 5 minutes.

Quantitative real-time reverse transcriptase polymerase chain reaction (RT-PCR) was performed for 40 PCR cycles by utilizing iQ^{TM} SYBR$^®$ Green Supermix (Bio-Rad). Mouse gene specific primers were designed from Primer Bank (http://pga.mgh.harvard.edu/primerbank/citation.html), and constructed by Integrated DNA Technologies, Inc. (IDT, Inc., Coralville, IA). Oligonucleotide primer sequences are listed as Table 2. Relative quantification of target gene expression was assayed using the comparative threshold (C_T) and computed by the $2^{-\Delta\Delta C_T}$ method described by the manufacturer (Bio-Rad). Changes in messenger RNA (mRNA) levels of specific genes were calculated according to the reference gene, 36B4.

3.3.4. Insulin-Stimulated Glucose Uptake Assay

3T3-L1 adipocytes at 8-10 days after differentiation initiation were used for insulin-stimulated glucose uptake assay. The steps followed the protocol previously described (305). Briefly, serum-starved adipocytes were washed and incubated for 15 minutes in Kreb's Ringer phosphate HEPES (KRPH) buffer (136 mM NaCl, 20 mM HEPES, 5 mM sodium phosphate buffer, 4.7 mM KCl, 1 mM $MgSO_4$, 1mM $CaCl_2$, pH 7.4) and then incubated with or without insulin (100 nM) for 30 minutes. Glucose uptake was initiated by adding [^{3}H]-2-deoxyglucose (2-DOG) to a final assay concentration for 10 minutes and stopped by washing the cells three times with ice-cold PBS buffer. Air-dried cells were then solublized in 0.2 N NaOH solution. The intracellular incorporation of [^{3}H]-2-deoxyglucose was measured by counting the radioactivity in half of the cell lysate with Packard liquid scintillation analyzer (Meriden, CT). The rest of the lysate was subjected for protein concentration determination by using BCA protein assay kit (Bio-Rad) with BSA as standard. The level of non-specific glucose uptake was determined in cells pretreated with cytochalasin B before insulin stimulation. For each group of cells, the glucose uptake values were denoted as "pmol radioactive 2-deoxyglucose taken up per minute and per mg protein", and the amount of [^{3}H]-2-deoxyglucose taken up was calculated according to the formula:

$$\frac{(\text{Observed cpm} - \text{cytochalasin B cpm}) \times 2/\text{total cpm} \times 25}{10 \times \text{mg protein per mL}}$$

Glucose uptake assay in GLUT4^{myc} L6 cells (kindly provided by Dr. Suresh Mathews, Auburn University) were performed in the same manner with slight

modifications that the insulin incubation was performed at 37ºC but not at room temperature.

For the assay associated with chemical inhibitor treatment, 3T3-L1 adipocytes were incubated with chemical inhibitors: BEL (10 or 50 μM), (S)-BEL (50 μM), (R)-BEL (50 μM), propranolol (150 μM), or MAFP (50 μM), respectively, or dimethyl sulfoxide (DMSO) vehicle for 30 minutes prior to the addition of insulin.

3.3.5. Preparation of protein samples from 3T3-L1 cells

The cell monolayer, with or without insulin or BEL treatments, was washed with ice-cold PBS buffer and scraped into ice cold lysis buffer (20mM Tris, 150 mM NaCl, 1mM EDTA, 1% Triton X-100) with protease inhibitor cocktail (1 tablet per 10 ml, Roche Applied Science). The cell lysate was homogenized on ice for 20 seconds for three times utilizing 60 Sonic Dismembrator (Fisher). The cell homogenate was spun at 10,000 g at 4 °C for 5 minutes to remove the insoluble material. Sample protein concentrations were assessed using Bio-Rad Protein Assay Reagent. The whole cell lysates were either subjected to immunoprecipitation or sodium dodecyl sulfate-polyacrylamide gel (SDS-PAGE) separation directly, or stored at -80 °C for future use.

3.3.6. Immunoprecipitation and Western Blotting

For immunoprecipitation with IRβ, 1 mL whole-cell lysates were precleared by addition of 100 μL protein A agrose beads (Invitrogen). Then 50 μL precleared protein sample was incubated and rotated with 4 μg anti- IRβ subunit antibody overnight at 4°C.

The resulted immune complexes were precipitated by rotation with 100 µL protein A agrose beads for 2 hours at 4°C. After pulse micro centrifugation, the pellets were washed three times in ice-old PBS buffer, and ready for subsequent protein electrophoresis.

Whole cell lysates or immunoprecipitates mixed with sample loading buffer (5% SDS, 5% 2-mercaptoethanol, 62.7 mM Tris-HCl, pH 6.8, 10% glycerol, 0.003% bromphenol blue) were boiled at 95°C for 5 minutes, separated in 10% SDS-PAGE gels, and then transferred to a nitrocellulose membrane (Amersham Biosciences) by the wet or semi-dry transfer method using transfer buffer (25 mM Tris, 192 mM Glycine, 20% Methanol).

Membranes were blocked in either 5% non-fat dry milk (NFDM) or 5% BSA (Fisher Scientific, Fairlawn, NJ) in Tris Buffered Saline (TBS) with Triton X 100 (TBS-T buffer, 10 mM Tris pH 7.4, 100 mM NaCl, 0.1% Tween-20). The blocked membranes were incubated with specific primary antibodies (diluted to 1:1000 in TBS-T containing 5% NFDM) as indicated, and then corresponding secondary antibodies (diluted to 1:2000 in TBS-T containing 5% NFDM). The membrane was developed using an enhanced chemiluminescent substrate for 5 minutes. The blots were imaged and analyzed using the UVP Bioimaging System and LabWorks software package (UVP, Upland, CA).

3.3.7. Fractionation Analysis of the Subcellular Distribution of GLUT4

The procedure for subcellular fractionation analysis of GLUT4 was described previously by Elmendorf (306). A schematic graph of this fractionation procedure is showed in Figure 2. All steps were performed on ice or at 4°C in a cold room. 3T3-L1

adipocytes at 10 days after withdrawal from differentiation medium, with or without specific treatments as indicated, were washed and scraped into HEPES-EDTA-sucrose (HES) buffer (20 mM HEPES, 1 mM EDTA, 255 mM sucrose, pH 7.4) containing protease inhibitors. The homogenate was prepared by passing the cell solution through a 22-gauge needle for 10 times on ice. After homogenization, the cell lysates were centrifuged at 19,000 g in a fixed-angle rotor (JA20 rotor, Beckman) for 20 minutes. The supernatant was subjected to another centrifugation for 20 minutes at 41,000 g to yield the high density microsome (HDM) fraction pellet. The resulting supernatant was removed and centrifuged at 180,000 g for 75 minutes to pellet the low density microsome (LDM) fraction. For plasma membrane (PM) fraction separation, the pellet resulted from the first 19,000 g centrifugation was suspended and washed in HES buffer by centrifugation at 19,000 g for 20 minutes, then resuspended in 5 mL of HES buffer, and layered onto a 6.3 mL sucrose cushion (38.5% sucrose, 20 mM HEPES, 1 mM EDTA, pH 7.4), followed by a centrifugation for 60 minutes at 100,000 g with a swing-out rotor (SW41, Beckman). The PM fraction was collected from the white fluffy band on the top of the sucrose cushion, resuspended in HES buffer, and repelleted by centrifugation for 20 minutes at 40,000 g. All pellets were finally suspended in appropriate volumes of HES buffer, and the LDM and PM fractions were subjected to SDS-PAGE and Western blotting for GLUT4 analysis.

3.3.8. Detection of GLUT4 in Lipid Raft Fractions

Lipid raft fractions were separated following the method developed by Macdonald and Pike (307). 3T3-L1 adipocytes, with or without BEL treatment, were treated for 30

minutes in medium containing insulin. Cells were then washed and scraped in base buffer (20mM Tris-Hcl, pH7.8, 250mM sucrose) containing 1mM $CaCl_2$, 1mM $MgCl_2$ and protease inhibitors. The cells were then lysed by passage through a 22 g×3" needle 20 times on ice. After centrifugation at 1,000g for 10 min, 2 ml of the postnuclear supernatants were mixed with equal volume of base buffer containing 50% Optiprep (Axis-Shield, Oslo, Norway), placed to the bottom of 12 ml ultracentrifuge tube (Beckman), and followed with a continuous gradient of 5% to 20% Optiprep in base buffer. Gradients were centrifuged for 90 min at 52,000 g using a SW-Ti55 rotor. Gradients were then fractionated into 12 fractions, and the lipid rafts fractions were verified by the distribution of lipid raft marker proteins, as well as protein and cholesterol concentrations. GLUT4 protein level was assessed in combined lipid raft factions 1-2, 3-4 and non-raft fractions 11-12 from cells with different treatment by western blotting analysis.
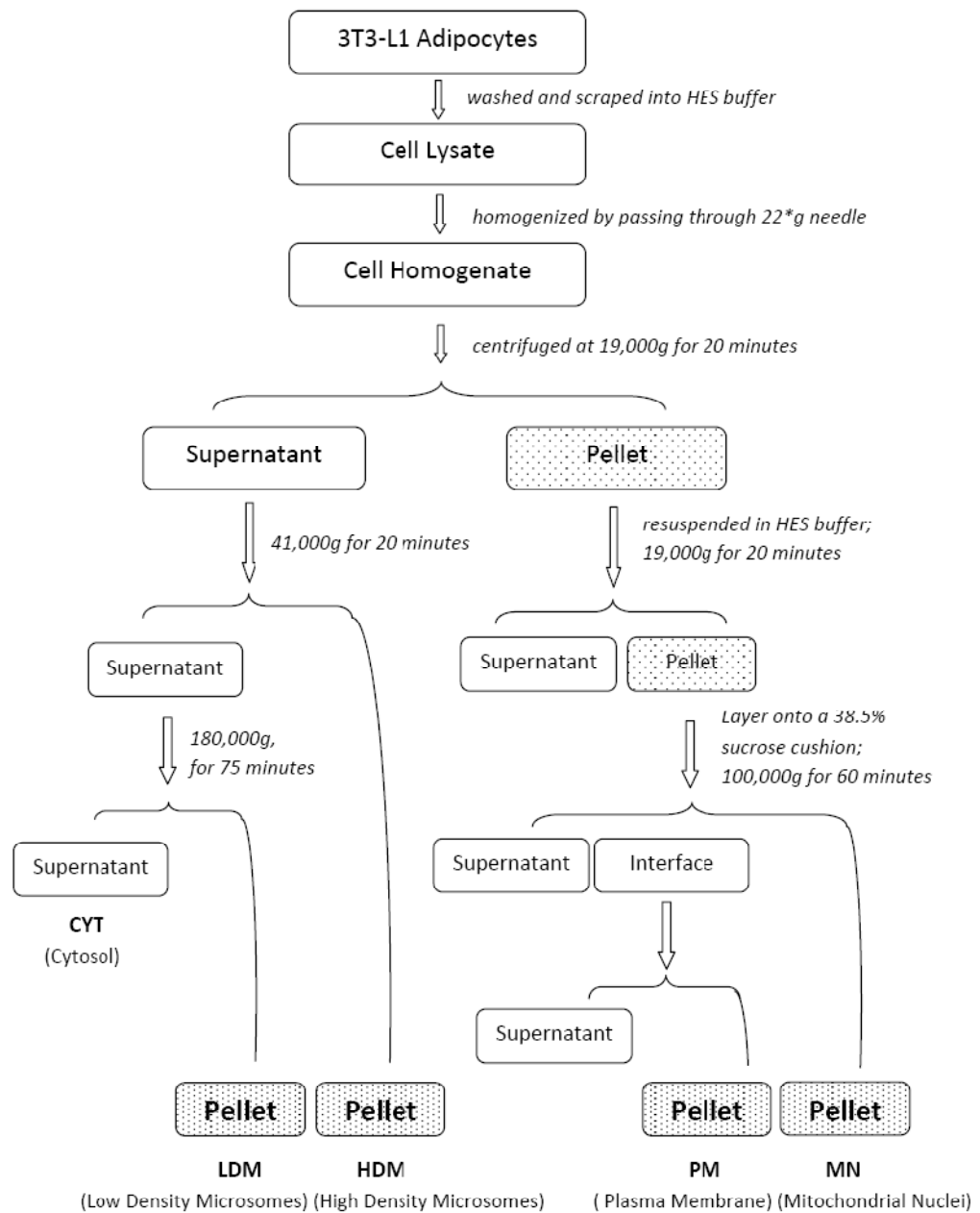
Figure 2. Procedure for preparation of subcellular fractionations. The figure has been modified based on (306).

3.3.9. Statistical Analysis

Data are presented as mean ± S.E. Statistical significance difference between treatments was determined using the Student's *t* tests, and statistical significance level is set as 0.05.

3.4. RESULTS

3.4.1. Gene Expression of iPLA$_2$ Is Increased during 3T3-L1 Adipocyte Differentiation

It has been previously shown that iPLA$_2\beta$ and iPLA$_2\gamma$ are required for the adipogenic program, which differentiates 3T3-L1 fibroblast into adipocytes under hormone stimulation (15). Since the upregulated gene expression of iPLA$_2\beta$ and iPLA$_2\gamma$ predicts their possible importance in 3T3-L1 adipocytes, we sought to confirm the alterations in the mRNA levels of iPLA$_2\beta$ and iPLA$_2\gamma$ during the differentiation of 3T3-L1 cells. In addition, we sought to determine the expression of another intracellular PLA$_2$, cPLA$_2$, which has not been shown to be involved in 3T3-L1 differentiation (15). Total RNA samples were isolated from the cells at day 0, 2, 4, 6, and 8 days post-differentiation and reverse transcribed into cDNA.

The results from quantitative real-time PCR analysis demonstrated that the mRNA levels of iPLA$_2\beta$ and iPLA$_2\gamma$ were both increased dramatically during the differentiation program. At day 8, the amounts of mRNA encoding iPLA$_2\beta$ and iPLA$_2\gamma$ were increased approximately 8 and 7.2 folds respectively (Figure 3). However, mRNA

level of $cPLA_2$ was reduced more than 80% during the differentiation of 3T3-L1 preadipocytes. These results are consistent with a previous study (15), and suggest that in 3T3-L1 adipocytes, $iPLA_2\beta$ and $iPLA_2\gamma$ may be important for specific physiological functions in 3T3-L1 adipocytes.

3.4.2. Insulin-Stimulated Glucose Uptake in 3T3-L1 Adipocytes Is Decreased by BEL-Induced $iPLA_2$ Inhibition

For adipocytes, proper response to insulin is essential to maintain normal cellular functions. To investigate the possible physiological roles of $iPLA_2$ in 3T3-L1 adipocytes, we first initiated a study to determine whether $iPLA_2$ has effects on insulin stimulated cellular glucose uptake. Since the functional significance of intracellular $iPLA_2$ can most easily be investigated using selective inhibitors, we utilized BEL, a chemical inhibitor specific for $iPLA_2$ to block $iPLA_2$ activity in vitro.

Fully differentiated 3T3-L1 adipocytes (day 8-10) were incubated with two different concentrations of BEL (10 μM or 50 μM) for 30 min at 37 °C, and the basal and insulin-stimulated glucose uptake were assessed by measuring intracellular incorporation of [^{3}H]-2-deoxyglucose.

As seen in Figure 4, insulin stimulation significantly increased to almost 14- fold of the basal 2-deoxyglucose uptake in 3T3-L1 cells. Compared to cells incubated in vehicle DMSO alone, 3T3-L1 adipocytes pretreated with BEL exhibit decreased intracellular incorporation of [^{3}H]-2-deoxyglucose under insulin stimulation. At 10 and 50μM BEL, insulin-stimulated glucose uptake was decreased approximately 30 and 50%,

respectively. There was no significant difference in basal glucose uptake with BEL treatment.

Since high concentrations of BEL have been shown to also inhibit the enzyme, Mg^{2+}-dependent phosphatidate phosphohydrolase-1 (PAP-1) (84), glucose uptake assays were performed in the presence of the PAP-1 inhibitor, propranolol (150 μM). There was no apparent difference in insulin-stimulated glucose uptake in propranolol-treated cells versus vehicle controls (Figure 5), excluding the possibility that PAP-1 contributes to the observed inhibitory effects of BEL.

3.4.3. Both iPLA$_2$β and iPLA$_2$γ Contribute to Glucose Uptake in Insulin-Stimulated Adipocytes

Previous research has demonstrated the specificity of the (S) - and (R)- enantiomers for preferentially inhibiting iPLA$_2$β and iPLA$_2$γ, respectively (132). To find out which iPLA2 was involved in the insulin-stimulated glucose uptake, 3T3-L1 adipocytes were pretreated with 50 μM (S) - or (R) - BEL, separately, and the basal and insulin-stimulated glucose uptake was compared to that in cells incubated in vehicle alone. As shown by Figure 6, the measured [^{3}H]-2-deoxyglucose in insulin-stimulated adipocytes was reduced approximately 35% by either (S) - or (R) - BEL. This finding demonstrates that both iPLA$_2$β and iPLA$_2$γ contribute similarly to the insulin-stimulated glucose uptake in 3T3-L1 adipocytes.

To further verify that PLA$_2$ activity was implicated in the insulin-stimulated glucose uptake, we used the PLA$_2$ inhibitor, methyl arachidonyl fluorophosphonate

(MAFP), which is reported as a suicide inhibitor for iPLA$_2$, cPLA$_2$ and AdPLA (10). As expected, MAFP treatment markedly reduced about 30% of the incorporation of [^{3}H]-2-deoxyglucose in insulin-stimulated 3T3-L1 adipocytes (Figure 6). Compared to BEL treatment, MAFP administration did not exhibit strong effects in insulin stimulated glucose, which may suggest that other PLA$_2$s like cPLA$_2$ and AdPLA are not included in this process. Together with the results above, it is suggested that the inhibitory effects of BEL on insulin-stimulated glucose uptake we observed in 3T3-L1 adipocytes are induced by inhibition of iPLA$_2$ activity, implicating a role for iPLA$_2$ in insulin-stimulated glucose uptake.

3.4.4. Exogenous Arachidonic Acid Reverses the BEL-Inhibitory Effect in Insulin-Stimulated Glucose Uptake

Arachidonic acid (AA) is one of the products of phospholipid hydrolysis catalyzed by iPLA$_2$, which has been implicated in mediating some of the physiological effects of iPLA$_2$. Recent studies have also established the relationship between AA treatment and adipocyte glucose uptake (308, 309). To determine whether BEL-suppressed arachidonic acid (AA) liberation was involved in insulin-stimulated glucose uptake, BEL-pretreated adipocytes were incubated with medium containing AA (10 or 100 μM) for 30 min, and subjected to insulin-stimulated glucose uptake assay. As demonstrated in Figure 7, 10 μM AA treatment did not exhibit significant effects on insulin-stimulated glucose uptake in BEL-pretreated cells, however, addition of 100 μM exogenous AA increased approximately 30% of insulin-stimulated uptake in BEL-pretreated adipocytes, and restored the inhibitory effect of BEL treatment. Previous

studies have shown that long-term AA administration influences the glucose uptake in both resting and insulin-stimulated adipocytes (309, 310). With this in mind, we further tested the effects of AA incubation on adipocytes not treated with BEL. There was a dose-dependent increase in both basal and insulin-stimulated glucose uptake induced by AA incubation, however, the increase was not statistically significant (Figure 8). Taken together, these results indicate that iPLA$_2$-stimulated release of AA is at least partially contributing to the insulin-stimulated glucose transport in 3T3-L1 adipocytes.

3.4.5. Insulin-Stimulated Glucose Uptake in L6-GLUT4 Myotubes Is Decreased by BEL-Induced iPLA$_2$ Inhibition

Analogous to adipocytes, skeletal muscle cells are sensitive to insulin and perform glucose uptake through the rapid translocation of GLUT4 glucose transporters to the plasma membrane. We also tested the effects of BEL treatment in insulin-stimulated glucose uptake in L6-GLUT4^{myc} myotubes. BEL administration dramatically reduced the glucose uptake in insulin-activated L6 cells. In cells treated with 10 µM BEL, the glucose uptake upon insulin administration was inhibited about 45% compared to the vehicle control (Figure 9). However, there was a nearly 30% reduction in basal glucose uptake observed in these cells, indicating that BEL influences myotubes in a way partially different from that in adipocytes. The results also showed that high concentration of BEL (50 µM) inhibited approximately 80% of basal glucose uptake and 90% of insulin-stimulated glucose uptake in L6-GLUT4^{myc} myotubes.

3.4.6. Inhibition of iPLA$_2$ by BEL Does Not Impair Insulin-Stimulated Phosphorylation of IR and Akt

One possible mechanism by which BEL treatment inhibited insulin-stimulated glucose uptake is through alteration in insulin signaling pathways. In 3T3-L1 adipocytes, insulin-stimulated phosphorylation of receptor (IR) and Akt are important for the initiation and transduction of insulin signaling (194). Therefore, we assessed the activity of IR and Akt by measuring their phosphorylation levels. Western blot analysis showed that insulin treatment increased the amount of phosphorylated-IR and phosphorylated-Akt dramatically, however, there was no significant difference in the phosphorylation levels of IR and Akt between BEL-treated and vehicle-treated cells (Figure 10 and Figure 11). These results indicate that the insulin signaling up to forehead of Akt is not affected by BEL treatment in 3T3-L1 adipocytes.

3.4.7. Inhibition of iPLA$_2$ by BEL Impacts the Insulin-Stimulated GLUT4 Translocation in 3T3-L1 adipocytes

In response to insulin, GLUT4 translocates to plasma membrane from the intracellular storage compartments, leading to the increased glucose transport into adipocytes (147). Since BEL treatment decreased the insulin-stimulated glucose transport in adipocytes, we next examined the effects of BEL treatment on the cellular localization of GLUT4. 3T3-L1 adipocytes with or without BEL (50 μM) treatment were stimulated by insulin and then subjected to subcellular fractionation. The GLUT4 levels in plasma membrane (PM) and low density microsome (LDM) fractions were assessed by western

blotting. In the absence of insulin, LDM showed the majority of GLUT4, while PM fraction contained a low level of background GLUT4. Upon insulin stimulation, an approximately 1.5-fold increase in the protein level of GLUT4 was observed in PM fraction. In contrast, in BEL-treated cells, there was a nearly 30% decrease in plasma membrane incorporated GLUT4 versus vehicle-treated cells (Figure 12).

3.4.8. Inhibition of iPLA$_2$ by BEL Alters GLUT4 Incorporation in Lipid Rafts

Lipid rafts are specialized compartments of the plasma membrane enriched in cholesterol and glycerolsphingolipids. Various studies have established the associations between GLUT4 and caveolae (substructure of lipid rafts), and suggested that lipid rafts are required for efficient localization of GLUT4 into plasma membrane (PM). Previously, we detected some effects of BEL on lipid raft structures and distributions of raft protein markers (data not shown). For this reason, we next examined whether these effects of BEL impact GLUT4 incorporation in lipid rafts. With or without BEL pretreatment, we subjected basal and insulin-stimulated 3T3-L1 adipocytes to non-detergent homogenization and gradient fractionation as described by Pike (307). As shown in Figure 13, throughout the generated 12 fractions, the first four fractions (Fraction1-4) were enriched in lipid raft marker proteins caveolin-1 and flotillin-1, which were identified as lipid raft (LR) fraction, whereas the non-raft (NR) protein β-actin was localized in the bottom fractions (Fraction 8-12). For GLUT4 incorporation detection, we combined LR and NR fractions according to the description above. Western blot analysis with anti-GLUT4 antibody showed an increase in GLUT4 protein presence in the LR fractions was observed under the insulin stimulation, however, the presence of GLUT4

was noticeably reduced in LR fractions when adipocytes were pretreated by BEL (Figure 11). With 10 μM BEL treatment, the GLUT4 protein in the first combined LR fraction (original fractions 1 and 2) was significantly attenuated; with 50 μM BEL treatment, levels of GLUT4 in both of the LR factions were both reduced to background level. Along with the distribution change in GLUT4 proteins, the localization of lipid raft marker protein caveolin-1 and flotillin-1 was also altered by BEL treatment. For both caveolin-1 and flotillin-1, BEL treatment introduced the shift of the proteins from the first (original fractions 1 and 2) to the second combined LR fractions (original fractions 3 and 4), as well as a reduction in the total protein levels in LR fractions (Figure 14). These findings imply that the BEL treatment impacts interactions of GLUT4 with lipid raft domains in plasma membrane.

3.5. DISCUSSION

Recently, numerous studies have indicated the essential roles of $iPLA_2$ in whole body metabolism, including adipocyte differentiation (15), insulin secretion (16-21, 23), glucose homeostasis (22, 23), hepatic adipogenesis (24, 25), and cardiac myocytes mitochondrial functioning (26, 27). These data have linked $iPLA_2$ to obesity, type 2 diabetes, fatty liver disease and other manifestations of the metabolic syndrome. However, the prospective significance of $iPLA_2$ in whole body homeostasis remains a puzzle. Su et.al (15) originally reported that $iPLA_2$ exhibited much higher gene expression compared to the background expression level of $cPLA_2$. With this in mind, we have hypothesized that $iPLA_2$ plays important roles in adipocyte biology. Propagating signals from insulin, as it relates to energy metabolism, is one of the major functions of

adipocytes. The objective of this study was to investigate the possible functions of $iPLA_2$ in insulin action within the adipocytes.

Using the selective inhibitor for $iPLA_2$, BEL, we established the involvement of $iPLA_2$ in insulin-stimulated glucose uptake in fully differentiated 3T3-L1 adipocytes. Our results also indicate the comparable contribution of $iPLA_2\beta$ and $iPLA_2\gamma$ in this process. Earlier studies have already described the "insulin-like" effects of phospholipase on glucose and amino acid uptake in adipocytes (311, 312), and previous studies have also shown that insulin enhances the phospholipase A_2 activities in adipocyte membranes resulting in global enrichment of lyso deviates and membrane fatty acids (304). The major types of phospholipase A_2 responsive to those events were not specified in these studies. However, our results suggest that $iPLA_2$ could represent the most prospective candidate. Among the PLA_2 family, $cPLA_2$ performs a Ca^{2+} dependent translocation into cellular membrane (13); $iPLA_2$ β, although originally purified from the cytosolic source, can be preferentially distributed in membrane fractions (313, 314); and $iPLA_2\gamma$ is reported to be a membrane-associated protein (54). Recently, a novel member of PLA_2, AdPLA, was identified in adipocytes, and found to be ubiquitously localized in both membrane and cytoplasmic compartments (10). In this study, we utilized another PLA_2 inhibitor, MAFP, parallel to BEL. In contrast to $iPLA_2$, $cPLA_2$ and AdPLA are efficiently inhibited by MAFP, but not BEL. Our results show that MAFP treatment does not exhibit extra effects on the insulin-induced glucose uptake compared to BEL, which may rules out the participation of $cPLA_2$s and AdPLA in this process.

As one of the primary products of reactions catalyzed by iPLA$_2$, AA has been reported to influence glucose uptake in adipocytes. In 2001, Nugent and coworkers demonstrated that exposure of fully differentiated 3T3-L1 adipocytes to 0.8 mM AA significantly enhanced the insulin-stimulated glucose uptake, and the maximum effects occurred at 4 hours post treatment when membrane phospholipid content of AA was markedly increased (309). In the present study, we observed similar but not significant trend of AA effects on the insulin-stimulated glucose uptake in 3T3-L1 cells with a lower concentration (100 μM) and shorter exposure time (30 minute). Most importantly, we found that the addition of exogenous AA successfully restored the reduced glucose uptake resulting from iPLA$_2$ inhibition by BEL, indicating that the AA, released through iPLA$_2$ enzymatic activity, is highly involved in insulin action on adipocyte glucose uptake. It is intriguing that another product of phospholipid hydrolysis, lysophospholipids, and its metabolites are also involved in adipocytes glucose transport. Two recent studies, performed by Yea and colleagues (315, 316) reported that lysophosphatidic acid (LPA) and lysophosphatidyl-serine (LPS) promoted glucose uptake in both L6 GLUT4^{myc} myotubes and 3T3-L1 adipocytes in a dose- and time-dependent manner. These studies provide supplementary evidence for the roles of iPLA$_2$ activity in glucose regulation. Furthermore, similar inhibitory effects of BEL were detected in L6-GLUT4^{myc} myotubes, which provides additional support for the conclusion that iPLA$_2$ is partially mediating insulin-stimulated glucose uptake.

To further evaluate the mechanism that iPLA$_2$ impacts adipocyte glucose transport under insulin stimulation, we attempted to dissect the molecular events

underlying the inhibitory effects of BEL. It is well known that insulin-stimulated glucose uptake in adipose tissue is mediated by the translocation of insulin-sensitive GLUT4 from intracellular storage vesicles to the plasma membrane. We further investigated the GLUT4 translocation in BEL-treated adipocytes to elucidate the mechanism by which BEL decreases the insulin-stimulated uptake. Our studies showed that BEL reduced the presence of GLUT4 in the PM fraction. Therefore, these results potentiate the relationship between iPLA$_2$ activity and GLUT4 translocation.

Additionally, specific membrane microdomains, known as lipid rafts, serve as sites for assembly of signaling complexes that play an important role in insulin action, especially the Cbl/CAP cascade (317). The insulin-responsive presence of GLUT4 in lipid rafts has been verified by previous studies (317). Our results also suggest similar findings: upon insulin stimulation, GLUT4 protein presence increases in the lipid raft fractions of 3T3-L1 adipocyte, and BEL treatment prevents the incorporation of GLUT4 in lipid rafts. It is also noteworthy that the distributions of caveolin-1 and flotillin-1 are also altered by BEL treatment. Previous studies have showed that caveolin and flotillin are colocalized in distinct subdomains of the plasma membrane, and that insulin induces the translocation of Cbl to these caveolin- and flotillin-enriched compartments through its interaction with CAP (168). Together with results provided in this study, BEL treatment could affect the GLUT4 translocation via the possible influence on the Cbl/CAP pathway.

To initiate the insulin-responsive GLUT4 translocation, insulin-activated phosphorylation cascade of the downstream components is imperative. Control over insulin signaling can be achieved by regulating the phosphorylation levels of several key

68

molecules, such as IR, IRS, PI3K and Akt (191). In the current study, we tried to determine whether the Akt kinase pathway, a pathway essential for glucose transport responsive to insulin stimulation, is affected by BEL-induced iPLA$_2$ inhibition in 3T3-L1 adipocytes. Interestingly, the immunoblotting showed that BEL pre-incubation did not influence the insulin-responsive phosphorylation of IR and Akt in 3T3-L1 adipocytes. Therefore, these results suggest that inhibition of iPLA$_2$ does not affect insulin-initiated signal transduction pathway leading to Akt kinase activation and works on the later stages of insulin action on glucose uptake.

Collectively, these findings in the present study demonstrate that iPLA$_2$, at least partially, mediating the insulin-stimulated glucose uptake in 3T3-L1 adipocytes. It is involved in the GLUT4 translocation without affecting Akt kinase pathway upon insulin stimulation. This novel function of iPLA$_2$ in 3T3-L1 adipocytes makes it a promising target for strategies for prevention and treatment of obesity, type 2 diabetes and other linked metabolic diseases.

Table 3. Oligonucleotide Primer Sequences for RT-PCR

Gene	Sequence
$iPLA_2\beta$	Fwd 5'-GCC TCG TCA ACA CCC TCA G -3'
	Rev 5'-CCT TCA CCC GGA ATG GGT TC -3'
$iPLA_2\gamma$	Fwd 5'-AGC CTT TTC CAT TAC ACA TAC GG-3'
	Rev 5'-CCT GGA GAA CTG GAT TTC CTT TC -3'
$cPLA_2$	Fwd 5'-CAG CAC ATT ATA GTG GAA CAC CA -3'
	Rev 5'- AGT GTC CAG CAT ATC GCC AAA-3'
36B4	Fwd 5'-AGA TTC GGG ATA TGC TGT TGG C-3'
	Rev 5'-TCG GGT CCT AGA CCA GTG TTC -3'
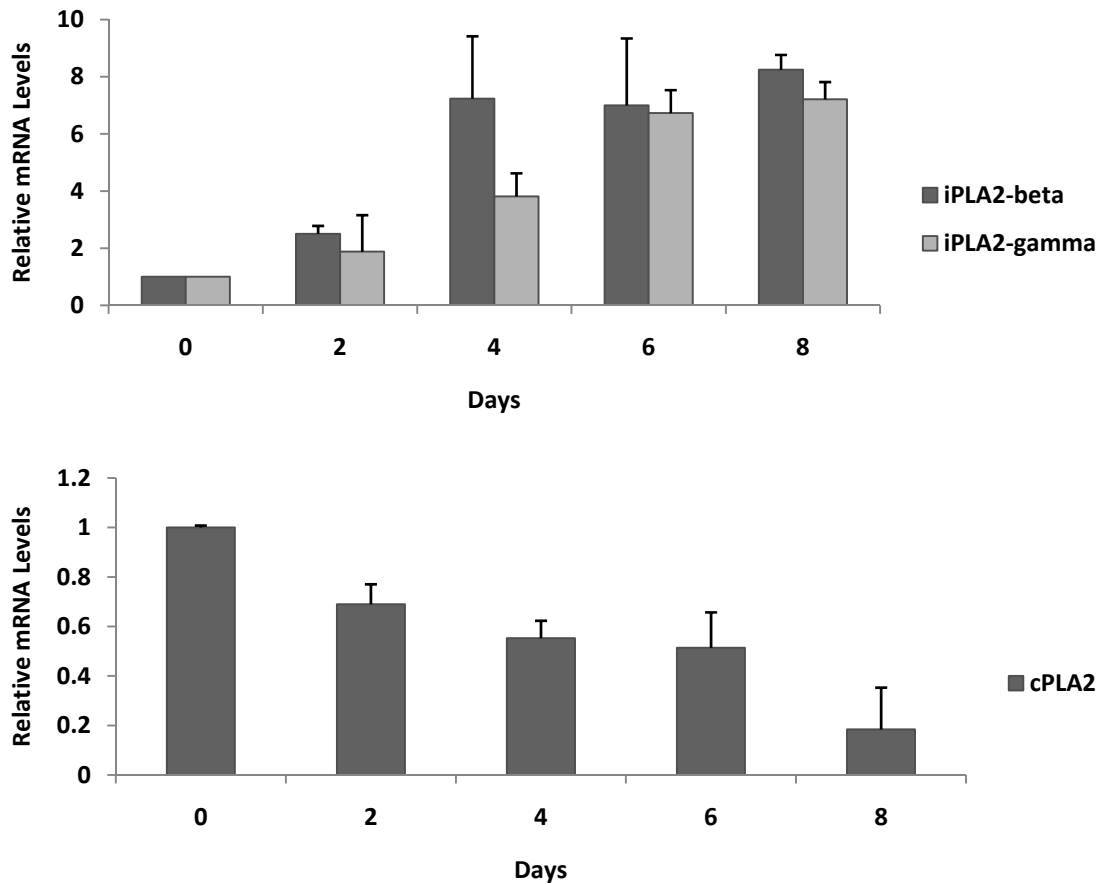
Figure 3. mRNA Levels of iPLA$_2$β, iPLA$_2$γ and cPLA$_2$ in 3T3-L1 cells during hormone-stimulated differentiation. 3T3-L1 fibroblasts were cultured and subjected to hormone-induced differentiation. During this process, total RNA was collected at day 0, 2, 4, 6, and 8 after the initiation of differentiation. Total RNA (1 μg) was then reverse transcribed to cDNA, followed by RT-PCR analysis. The mRNA levels of iPLA$_2$β, iPLA$_2$γ and cPLA$_2$ were determined using 36B4 as the internal reference gene. The relative mRNA levels are computed using the mRNA levels at day 0 as internal standard, and the fold changes are represented as mean ± S.E. of three independent experiment.

71
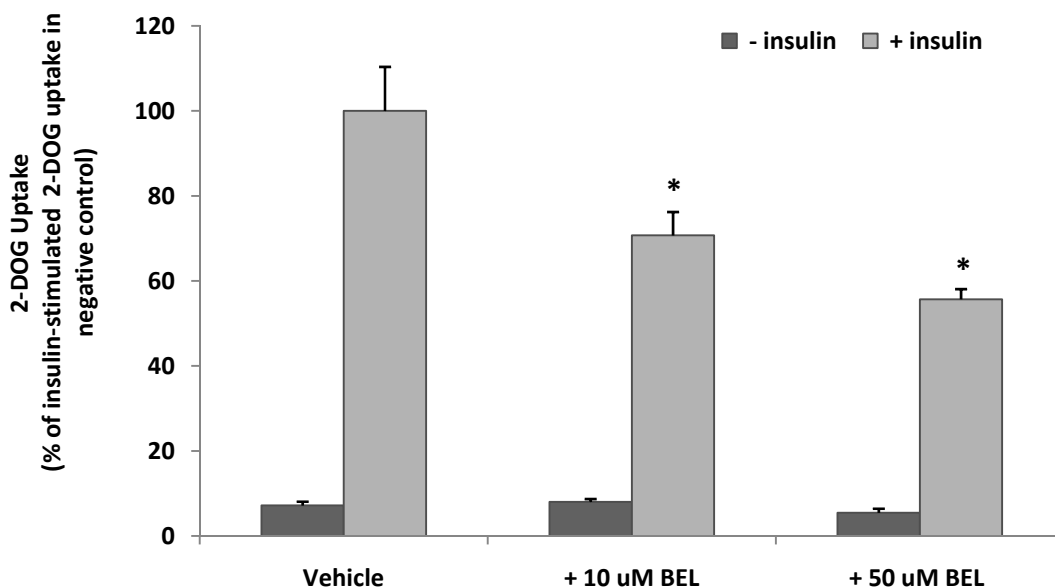
Figure 4. Effects of BEL on insulin-stimulated glucose uptake in 3T3-L1 adipocytes.
Day 8-10 3T3-L1 adipocytes in multiple-well plates were serum starved for 2 hours, and
then pretreated for 30 minutes with two concentrations of BEL (10 or 50 μM) or vehicle
DMSO, separately. Cells were then untreated (dark grey, left) or stimulated with 100 nM
insulin (light grey, right) for 30 minutes and assayed for [^{3}H]-2-DOG uptake over 10
minutes in the presence of 10 or 50 μM BEL or vehicle. Data are mean ± S.E. from three
or more independent experiments performed in triplicate, normalized to insulin-
stimulated uptake in vehicle treated adipocytes. Statistical significance of treatments on
basal or insulin-stimulated 2-DOG uptake was determined by comparing the means of
basal or insulin-stimulated 2-DOG uptake of cells treated with BEL (10 or 50 μM) to that
from the vehicle controls using 2-sample student's *t* test (*, *p*<0.05).

Figure 5. Insulin-stimulated glucose uptake in 3T3-L1 adipocytes treated with propranolol. Day 8-10 3T3-L1 adipocytes in multiple-well plates were serum starved for 2 hours, and then pretreated for 30 minutes with 150 µM propranolol or vehicle DMSO, separately. Cells were then untreated (dark grey, left) or stimulated with 100 nM insulin (light grey, right) for 30 minutes and assayed for [³H]-2-DOG uptake over 10 minutes in the presence of 150 µM propranolol or vehicle. Data are mean ± S.E. from three or more independent experiments performed in triplicate, normalized to insulin-stimulated uptake in vehicle treated adipocytes. Statistical significance of treatments on basal or insulin-stimulated 2-DOG uptake was determined by comparing the means of basal or insulin-stimulated 2-DOG uptake of cells treated with propranolol to that from the vehicle controls using 2-sample student's *t* test (*, *p*<0.05).

Figure 6. Effects of PLA$_2$ inhibitors on insulin-stimulated glucose uptake in 3T3-L1 adipocytes. Day 8-10 3T3-L1 adipocytes in multiple-well plates were serum starved for 2 hours, and then pretreated for 30 minutes with vehicle DMSO or three different PLA$_2$ inhibitors, (R)-BEL(50 μM), (S)-BEL (50 μM), and MAFP (50 μM), separately. Cells were then untreated (dark grey, *left*) or stimulated with 100 nM insulin (light grey, *right*) for 30 minutes and assayed for [^{3}H]-2-DOG uptake over 10 minutes in the presence of inhibitors or vehicle. Data are mean ± S.E. from three or more independent experiments performed in triplicate, normalized to insulin-stimulated uptake in vehicle treated adipocytes. Statistical significance of treatments on basal or insulin-stimulated 2-DOG uptake was determined by comparing the means of basal or insulin-stimulated 2-DOG uptake of cells treated with different inhibitors to that from vehicle-treated cells using 2-sample student's *t* test (*, *p*<0.05).
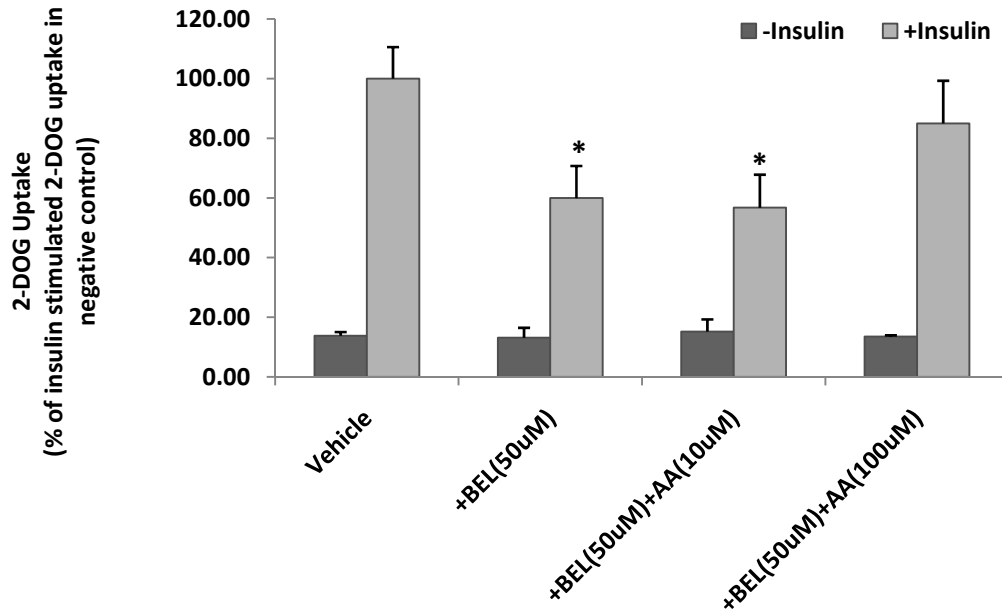
Figure 7. Exogenous arachidonic acid effects on insulin-stimulated glucose uptake in BEL pretreated adipocytes. Day 8-10 3T3-L1 adipocytes in multiple-well plates were serum starved for 2 hours, and then subjected for four different treatment procedures: vehicle control, 30 minutes pretreatment with BEL (50 µM), 30 minutes pretreatment with BEL (50 µM) followed by 30 minutes AA (10 µM) incubation, and 30 minutes pretreatment with BEL (50 µM), 30 minutes pretreatment with BEL (50 µM) followed by 30 minutes AA (100 µM) incubation. Cells were then untreated (dark grey, *left*) or stimulated with 100 nM insulin (light grey, *right*) for 30 minutes and assayed for $[^3H]$-2-DOG uptake over 10 minutes in the presence of BEL and/or AA or vehicle. Data are mean ± S.E. from three or more independent experiments performed in triplicate, normalized to vehicle insulin-stimulated uptake. Statistical significance of treatments on basal or insulin-stimulated 2-DOG uptake was determined by comparing the means of 2-DOG uptake of cells treated with BEL or/and AA with that from vehicle controls using 2-sample student's *t* test (*, $p<0.05$).
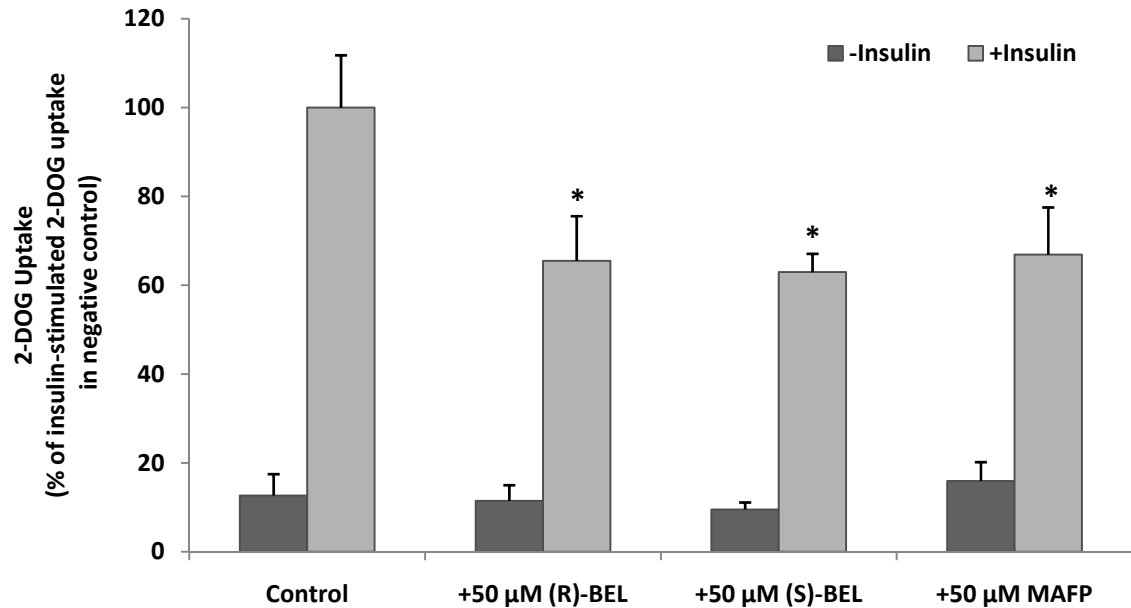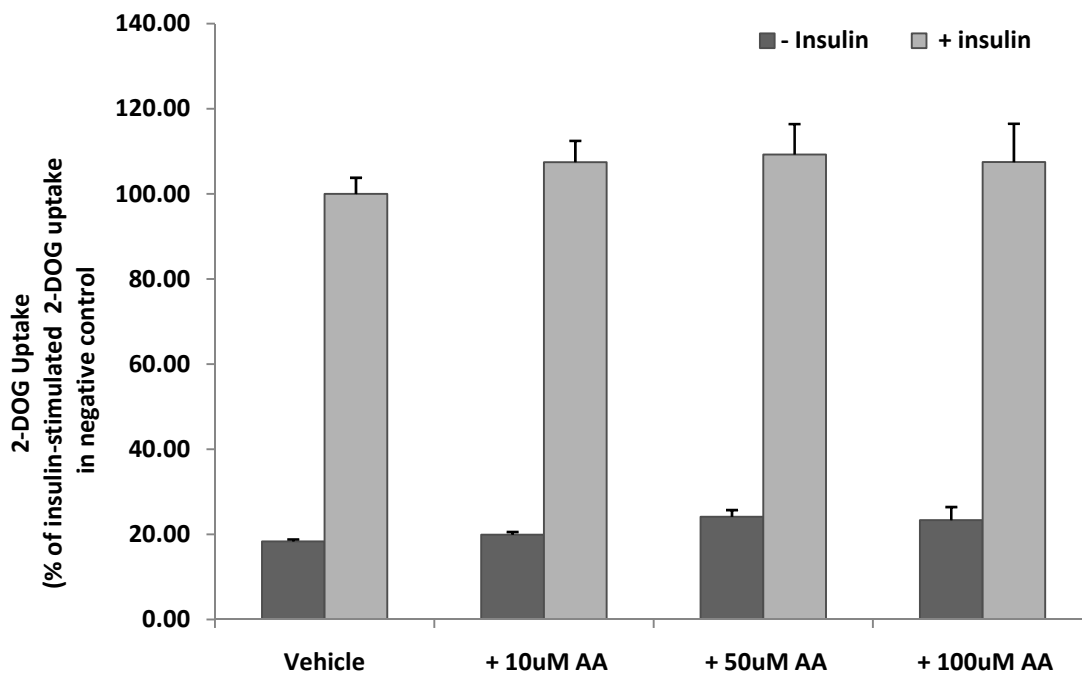
Figure 8. Exogenous arachidonic acid effects on Insulin-stimulated glucose uptake in 3T3-L1 adipocytes. Day 8-10 3T3-L1 adipocytes in multiple-well plates were serum starved for 2 hours, and then incubated with AA (10, 50 or 100 µM) for 30 minutes. Cells were then untreated (dark grey, *left*) or stimulated with 100 nM insulin (light grey, *right*) for 30 minutes and assayed for [³H]-2-DOG uptake over 10 minutes in the presence of AA (10, 50 or 100 µM) or vehicle. Data are mean ± S.E. from three or more independent experiments performed in triplicate, normalized to vehicle insulin-stimulated uptake. Statistical significance of treatments on basal or insulin-stimulated 2-DOG uptake was determined by comparing the means of 2-DOG uptake of cells treated with AA to that from vehicle controls using 2-sample student's *t* test.
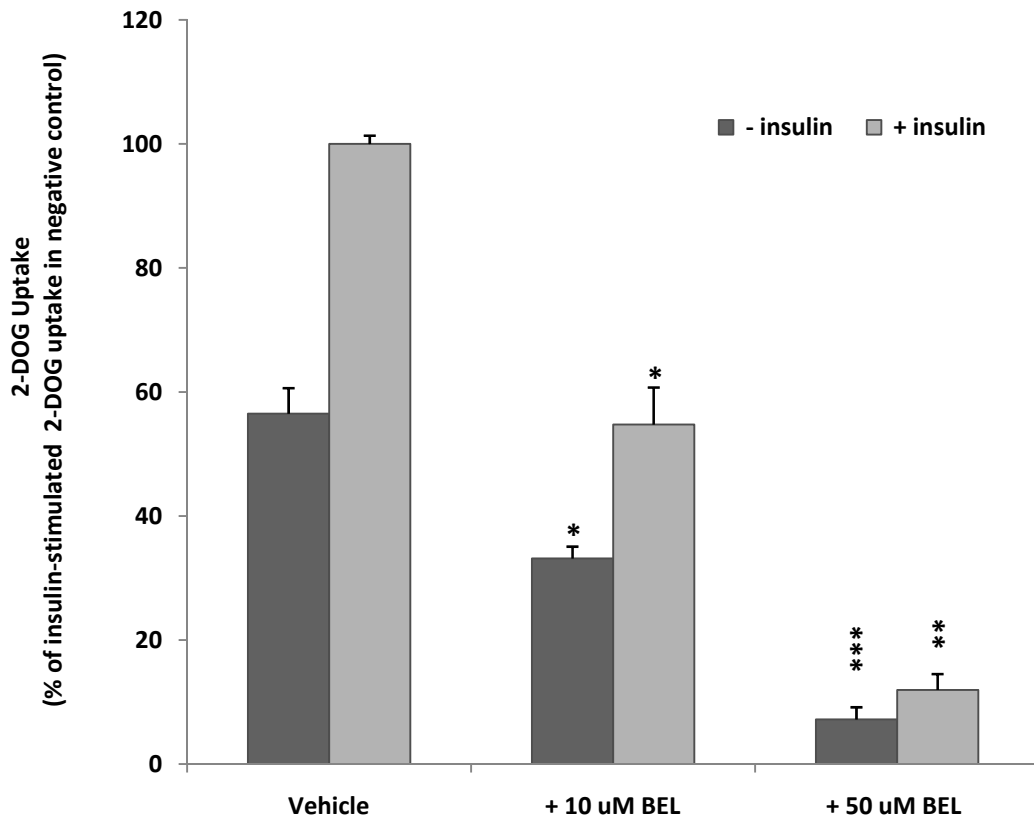
Figure 9. BEL effects on insulin-stimulated glucose uptake in L6-GLUT4 myotubes.
L6-GLUT4^{myc} myotubes were serum starved for overnight, and then incubated with BEL (10 or 50 µM) for 30 minutes or vehicle DMSO, separately. Cells were then untreated (dark grey, *left*) or stimulated with 100 nM insulin (light grey, *right*) for 30 minutes and assayed for [^{3}H]-2-DOG uptake over 10 minutes in the presence of 10 or 50 µM BEL or vehicle. Data are mean ± S.E. from three or more independent experiments performed in triplicate, normalized to insulin-stimulated uptake in vehicle treated adipocytes. Statistical significance of treatments on basal or insulin-stimulated 2-DOG uptake was determined by comparing the means of basal or insulin-stimulated 2-DOG uptake of cells treated with BEL (10 or 50 µM) to that from the vehicle controls using 2-sample student's *t* test (*, *p<0.05*; **, *p<0.01*, ***, *p<0.001*).
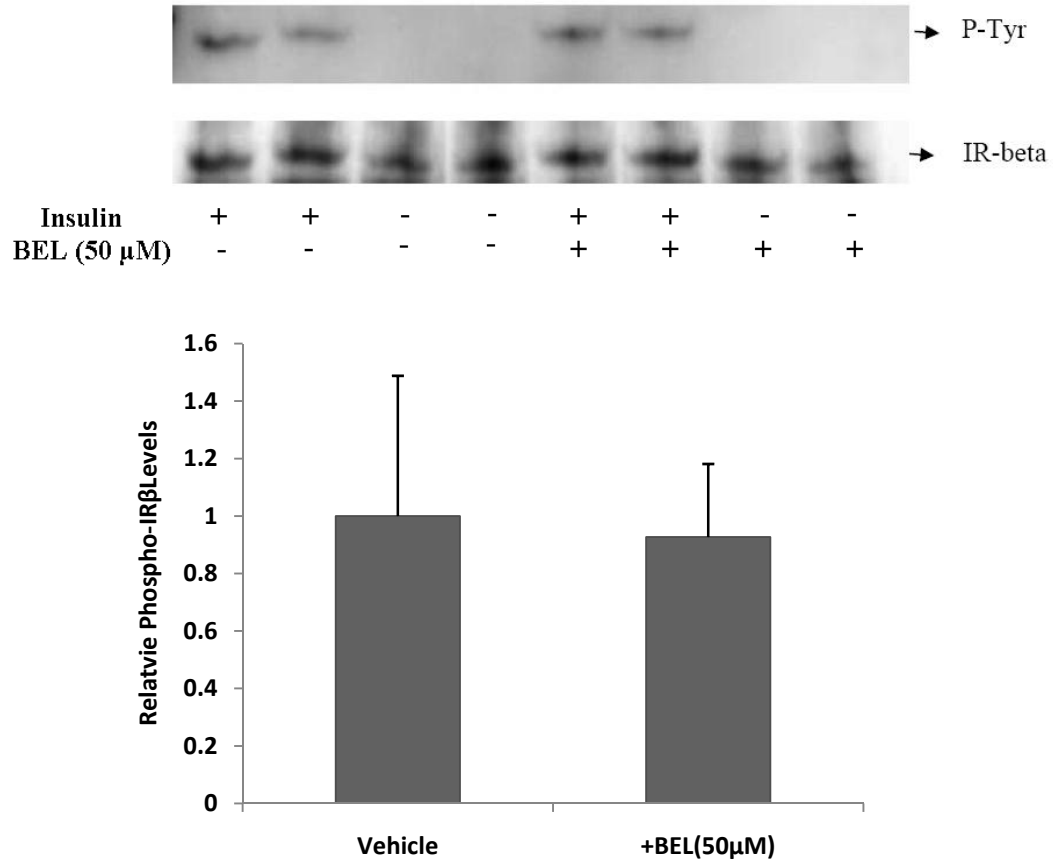
Figure 10. Effects of BEL on insulin-dependent insulin receptor phosphorylation. Day 8-10 3T3-L1 adipocytes in 60 mm dishes were serum starved for 2 hours, and then treated with or without BEL (50 µM) for 30 minutes. After consequent insulin (100 nM) incubation for 30 minutes, insulin-dependent tyrosine phosphorylation of insulin receptor β subunit (IRβ) levels were assessed by immunoprecipitation with anti-IR antibody and immunoblotting with anti-phosphotyrosine antibody. Shown are representative blot (*top*) and densitometry analysis (*bottom*) of independent experiments in which results represent the mean ± S.E. of phospho-tyrosine level relative to total IR level (relative phospho-IRβ level), and relative phospho-IRβ level in controls (+Insulin- BEL) was assigned a value of 1.
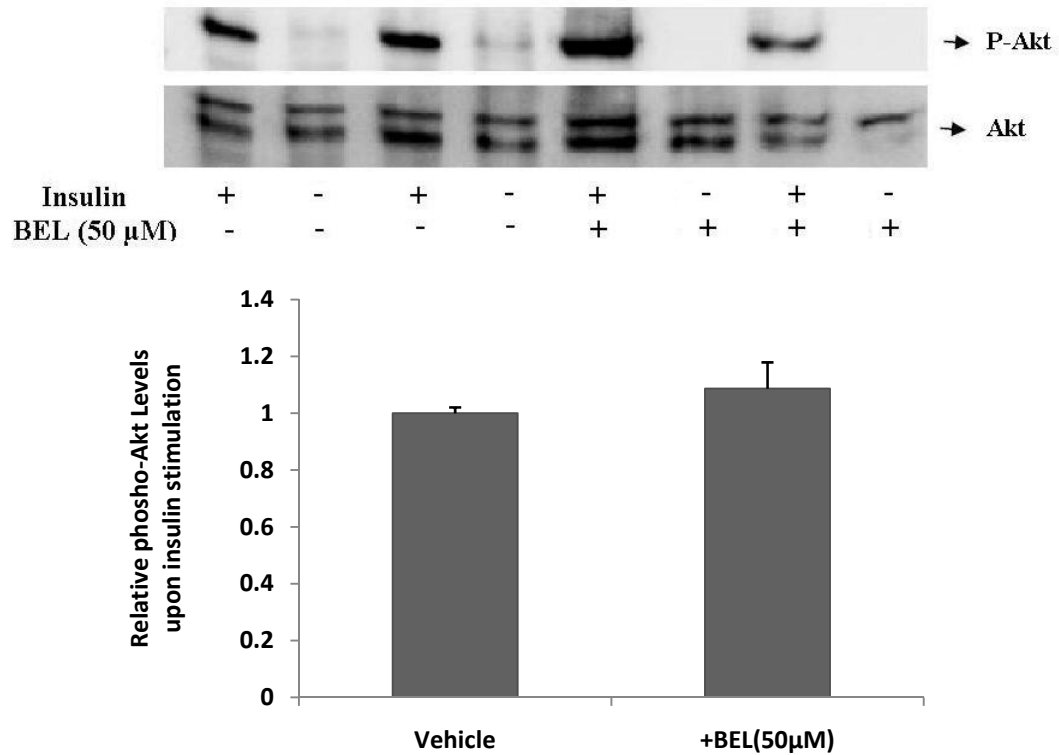
Figure 11. Effects of BEL on insulin-dependent Akt phosphorylation. Day 8-10 3T3-L1 adipocytes in 60 mm dishes were serum starved for 2 hours, and then treated with or without BEL (50 µM) for 30 minutes. After consequent insulin (100 nM) incubation for 30 minutes, insulin-dependent threonine phosphorylation of Akt was assessed by western blot analysis with anti-phospho-Akt antibody and anti-Akt antibody. Shown are representative blot (*top*) and densitometry analysis (*bottom*) of independent experiments in which results represent the mean ± S.E. of phospho-Akt level relative to total Akt level (relative phospho-Akt level), and relative phospho-Akt level in controls (+Insulin - BEL) was assigned a value of 1.
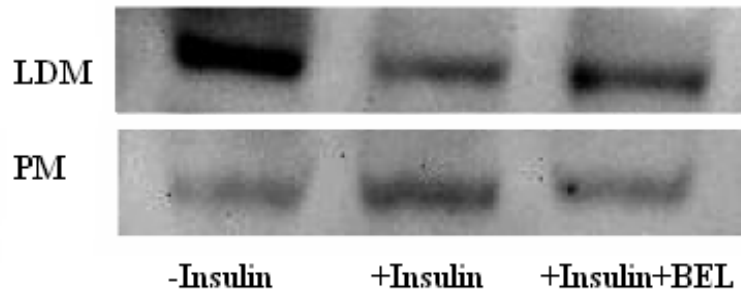
Figure 12. BEL effects on insulin-induced GLUT4 translocation to plasma membrane. Day 8-10 3T3-L1 adipocytes in 100 mm dishes were serum starved for 2 hours, and then treated with or without BEL (50 µM) for 30 minutes. Pretreated cells were stimulated by insulin (100 nM) for 30 minutes, and subcellular membrane fractions were obtained by differential centrifugation procedure. To detected GLUT4 protein levels, equal amount of low-density microsomal protein (LDM) and plasma membrane protein (PM) were separated by SDS-PAGE and assessed by western blot analysis with anti-GLUT4 antibody.
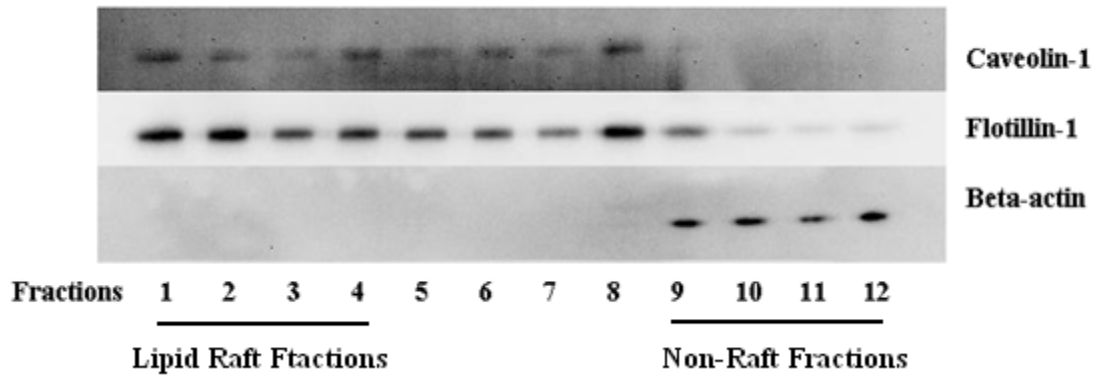
Figure 13. Distribution of proteins between lipid raft and non-raft fractions.
Differentiated 3T3-L1 adipocytes (day 8-10) were harvested and lysed in base buffer on
ice. The cell lysate was mixed with equal volume of base buffer containing 50%
Optiprep, placed to the bottom of 12 ml ultracentrifuge tube, and followed with a
continuous gradient of 5% to 20% Optiprep in base buffer. Gradients were then
fractionated into 12 fractions, and the lipid raft fractions were verified by the distribution
of lipid raft marker proteins, as well as protein and cholesterol concentrations. GLUT4
protein level was assessed in combined lipid raft factions 1-2, 3-4 and non-raft fractions
11-12 from cells with different treatment by western blotting analysis. Equal amount of
proteins were separated by SDS-PAGE gel and western blot analysis. Caveolin-1 and
Flotillin-1 were utilized as lipid raft markers, while β-actin was used as marker for non-
raft proteins.

81
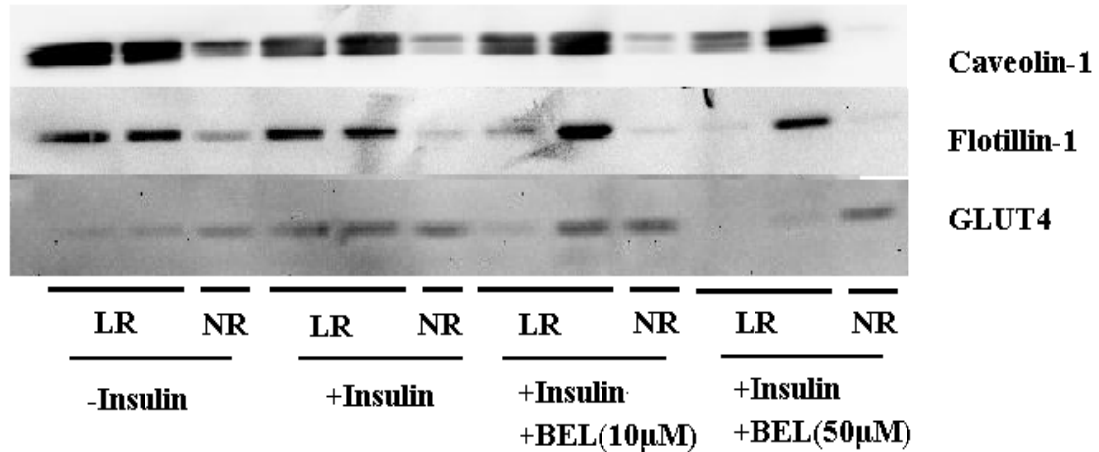
Figure 14. BEL effects on insulin-induced GLUT4 incorporation into lipid rafts. Day 8-10 3T3-L1 adipocytes in 100 mm dishes were serum starved for 2 hours. With or without BEL pretreatment (10 or 50 μM) for 30 minutes, the cells were stimulated by 100 nM insulin for 30 Minutes. The cells were then harvested and fractionated by Optiprep gradients centrifugation. For each treatment, GLUT4 protein level was assessed in combined lipid raft (LR) factions 1-2, 3-4 and non-raft (NR) fractions 11-12 from cells with different treatment by western blotting analysis. Equal amount of proteins were separated by SDS-PAGE gel and western blot analysis. Caveolin-1 and Flotillin-1 were utilized as lipid raft markers, while β-actin was used as marker for non-raft proteins.

CHAPTER 4. SMALL INTERFERING RNA KNOCKDOWN OF CALCIUM-INDEPENDENT PHOSPHOLIPASE A$_2$ INHIBITS INSULIN-STIMULATED GLUCOSE UPTAKE IN 3T3-L1 ADIPOCYTES

4.1. ABSTRACT

In our previous study, in order to determine the involvement of iPLA$_2$ in adipocyte insulin actions on glucose uptake, we used BEL, a selective suicide inhibitor of iPLA$_2$, to inhibit the iPLA$_2$ activity in 3T3-L1 adipocytes. In the present study, we preformed a more selective approach, small interfering RNA to investigate the role of iPLA$_2$ in 3T3-L1 adipocytes. 3T3-L1 adipocytes at day 6 post differentiation were transfected by 50 μM siRNA against iPLA$_2\beta$ or iPLA$_2\gamma$, respectively, by electroporation. Our primary results showed that selective delivery of siRNA efficiently inhibited the gene expression of iPLA$_2\beta$ and iPLA$_2\gamma$ by a ~70% reduction in the mRNA levels of iPLA$_2\gamma$, and a nearly 80% reduction in mRNA levels of iPLA$_2\beta$ in 3T3-L1 adipocytes. Consistent to the gene silencing effects, the glucose uptake under insulin stimulation in adipocytes transfected with siRNA selective to iPLA$_2\beta$ and iPLA$_2\gamma$ was diminished also: the insulin-stimulated glucose uptake was reduced about 40% in 3T3-L1 adipocytes transfected by either iPLA$_2\beta$ or iPLA$_2\gamma$ siRNAs. All these results further enforced the essential role of iPLA$_2$ in insulin-stimulated glucose uptake.

4.2. INTRODUCTION

Calcium-independent phospholipase A_2 (iPLA$_2$) is one of the major types of phospholipase hydrolase family catalyzing the release of free fatty acid from the sn-2 position of membrane glycerophospholipids. In most iPLA$_2$ activity studies, chemical inhibitors facilitate the distinguishing of iPLA$_2$ from other PLA$_2$ types, and they are also widely used to assess the role of iPLA$_2$ in particular cellular processes. BEL is the most prominent chemical inhibitor for iPLA$_2$ since it is the only inhibitor that selectively targets iPLA$_2$ over other calcium-dependent PLA$_2$s, and inhibits all known iPLA$_2$s (84-86). Recently, increasing research groups started to using, targeted gene tools to selective inhibit iPLA$_2$s (28, 84-86).

Small interfering RNA is one of the important gene silencing strategies to decrease the expression and activity of almost any given enzyme (15, 57, 90). SiRNA cuts down the level of mRNA encoding a specific protein via an endogenous cellular mechanism. By combining and degrading the target protein mRNA, this technique ideally leads to a reduction of the protein level and enzymatic activity if applicable. In previous studies, siRNA selectively targets iPLA$_2\beta$ or iPLA$_2\gamma$ were utilized to determine the roles of iPLA$_2$ in numerous biological processes, including adipocytes differentiation (15), glucose- induced insulin secretion (90), gene expression (318), AA release and eicosanoids metabolism (57).

Our previous study has shown that BEL treatment decreased insulin-stimulated glucose uptake and such an effect is mediated via decreased translocation of GLUT4 to

PM. To further confirm the roles of iPLA$_2$, in the present study, we applied siRNA in 3T3-L1 to selectively downregulate the gene expression of iPLA$_2\beta$ and iPLA$_2\gamma$ and examined whether the insulin-stimulated glucose uptake in the 3T3-L1 adipocyte with iPLA$_2\beta$ or iPLA$_2\gamma$ knockdown was affected by gene silencing.

4.3. MATERIALS AND METHODS

4.3.1. Materials

3T3-L1 cells were purchased from ATCC (Manassas, VA). Fetal calf serum (FCS), Fetal bovine serum (FBS), glutamine, penicillin streptomycin and Dulbecco's modified Eagle's medium (DMEM) were obtained from Invitrogen, Inc. (Carlsbad, CA). Phosphate-buffered saline (PBS) was purchased from Mediatech, Inc. (Manassas, VA). Reagents for RNA extraction, reverse transcription and quantitative polymerase chain reaction (PCR) were obtained from Bio-Rad (Hercules, CA). SiRNA oligonucleotides were constructed by Ambion (Austin, TX). CMV-LacZ plasmid and detection kit were kindly provided by Dr. Suresh Mathews (Auburn University). Radiolabeled 2-deoxyglucose was obtained from Perkin Elmer (Waltham, MA). All other chemicals were obtained from Sigma except those as indicated.

4.3.2. Cell Culture of 3T3-L1 Fibroblasts and Adipocytes

3T3-L1 fibroblasts were grown in DMEM containing 5% D-glucose, 10% FCS, 1% L-glutamine, and 1% penicillin streptomycin at 37 °C and 5% CO_2. The medium was changed every other day until 100% confluent. Two days after confluence (Day 0), cell

differentiation into adipocytes was introduced by changing the medium to DMEM containing 5% D-glucose, 10% FBS, 1% L-glutamine, 1% penicillin streptomycin, 4 µg/ml insulin, 0.5 mM 3-isobutyl-1-methylxanthine (IBMX), and 0.25 mM dexamethasone. Subsequent medium changes contained 4 µg/ml insulin and occurred every three days until the cells were fully differentiated and harvested for succeeding experiments. Prior to use, cells were washed three times in sterile PBS buffer and serum-starved in serum free DMEM with 0.1% bovine serum albumin (BSA) (Fisher, Waltham, MA) for 2 hours.

4.3.3. Transfection of 3T3-L1 Adipocytes by Electroporation

The procedure of 3T3-L1 adipocyte electroporation was described previously (319). Four 100 mm dishes of 3T3-L1 adipocytes (at day 5 or 6 postdifferentiation) were trypsinized and resuspended in 12 mL complete medium (DMEM containing 5% D-glucose, 10% FBS, 1% L-glutamine without antibiotics). The cells were then pelleted by centrifugation at 200 g and room temperature for 5 minutes and washed in 40 mL sterile D-PBS for 3 times. The cell pellet was suspended in 1.5-2 mL sterile D-PBS to achieve a final cell concentration approximately at 2×10^7 cells per mL. 0.5 mL cell solution was transferred to an electroporation cuvet, and mixed with specific amount of CMV-Laz plasmid DNA (50 µg) or siRNA (50 nM). The electroporation was performed by Bio-Rad Gene Pulse Xcell at the setting as 0.18 kV, and 950 µF capacitance. Right after electroporation, cells were mixed with 2.5 mL fresh complete medium and incubated for 10 minutes at room temperature, than reseeded to 24- well plates (0.5 mL per well), and incubated at 37 °C and 5% CO_2. The medium were changed to normal growth medium

containing 5% D-glucose, 10% FBS, 1% L-glutamine, and 1% penicillin streptomycin 12 hours after electroporation.

The siRNA directed against iPLA$_2$β and iPLA$_2$γ were constructed employing the Ambion Silencer siRNA construction kit according to the protocol provided by manufacturer. The siRNA sequences were listed in Table 4. The siRNA (50 nM) was delivered into 3T3-L1 adipocytes through electroporation as described above. For all transfection experiments, scramble siRNA were used as negative controls. Fourth-eight hours after transfection, the cells were subjected to post-transfection analyses, including mRNA level analysis by reverse transcription and quantitative PCR, and glucose uptake assay.

4.3.4. Evaluation of Transfection Efficiency

3T3-L1 adipocytes transfected with CMV-LacZ plasmid DNA were subjected to β-galactosidase staining 48 hours post electroporation. β-galactosidase was visualized utilizing the In Situ β-Galactosidase Staining kit (Stratagene, Ceder Creek, TX) according to the procedure provide by manufacturer. Briefly, cells were washed three times in ice-cold PBS followed by fixation using fixing solution for 10 minutes. Next, the cells were stained with 5-bromo-4-chloro-3-indoyl-β-D-galactopyranoside (X-Gal) diluted in staining solution. Cells expressing β-galactosidase appeared blue, which was visualized and captured using a Canon PowerShot S31S-attached Nikon TS100-F inverted microscope.

4.3.5. Reverse Transcription and Quantitative PCR

Following the protocol provided by the manufacturer of RNA extraction kit from Qiagen (Valencia, CA), total RNA was extracted from 3T3-L1 adipocytes transfected by siRNA selectively targeting against iPLA$_2\beta$ or iPLA$_2\gamma$, or scramble siRNA. The RNA concentration and purity were assayed by determining the absorbency of the RNA sample at 260 nm and 280 nm using DV® 530 Life Science UV/Vis spectrophotometer (Beckman, Fullerton, CA).Complementary DNA (cDNA) was synthesized from 1μg of the total RNA of each sample according to the manufacturer's protocol using an iScript^{TM} cDNA Synthesis Kit (Bio-Rad). The cDNA synthesis was initiated by incubating the reaction mixture in 25°C for 5 minutes, extended by 42°C incubation for 30 minutes and then inactivated by 85°C incubation for 5 minutes.

Quantitative real-time reverse transcriptase polymerase chain reaction (RT-PCR) was performed for 40 PCR cycles by utilizing iQ^{TM} SYBR$^®$ Green Supermix (Bio-Rad). Mouse gene specific primers were designed from Primer Bank (http://pga.mgh.harvard.edu/primerbank/citation.html), and constructed by Integrated DNA Technologies, Inc. (IDT, Inc., Coralville, IA). Oligonucleotide primer sequences are listed as Table 2. Relative quantification of target gene expression was assayed using the comparative threshold (C_T) and computed by the $2^{-\Delta\Delta C_T}$ method described by the manufacturer (Bio-Rad). Changes in messenger RNA (mRNA) levels of specific genes were calculated according to the reference gene, 36B4.

4.3.6. Insulin-Stimulated Glucose Uptake Assay

3T3-L1 adipocytes at 48 Hours after siRNA transfection were subjected to insulin-stimulated glucose uptake assay. The steps followed the protocol previously described (305). Briefly, serum-starved adipocytes were washed and incubated for 15 minutes in Kreb's Ringer phosphate HEPES (KRPH) buffer (136 mM NaCl, 20 mM HEPES, 5 mM sodium phosphate buffer, 4.7 mM KCl, 1 mM $MgSO_4$, 1mM $CaCl_2$, pH 7.4) and then incubated with or without insulin (100 nM) for 30 minutes. Glucose uptake was initiated by adding [^{3}H]-2-deoxyglucose (2-DOG) to a final assay concentration for 10 minutes and stopped by washing the cells three times with ice-cold PBS buffer. Air-dried cells were then solublized in 0.2 N NaOH solution. The intracellular incorporation of [^{3}H]-2-deoxyglucose was measured by counting the radioactivity in half of the cell lysate with Packard liquid scintillation analyzer (Meriden, CT). The rest of the lysate was subjected for protein concentration determination by using BCA protein assay kit (Bio-Rad) with BSA as standard. The level of non-specific glucose uptake was determined in cells pretreated with cytochalasin B before insulin stimulation. For each group of cells, the glucose uptake values were denoted as "pmol radioactive 2-deoxyglucose taken up per minute and per mg protein", and the amount of [^{3}H]-2-deoxyglucose taken up was calculated according to the formula:

$$\frac{(\text{Observed cpm} - \text{cytochalasin B cpm}) \times 2/\text{total cpm} \times 25}{10 \times \text{mg protein per mL}}$$

The 3T3-L1 adipocytes transfected by scrambled siRNA were used to be negative controls.

4.3.7. Statistical Analysis

Data are presented as mean ± S.E. Statistical significance difference between treatments was determined using the Student's *t* tests, and statistical significance level is set as 0.05.

4.4. RESULTS AND DISCUSSION

4.4.1. Electroporation Introduces Foreign Plasmids into 3T3-L1 Adipocytes

The introduction of DNA or genes of interest into adipocytes by standard transfection protocols such as calcium phosphate, DEAE-dextran, and liposome-mediated transfection are very inefficient (319). It is also difficult that transgenes can be expressed in adipocytes, and this genetic tool is substantially more burdensome. Furthermore, the production of recombinant adenoviruses to use in infection of insulin-responsive tissues is comparative more time-consuming and requires very high titers of adenovirus. Therefore, it is relatively more efficient, simple, and fast to transfect adipocytes using electroporation (319). Differentiated 3T3-L1 adipocytes were electroporated to deliver the foreign nucleotides. A large number of 3T3-L1 cells were killed during the electroporation procedure, and a lipid-droplet-loss was observed in electroporated cells. However, the living cells successfully attached to the cell culture plates in 3~5 hours after the electroporation.   As showed in Figure 15, there were no noticeable changes in the adipocyte appearance before or after electroporation. To determine the efficiency of electroporation, we transfected 3T3-L1 adipocytes with CMV-LacZ plasmid to express β-Galactosidase, which is an enzyme that catalyzes the hydrolysis of β-galactosides,

including lactose. Transfected cells expressing β-galactosidase can cleave X-Gal to produce a blue stain. The transfection efficiency is determined by counting stained and unstained cells under a microscope and calculating the percentage of stained cells in the total population. Using 50 μg of CMV-LacZ plasmid DNA, we obtained an electroporation efficiency of less than 30% (Figure 16), which is relatively low. According to the original protocol (319), the efficiency is closely correlated with the amount of plasmid used. When 600 μg of CMV-LacZ plasmid DNA was used, the transfected adipocytes displayed 80%-90% efficiency (319). Due to the source limitation, we did not utilize the huge amount of plasmid DNA in this study. However, the 30% transfection efficiency was reasonable considering the small amount of plasmid DNA used in the current study.

4.4.2. SiRNA Reduces the Amount of mRNA Levels of iPLA$_2$β and iPLA$_2$γ in 3T3-L1 Adipocytes

To test whether siRNA can induce gene-selective silencing in 3T3-L1 adipocytes, we tested mRNA and protein levels of iPLA$_2$β and iPLA$_2$γ in transfected 3T3-L1 Adipocytes. Results from RT-PCR showed that both genes were dramatically reduced by siRNA transfection (Figure 17): iPLA$_2$γ mRNA level was attenuated by ≈70%, and the suppressed iPLA$_2$β mRNA level was up to 80%, indicating that siRNA gene silencing technique effectively reduced the gene expression of iPLA$_2$β and iPLA$_2$γ in 3T3-L1 adipocytes.

91

4.4.3. Pretreatment of siRNAs Targeting iPLA$_2\beta$ or iPLA$_2\gamma$ Inhibits Insulin-Stimulated Glucose Uptake in 3T3-L1 Adipocytes

Previous studies show that inhibition of iPLA$_2$ activity utilizing chemical inhibitors significantly decreased the insulin-stimulated glucose uptake in 3T3-L1 adipocytes without affecting the basal glucose uptake levels (Chapter 3). Considering the intense diminution of iPLA$_2\beta$ and iPLA$_2\gamma$ mRNA levels observed in transfected cells, we assessed effect of iPLA2β or iPLA2γ siRNA transfection on the insulin-stimulated glucose uptake in the 3T3-L1 adipocyte. Compared to negative control electroporated with scrambled siRNA, selective attenuation of iPLA$_2\beta$ significantly reduced the insulin-stimulated glucose uptake by approximately 40% (Figure 18). Similar inhibitory effects were observed in adipocytes transfected by iPLA$_2\gamma$ siRNA. This results are consistent with previous studies utilizing (S)-and (R)-BEL (Figure 6 in Chapter 3). Collectively, our results have shown that selective knockdown of iPLA$_2\beta$ and iPLA$_2\gamma$ inhibits insulin-stimulated glucose uptake in 3T3-L1 adipocytes, indicating the important roles of iPLA$_2$ in adipocyte biology. Combined with the results from previous studies using BEL, we conclude that insulin-stimulated glucose uptake is mediated, at least in part, by iPLA$_2$ enzymatic activity, which indicates that iPLA$_2$ may represent a novel therapeutic target for the treatment of insulin resistance and associated diseases.

Table 4. Oligonucleotides siRNA sequences.

Gene		Sequence
iPLA$_2$β-1	Sense	5'- CGC UGC AAC CAA AAC AUU Att-3'
	Antisense	5'- UAA UGU UUU GGU UGC AGC Ggg-3'
iPLA$_2$β-2	Sense	5'- GCC UGG UCA UUA UCC AGC Utt-3'
	Antisense	5'- AGC UGG AUA AUG ACC AGG Cct-3'
iPLA$_2$γ-1	Sense	5'- CAA GAG UGA GUA UUG AUA Att-3'
	Antisense	5'- UUA UCA AUA CUC ACU CUU Gca-3'
iPLA$_2$γ-2	Sense	5'- GGC UGA GAC AAG UUA AGG Att-3'
	Antisense	5'- UCC UUA ACU UGU CUC AGC Cgt-3'
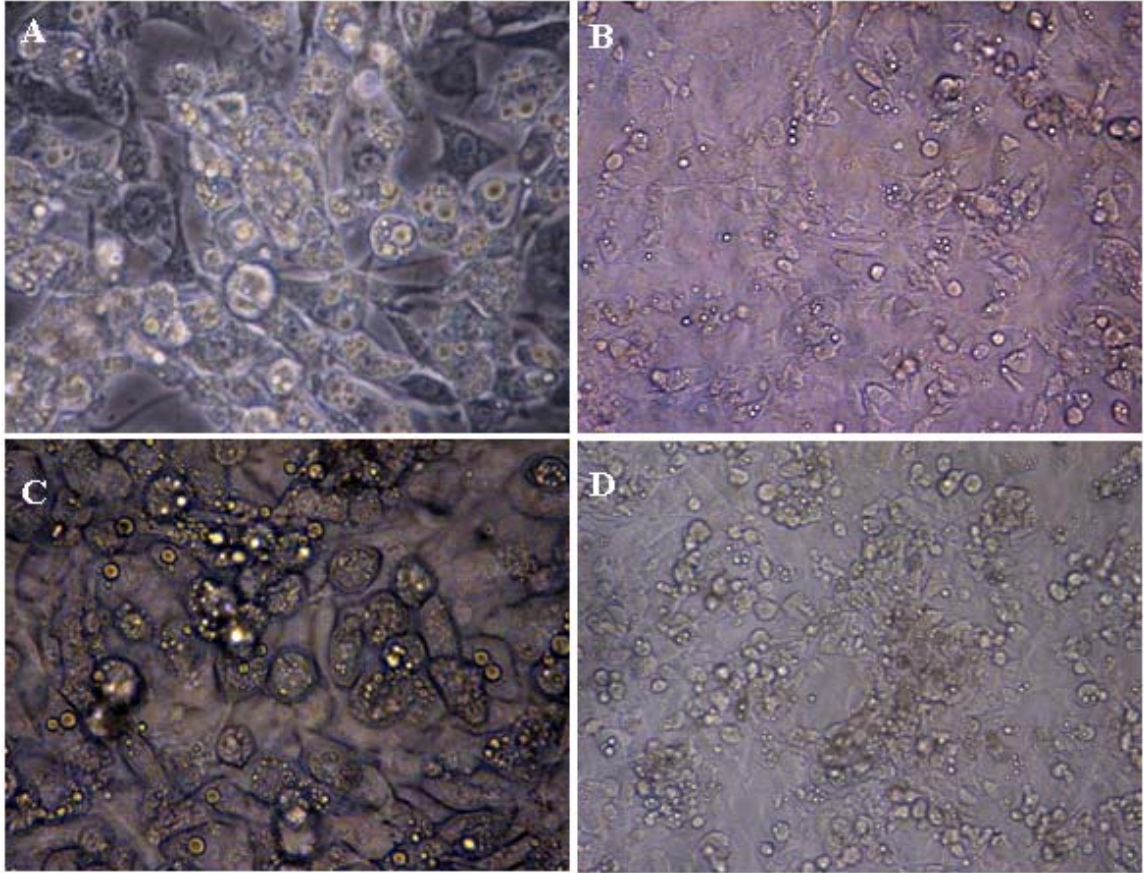
Figure 15. 3T3-L1 adipocytes after electroporation. Day 5 3T3-L1 adipocytes were electroporated with a Bio-Rad gene pulser system at the setting of 0.18kV and 960 µF capacitance. The state of adipocytes after electroporation was compared to those without electroporation. (A) 3T3-L1 adipocytes with electroporation viewed at 400 ×; (B) 3T3-L1 adipocytes with electroporation viewed at 200 × ; (C) 3T3-L1 cells without electroporation viewed at 400 ×; (D) 3T3-L1 cells without electroporation at 200 × under microscope.
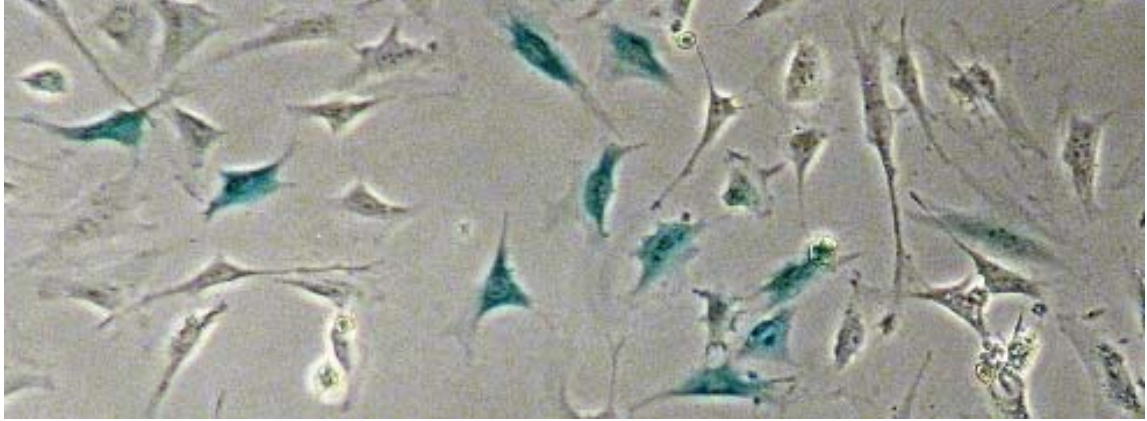
Figure 16. Electroporation Efficiency in 3T3-L1 adipocytes. Day 5 3T3-L1 adipocytes were electroporated with 50 μg CMV-LacZ plasmid DNA, and transfection/expression of β-galactosidase efficiency was determined by In Situ β-galactosidase staining kit. Cells taking up the blue stain express β-galactosidase, which is used as a measure of transfection efficiency. The stained and unstained cells in randomly selected fields were counted. The transfection efficiency is the percentage of stained cells in the total population.
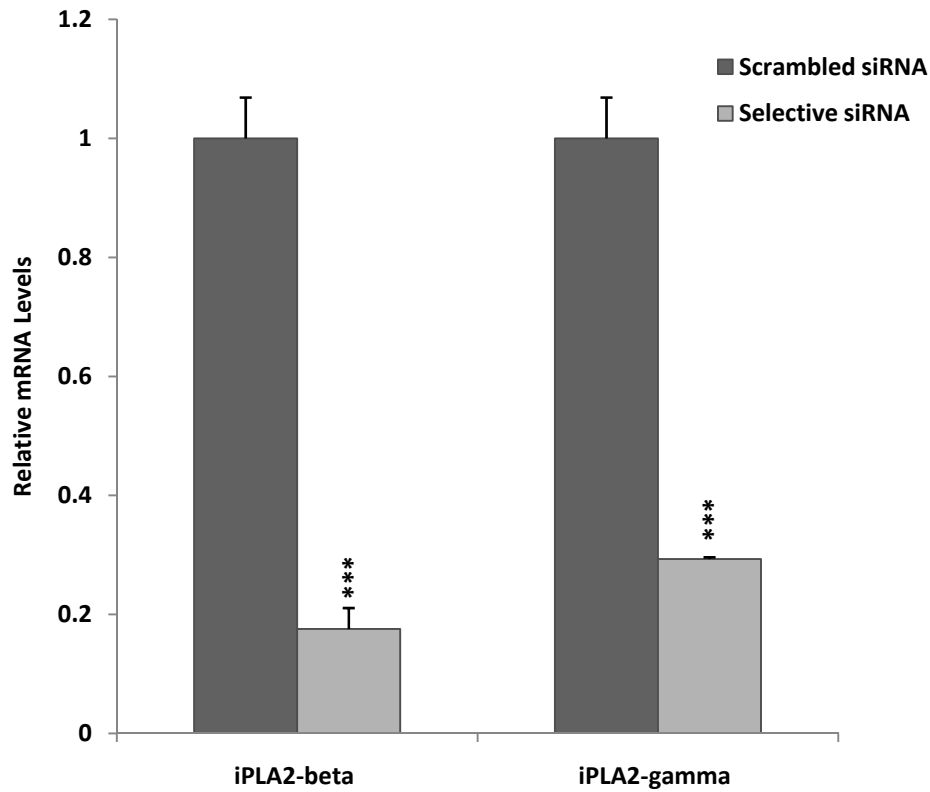
Figure 17. Effects of siRNA transfection on the mRNA levels of iPLA$_2$β and iPLA$_2$γ in 3T3-L1 Adipocytes. Day 6 3T3-L1 adipocytes were cultured and transfected with 50 nM negative control siRNA, siRNA directed against iPLA$_2$β and iPLA$_2$γ by electroporation. 48 hours after transfection, total RNA was collected and reverse transcribed to cDNA. RT-PCR analysis was performed to determine the mRNA levels of iPLA$_2$β and γ utilizing 36B4 as the reference gene. The relative mRNA levels are computed using the mRNA levels in negative control cells (scrambled siRNA treated) as internal standard, and the fold changes are represented as mean ± S.E. of independent experiments. Statistical significance of siRNA treatments on mRNA levels was determined by comparing the mean of mRNA level of iPLA$_2$β or iPLA$_2$γ of cells transfected by selective siRNA with that from cells treated with scramble siRNA using 2-sample student's *t* test (***, $p<0.001$).
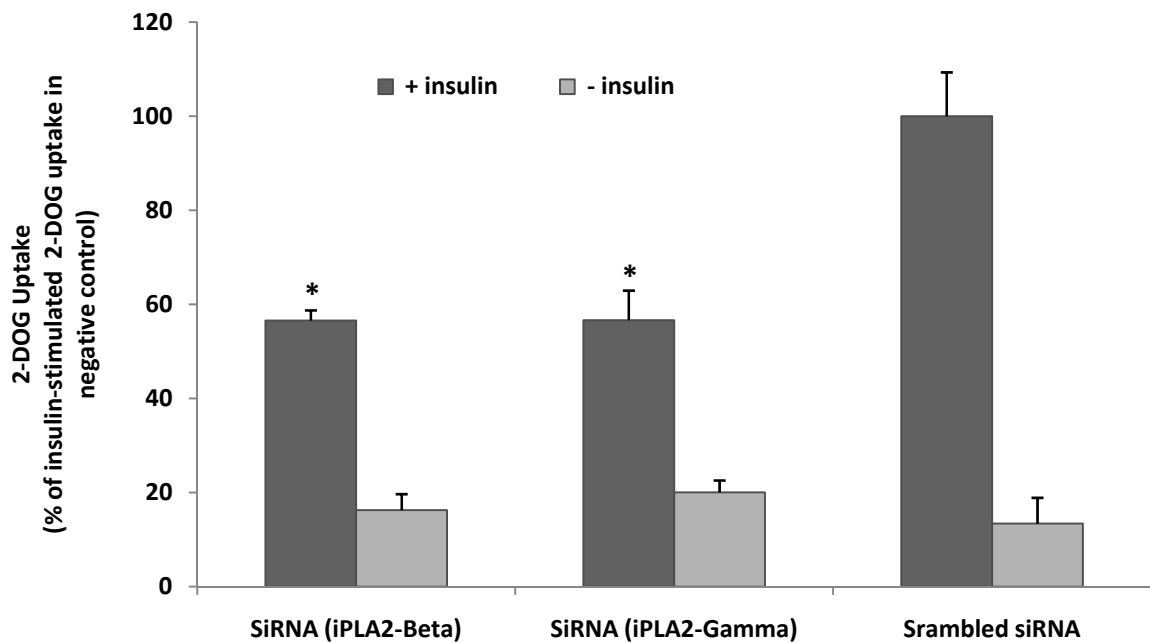
Figure 18. Effects of siRNA gene silencing of iPLA$_2$β and iPLA$_2$γ on insulin-stimulated glucose uptake in 3T3-L1 adipocytes. Day 6 3T3-L1 adipocytes were cultured and transfected with 50 nM negative control siRNA, siRNA directed against iPLA$_2$β and γ by electroporation. 48 hours after transfection, cells were serum-starved, and then stimulated by 100 nM insulin for 30 minutes. 2-Deoxygluocse uptake in these adipocytes was measured over 10 minutes. Data are mean ± S.E. from three or more independent experiments performed in triplicate, normalized to negative control insulin-stimulated uptake. Statistical significance of treatments on basal or insulin-stimulated 2-DOG uptake was determined by comparing the mean of basal or insulin-stimulated 2-DOG uptake of cells transfected by selective siRNA with that from cells treated with scramble siRNA using 2-sample student's *t* test (*, *p*<0.05).

97

CHAPTER 5. SUMMARY AND FUTURE STUDIES

In this dissertation, we demonstrate a role for iPLA$_2$ in glucose transport in insulin-stimulated 3T3-L1 adipocytes. We found that adipocyte insulin-stimulated glucose uptake was significantly reduced with BEL-induced iPLA$_2$ inhibition. In agreement with the BEL treatment results, selective knockdown of iPLA$_2$β or iPLA$_2$γ using siRNA technique significantly decreased the insulin-stimulated glucose uptake in the 3T3-L1 adipocytes. We further explored the mechanism for the inhibitory effect of BEL. The results showed that the impaired insulin action on glucose transport was not due to the alterations in insulin signaling pathways, but due to decreased incorporation of GLUT4 into the plasma membrane or lipid raft microdomains.

Although the regulation of GLUT4 trafficking have been areas of intensive investigation since its identification, the mechanisms involved in our results remain to be established. As far as the biological functions of iPLA$_2$ are concerned, three possible mechanisms by which insulin-stimulated glucose uptake is regulated by iPLA$_2$ enzymatic activity are proposed here:

1. Activation of PPARγ: PPARγ is believed to be a prominent effector controlling insulin sensitivity. Evidence is accumulating to indicate that PPARγ activation can affect insulin signaling in adipose tissue through upregulation of a number of downstream

molecules, including IRS proteins, the p85 subunit of PI3K and CAP - all of which might be predicted to enhance GLUT4 activity (320). Recent studies have shown that iPLA$_2$ could serve as PPARγ activator through providing lipids or lipid precursors during the adipocytes differentiation (15). Additionally, AA exposure potentiates the insulin-stimulated glucose uptake by increasing GLUT4 level at the plasma membrane, and this potentiation is proved to be dependent on PPARγ activation (309). It is possible that iPLA$_2$ inhibition prevents PPARγ activation, leading to the reduced insulin response in adipocytes.   It was unclear; however, whether short term treatments would be sufficient to cause such effects. The non-altered Akt and IR phosphorylation may let us exclude PPARγ in the present study. Long term BEL treatment or selective gene knockdown would help us to better understand this possible mechanism.

2. Alterations of phospholipid membrane structure: One of the most important cellular functions of iPLA$_2$ is controlling the membrane glycerophospholipid metabolism. By regulating the cleavage of pre-existing membrane PL, the reincorporation of generated fatty acids into membrane PL molecules, and reacylating the lysoPL with a different fatty acid, iPLA$_2$s are highly involved in the ongoing deacylation/reacylation cycle critical for membrane homeostasis (12). More importantly, the accumulation of lysophospholipids and free fatty acids may increase the membrane fluidity or promote non-bilayer structures, and eventually stimulate the fusion of biological membranes. Recent studies have confirmed the linkage of iPLA$_2$ activity and several exocytosis processes, including glucose-stimulated insulin secretion in pancreatic β cells (89, 111, 112), lysozyme secretion in U397 cells (110), exocytosis of amylase from parotid acinar

cells (113), and lysosome-mediated IL-1β secretion (114). Similar to these secretion or exocytosis procedures, GLUT4 translocation to the plasma membrane requires the formation and transport of vesicle, as well as the fusion of bilayers of vesicle and plasma membrane (218). Therefore, it is reasonable to postulate that GLUT 4 translocation is at least partly dependent on iPLA$_2$ activity. In addition, alterations in the fatty acid composition of membrane phospholipids can affect specific membrane microdomains, such as lipid rafts (310), which serves as sites for assembly of signaling complexes that play an important role in insulin action, especially the Cbl/CAP cascade (317). To our knowledge, no studies to date have discussed the relation between iPLA$_2$ activities or BEL effects on lipid raft structures; however, the observed alteration in GLUT4 distributions indicates this possibility.

3. Regulations of Ca^{2+} homeostasis: Calcium-independent PLA$_2$ has recently been shown to regulate Ca^{2+} entry by replenishing the depleted intracellular Ca^{2+} stores. It has been observed in a variety of cells and tissues that both chemical and genetic inhibition of iPLA$_2$β activation result in the block of store-operated Ca^{2+} channels (SOC), and the Ca^{2+} influx can be restored by LPC (105-108). These studies suggest that the iPLA$_2$ activity is necessary for the activation of SOC. The iPLA$_2$ is also reported to regulate the Ca^{2+} influx by transient receptor potential (TRP) channels (108, 109). In many exocytosis processes, increased cytosolic calcium is known to be required. BEL treatment has been shown to inhibit such processes, including release of neurotransmitter (115) and mast cell granule (116). Therefore, the regulatory roles of iPLA$_2$ on calcium entry may explain some aspects of its importance in secretion.

Similar to these proteins, the movement of GLUT4 has been shown to be controlled by Ca^{2+}, and it appears to be caused by physically associated signaling molecules that sense local Ca^{2+} increases at the mouth of the channels (240, 321). The Ca^{2+}-binding protein calmodulin has a central role in this process. As reviewed by Lanner (321), the late steps of insulin signaling contains an increase in the concentrations of intracellular Ca^{2+} and Ca^{2+} sensing proteins, which serve as modulators for GLUT4 exocytosis in either direct or indirect manner. Some research groups found that using Ca^{2+} chelators or calmodulin antagonists in insulin-sensitive cells or tissues decreases the glucose uptake upon insulin administration and reduces the level of GLUT4 in plasma membrane (240, 322). Of note is the work of Lanner and coworkers in 2006 (240), who demonstrated that inhibition of Ca^{2+} influx by 2-aminoethoxydiphenyl borate (2-APB) decreased insulin-mediated glucose uptake in skeletal muscle but did not affect the phosphorylation state of PKB/Akt or the MAP kinase ERK1/2. In the current study, we also show that BEL treatment influence the insulin actions in 3T3-L1 adipocytes in the similar way as 2-APB. Consequently, possible Ca^{2+} influx blocking resulting from $iPLA_2$ inhibition contributes to the inhibitory effects of BEL on insulin action observed in this study.

The present results constitute the first demonstration of an important role of $iPLA_2$ in insulin action on glucose uptake. It is involved in some aspects of the GLUT4 translocation in response to insulin without affecting insulin signal pathway up to forehead of Akt kinase. Although further studies are needed to identify the specific underlying mechanism, this novel function of $iPLA_2$ in 3T3-L1 adipocytes makes it a

promising target for strategies for prevention and treatment of obesity, type 2 diabetes and other linked metabolic diseases.

REFERENCES

1.   Obesity and Overweight. 2009 [cited 2009 July, 01]; Available from: http://www.who.int/mediacentre/factsheets/fs311/en/index.html

2.   Kopelman PG. Obesity as a medical problem. Nature. 2000 Apr 6;404:635-43.

3.   About Obesity. 2009 [cited 2009 July, 01]; Available from: http://www.iotf.org/aboutobesity.asp

4.   Flier JS. Obesity wars: molecular progress confronts an expanding epidemic. Cell. 2004 Jan 23;116:337-50.

5.   National Diabetes Fact Sheet 2009 [cited 2009 July, 01]; Available from: http://apps.nccd.cdc.gov/DDTSTRS/default.aspx

6.   Trayhurn P, Wang B, Wood IS, Trayhurn P, Wang B, Wood IS. Hypoxia in adipose tissue: a basis for the dysregulation of tissue function in obesity?[see comment]. British Journal of Nutrition. 2008 Aug;100:227-35.

7.   Hajer GR, van Haeften TW, Visseren FL, Hajer GR, van Haeften TW, Visseren FLJ. Adipose tissue dysfunction in obesity, diabetes, and vascular diseases. European Heart Journal. 2008 Dec;29:2959-71.

8.   Guilherme A, Virbasius JV, Puri V, Czech MP, Guilherme A, Virbasius JV, Puri V, Czech MP. Adipocyte dysfunctions linking obesity to insulin resistance and type 2 diabetes. Nature Reviews Molecular Cell Biology. 2008 May;9:367-77.

9.   Schaloske RH, Dennis EA. The phospholipase A2 superfamily and its group numbering system. Biochim Biophys Acta. 2006 Nov;1761:1246-59.

10.   Duncan RE, Sarkadi-Nagy E, Jaworski K, Ahmadian M, Sul HS. Identification and functional characterization of adipose-specific phospholipase A2 (AdPLA). J Biol Chem. 2008 Sep 12;283:25428-36. Epub 2008 Jul 9.

11.   Balsinde J, Balboa MA. Cellular regulation and proposed biological functions of group VIA calcium-independent phospholipase A2 in activated cells. Cell Signal. 2005 Sep;17:1052-62.

12.   Balsinde J, Dennis EA. Function and inhibition of intracellular calcium-independent phospholipase A2. J Biol Chem. 1997 Jun 27;272:16069-72.

103

13.   Kudo I, Murakami M. Phospholipase A2 enzymes. Prostaglandins Other Lipid Mediat. 2002 Aug;68-69:3-58.

14.   Akiba S, Sato T. Cellular function of calcium-independent phospholipase A2. Biol Pharm Bull. 2004 Aug;27:1174-8.

15.   Su X, Mancuso DJ, Bickel PE, Jenkins CM, Gross RW. Small interfering RNA knockdown of calcium-independent phospholipases A2 beta or gamma inhibits the hormone-induced differentiation of 3T3-L1 preadipocytes. J Biol Chem. 2004 May 21;279:21740-8.

16.   Song K, Zhang X, Zhao C, Ang NT, Ma ZA. Inhibition of Ca2+-independent phospholipase A2 results in insufficient insulin secretion and impaired glucose tolerance. Mol Endocrinol. 2005 Feb;19:504-15.

17.   Bao S, Jin C, Zhang S, Turk J, Ma Z, Ramanadham S. Beta-cell calcium-independent group VIA phospholipase A(2) (iPLA(2)beta): tracking iPLA(2)beta movements in response to stimulation with insulin secretagogues in INS-1 cells. Diabetes. 2004 Feb;53 Suppl 1:S186-9.

18.   Bao S, Miller DJ, Ma Z, Wohltmann M, Eng G, Ramanadham S, Moley K, Turk J, Bao S, et al. Male mice that do not express group VIA phospholipase A2 produce spermatozoa with impaired motility and have greatly reduced fertility. Journal of Biological Chemistry. 2004 Sep 10;279:38194-200.

19.   Bao S, Li Y, Lei X, Wohltmann M, Jin W, Bohrer A, Semenkovich CF, Ramanadham S, Tabas I, Turk J. Attenuated free cholesterol loading-induced apoptosis but preserved phospholipid composition of peritoneal macrophages from mice that do not express group VIA phospholipase A2. J Biol Chem. 2007 Sep 14;282:27100-14.

20.   Stein DT, Esser V, Stevenson BE, Lane KE, Whiteside JH, Daniels MB, Chen S, McGarry JD. Essentiality of circulating fatty acids for glucose-stimulated insulin secretion in the fasted rat. Journal of Clinical Investigation. 1996 Jun 15;97:2728-35.

21.   Sanchez JC, Converset V, Nolan A, Schmid G, Wang S, Heller M, Sennitt MV, Hochstrasser DF, Cawthorne MA. Effect of rosiglitazone on the differential expression of obesity and insulin resistance associated proteins in lep/lep mice. Proteomics. 2003 Aug;3:1500-20.

22.   Bao S, Song H, Wohltmann M, Ramanadham S, Jin W, Bohrer A, Turk J. Insulin secretory responses and phospholipid composition of pancreatic islets from mice that do not express Group VIA phospholipase A2 and effects of metabolic stress on glucose homeostasis. J Biol Chem. 2006 Jul 28;281:20958-73.

23.   Bao S, Jacobson DA, Wohltmann M, Bohrer A, Jin W, Philipson LH, Turk J. Glucose homeostasis, insulin secretion, and islet phospholipids in mice that overexpress

iPLA2beta in pancreatic beta-cells and in iPLA2beta-null mice. Am J Physiol Endocrinol Metab. 2008 Feb;294:E217-29.

24.   Fajas L, Schoonjans K, Gelman L, Kim JB, Najib J, Martin G, Fruchart JC, Briggs M, Spiegelman BM, Auwerx J. Regulation of peroxisome proliferator-activated receptor gamma expression by adipocyte differentiation and determination factor 1/sterol regulatory element binding protein 1: implications for adipocyte differentiation and metabolism. Mol Cell Biol. 1999 Aug;19:5495-503.

25.   Wilkins WP, 3rd, Barbour SE. Group VI phospholipases A2: homeostatic phospholipases with significant potential as targets for novel therapeutics. Curr Drug Targets. 2008 Aug;9:683-97.

26.   Mancuso DJ, Han X, Jenkins CM, Lehman JJ, Sambandam N, Sims HF, Yang J, Yan W, Yang K, et al. Dramatic accumulation of triglycerides and precipitation of cardiac hemodynamic dysfunction during brief caloric restriction in transgenic myocardium expressing human calcium-independent phospholipase A2gamma. J Biol Chem. 2007 Mar 23;282:9216-27.

27.   Mancuso DJ, Sims HF, Han X, Jenkins CM, Guan SP, Yang K, Moon SH, Pietka T, Abumrad NA, et al. Genetic ablation of calcium-independent phospholipase A2gamma leads to alterations in mitochondrial lipid metabolism and function resulting in a deficient mitochondrial bioenergetic phenotype. J Biol Chem. 2007 Nov 30;282:34611-22.

28.   Jenkins CM, Mancuso DJ, Yan W, Sims HF, Gibson B, Gross RW. Identification, cloning, expression, and purification of three novel human calcium-independent phospholipase A2 family members possessing triacylglycerol lipase and acylglycerol transacylase activities. J Biol Chem. 2004 Nov 19;279:48968-75.

29.   Funk CD. Prostaglandins and leukotrienes: advances in eicosanoid biology. Science. 2001 Nov 30;294:1871-5.

30.   Tsuboi K, Sugimoto Y, Ichikawa A. Prostanoid receptor subtypes. Prostaglandins Other Lipid Mediat. 2002 Aug;68-69:535-56.

31.   Breyer RM, Kennedy CR, Zhang Y, Breyer MD. Structure-function analyses of eicosanoid receptors. Physiologic and therapeutic implications. Annals of the New York Academy of Sciences. 2000 Apr;905:221-31.

32.   Moolenaar WH, van Meeteren LA, Giepmans BN. The ins and outs of lysophosphatidic acid signaling. Bioessays. 2004 Aug;26:870-81.

33.   Meyer zu Heringdorf D, Jakobs KH, Meyer zu Heringdorf D, Jakobs KH. Lysophospholipid receptors: signalling, pharmacology and regulation by lysophospholipid metabolism. Biochimica et Biophysica Acta. 2007 Apr;1768:923-40.

34.   Balsinde J, Winstead MV, Dennis EA. Phospholipase A(2) regulation of arachidonic acid mobilization. FEBS Lett. 2002 Oct 30;531:2-6.

35.   Chiba H, Michibata H, Wakimoto K, Seishima M, Kawasaki S, Okubo K, Mitsui H, Torii H, Imai Y. Cloning of a gene for a novel epithelium-specific cytosolic phospholipase A2, cPLA2delta, induced in psoriatic skin. J Biol Chem. 2004 Mar 26;279:12890-7.

36.   Six DA, Dennis EA. The expanding superfamily of phospholipase A(2) enzymes: classification and characterization. Biochim Biophys Acta. 2000 Oct 31;1488:1-19.

37.   Burke JE, Dennis EA, Burke JE, Dennis EA. Phospholipase A2 structure/function, mechanism, and signaling. Journal of Lipid Research. 2009 Apr;50 Suppl:S237-42.

38.   Burke JE, Dennis EA. Phospholipase A2 structure/function, mechanism, and signaling. J Lipid Res. 2009 Apr;50 Suppl:S237-42.

39.   Singer AG, Ghomashchi F, Le Calvez C, Bollinger J, Bezzine S, Rouault M, Sadilek M, Nguyen E, Lazdunski M, et al. Interfacial kinetic and binding properties of the complete set of human and mouse groups I, II, V, X, and XII secreted phospholipases A2. J Biol Chem. 2002 Dec 13;277:48535-49.

40.   Murakami M, Masuda S, Shimbara S, Bezzine S, Lazdunski M, Lambeau G, Gelb MH, Matsukura S, Kokubu F, et al. Cellular arachidonate-releasing function of novel classes of secretory phospholipase A2s (groups III and XII). J Biol Chem. 2003 Mar 21;278:10657-67.

41.   Seilhamer JJ, Pruzanski W, Vadas P, Plant S, Miller JA, Kloss J, Johnson LK. Cloning and recombinant expression of phospholipase A2 present in rheumatoid arthritic synovial fluid. J Biol Chem. 1989 Apr 5;264:5335-8.

42.   Oestvang J, Johansen B. PhospholipaseA2: a key regulator of inflammatory signalling and a connector to fibrosis development in atherosclerosis. Biochim Biophys Acta. 2006 Nov;1761:1309-16.

43.   Ghosh M, Tucker DE, Burchett SA, Leslie CC, Ghosh M, Tucker DE, Burchett SA, Leslie CC. Properties of the Group IV phospholipase A2 family. Progress in Lipid Research. 2006 Nov;45:487-510.

44.   Ghosh M, Tucker DE, Burchett SA, Leslie CC. Properties of the Group IV phospholipase A2 family. Prog Lipid Res. 2006 Nov;45:487-510.

45.   Abe A, Shayman JA. Purification and characterization of 1-O-acylceramide synthase, a novel phospholipase A2 with transacylase activity. J Biol Chem. 1998 Apr 3;273:8467-74.

46.   Hiraoka M, Abe A, Shayman JA. Cloning and characterization of a lysosomal phospholipase A2, 1-O-acylceramide synthase. J Biol Chem. 2002 Mar 22;277:10090-9.

47.   Ackermann EJ, Kempner ES, Dennis EA. Ca(2+)-independent cytosolic phospholipase A2 from macrophage-like P388D1 cells. Isolation and characterization. J Biol Chem. 1994 Mar 25;269:9227-33.

48.   Ross MI, Deems RA, Jesaitis AJ, Dennis EA, Ulevitch RJ. Phospholipase activities of the P388D1 macrophage-like cell line. Arch Biochem Biophys. 1985 Apr;238:247-58.

49.   Ackermann EJ, Conde-Frieboes K, Dennis EA. Inhibition of macrophage Ca(2+)-independent phospholipase A2 by bromoenol lactone and trifluoromethyl ketones. J Biol Chem. 1995 Jan 6;270:445-50.

50.   Tang J, Kriz RW, Wolfman N, Shaffer M, Seehra J, Jones SS. A novel cytosolic calcium-independent phospholipase A2 contains eight ankyrin motifs. J Biol Chem. 1997 Mar 28;272:8567-75.

51.   Balboa MA, Balsinde J, Jones SS, Dennis EA. Identity between the Ca2+-independent phospholipase A2 enzymes from P388D1 macrophages and Chinese hamster ovary cells. J Biol Chem. 1997 Mar 28;272:8576-80.

52.   Larsson PK, Claesson HE, Kennedy BP. Multiple splice variants of the human calcium-independent phospholipase A2 and their effect on enzyme activity. J Biol Chem. 1998 Jan 2;273:207-14.

53.   Ma Z, Wang X, Nowatzke W, Ramanadham S, Turk J. Human pancreatic islets express mRNA species encoding two distinct catalytically active isoforms of group VI phospholipase A2 (iPLA2) that arise from an exon-skipping mechanism of alternative splicing of the transcript from the iPLA2 gene on chromosome 22q13.1. Journal of Biological Chemistry. 1999 Apr 2;274:9607-16.

54.   Mancuso DJ, Jenkins CM, Gross RW. The genomic organization, complete mRNA sequence, cloning, and expression of a novel human intracellular membrane-associated calcium-independent phospholipase A(2). J Biol Chem. 2000 Apr 7;275:9937-45.

55.   Tanaka H, Takeya R, Sumimoto H. A novel intracellular membrane-bound calcium-independent phospholipase A(2). Biochem Biophys Res Commun. 2000 Jun 7;272:320-6.

56.   Yang J, Han X, Gross RW. Identification of hepatic peroxisomal phospholipase A(2) and characterization of arachidonic acid-containing choline glycerophospholipids in hepatic peroxisomes. FEBS Lett. 2003 Jul 10;546:247-50.

57.   Murakami M, Masuda S, Ueda-Semmyo K, Yoda E, Kuwata H, Takanezawa Y, Aoki J, Arai H, Sumimoto H, et al. Group VIB Ca2+-independent phospholipase A2gamma promotes cellular membrane hydrolysis and prostaglandin production in a manner distinct from other intracellular phospholipases A2. J Biol Chem. 2005 Apr 8;280:14028-41.

58.   Glynn P. Neuropathy target esterase. Biochem J. 1999 Dec 15;344 Pt 3:625-31.

59.   Glynn P. Neuropathy target esterase and phospholipid deacylation. Biochim Biophys Acta. 2005 Sep 15;1736:87-93.

60.   van Tienhoven M, Atkins J, Li Y, Glynn P. Human neuropathy target esterase catalyzes hydrolysis of membrane lipids. J Biol Chem. 2002 Jun 7;277:20942-8.

61.   Kinsey GR, Cummings BS, Beckett CS, Saavedra G, Zhang W, McHowat J, Schnellmann RG. Identification and distribution of endoplasmic reticulum iPLA2. Biochem Biophys Res Commun. 2005 Feb 4;327:287-93.

62.   Wolf C, Colard-Torquebiau O, Bereziat G, Polonovski J. [Phospholipase A2 of the adipocyte cytoplasmic membrane]. Biochimie. 1977;59:115-8.

63.   Nowatzke W, Ramanadham S, Ma Z, Hsu FF, Bohrer A, Turk J. Mass spectrometric evidence that agents that cause loss of Ca2+ from intracellular compartments induce hydrolysis of arachidonic acid from pancreatic islet membrane phospholipids by a mechanism that does not require a rise in cytosolic Ca2+ concentration. Endocrinology. 1998 Oct;139:4073-85.

64.   Jenkins CM, Wolf MJ, Mancuso DJ, Gross RW. Identification of the calmodulin-binding domain of recombinant calcium-independent phospholipase A2beta. implications for structure and function. J Biol Chem. 2001 Mar 9;276:7129-35.

65.   Akiba S, Ohno S, Chiba M, Kume K, Hayama M, Sato T. Protein kinase Calpha-dependent increase in Ca2+-independent phospholipase A2 in membranes and arachidonic acid liberation in zymosan-stimulated macrophage-like P388D1 cells. Biochem Pharmacol. 2002 Jun 1;63:1969-77.

66.   Martinez J, Moreno JJ. Role of Ca2+-independent phospholipase A2 on arachidonic acid release induced by reactive oxygen species. Arch Biochem Biophys. 2001 Aug 15;392:257-62.

67.   Akiba S, Mizunaga S, Kume K, Hayama M, Sato T. Involvement of group VI Ca2+-independent phospholipase A2 in protein kinase C-dependent arachidonic acid liberation in zymosan-stimulated macrophage-like P388D1 cells. Journal of Biological Chemistry. 1999 Jul 9;274:19906-12.

68.   Maggi LB, Jr., Moran JM, Scarim AL, Ford DA, Yoon JW, McHowat J, Buller RM, Corbett JA. Novel role for calcium-independent phospholipase A(2) in the

macrophage antiviral response of inducible nitric-oxide synthase expression. J Biol Chem. 2002 Oct 11;277:38449-55.

69.   Smani T, Zakharov SI, Leno E, Csutora P, Trepakova ES, Bolotina VM. Ca2+-independent phospholipase A2 is a novel determinant of store-operated Ca2+ entry. J Biol Chem. 2003 Apr 4;278:11909-15.

70.   Yellaturu CR, Rao GN. A requirement for calcium-independent phospholipase A2 in thrombin-induced arachidonic acid release and growth in vascular smooth muscle cells. J Biol Chem. 2003 Oct 31;278:43831-7.

71.   Lio YC, Dennis EA. Interfacial activation, lysophospholipase and transacylase activity of group VI Ca2+-independent phospholipase A2. Biochim Biophys Acta. 1998 Jun 15;1392:320-32.

72.   Birbes H, Drevet S, Pageaux JF, Lagarde M, Laugier C. Involvement of calcium-independent phospholipase A2 in uterine stromal cell phospholipid remodelling. European Journal of Biochemistry. 2000 Dec;267:7118-27.

73.   Birbes H, Gothie E, Pageaux JF, Lagarde M, Laugier C. Hydrogen peroxide activation of Ca(2+)-independent phospholipase A(2) in uterine stromal cells. Biochemical & Biophysical Research Communications. 2000 Sep 24;276:613-8.

74.   Xu J, Yu S, Sun AY, Sun GY. Oxidant-mediated AA release from astrocytes involves cPLA(2) and iPLA(2). Free Radic Biol Med. 2003 Jun 15;34:1531-43.

75.   Xu J, Yu S, Sun AY, Sun GY, Xu J, Yu S, Sun AY, Sun GY. Oxidant-mediated AA release from astrocytes involves cPLA(2) and iPLA(2). Free Radical Biology & Medicine. 2003 Jun 15;34:1531-43.

76.   Balboa MA, Balsinde J. Involvement of calcium-independent phospholipase A2 in hydrogen peroxide-induced accumulation of free fatty acids in human U937 cells. J Biol Chem. 2002 Oct 25;277:40384-9.

77.   Lauber K, Bohn E, Krober SM, Xiao YJ, Blumenthal SG, Lindemann RK, Marini P, Wiedig C, Zobywalski A, et al. Apoptotic cells induce migration of phagocytes via caspase-3-mediated release of a lipid attraction signal. Cell. 2003 Jun 13;113:717-30.

78.   Ramanadham S, Hsu FF, Zhang S, Jin C, Bohrer A, Song H, Bao S, Ma Z, Turk J, et al. Apoptosis of insulin-secreting cells induced by endoplasmic reticulum stress is amplified by overexpression of group VIA calcium-independent phospholipase A2 (iPLA2 beta) and suppressed by inhibition of iPLA2 beta. Biochemistry. 2004 Feb 3;43:918-30.

79.   Mancuso DJ, Jenkins CM, Sims HF, Cohen JM, Yang J, Gross RW. Complex transcriptional and translational regulation of iPLAgamma resulting in multiple gene

products containing dual competing sites for mitochondrial or peroxisomal localization. Eur J Biochem. 2004 Dec;271:4709-24.

80.   Lio YC, Reynolds LJ, Balsinde J, Dennis EA. Irreversible inhibition of Ca(2+)-independent phospholipase A2 by methyl arachidonyl fluorophosphonate. Biochim Biophys Acta. 1996 Jul 12;1302:55-60.

81.   Daniels SB, Cooney E, Sofia MJ, Chakravarty PK, Katzenellenbogen JA. Haloenol lactones. Potent enzyme-activated irreversible inhibitors for alpha-chymotrypsin. J Biol Chem. 1983 Dec 25;258:15046-53.

82.   Balsinde J, Bianco ID, Ackermann EJ, Conde-Frieboes K, Dennis EA. Inhibition of calcium-independent phospholipase A2 prevents arachidonic acid incorporation and phospholipid remodeling in P388D1 macrophages. Proceedings of the National Academy of Sciences of the United States of America. 1995 Aug 29;92:8527-31.

83.   Washburn WN, Dennis EA. Suicide-inhibitory bifunctionally linked substrates (SIBLINKS) as phospholipase A2 inhibitors. Mechanistic implications. J Biol Chem. 1991 Mar 15;266:5042-8.

84.   Balsinde J, Dennis EA. Bromoenol lactone inhibits magnesium-dependent phosphatidate phosphohydrolase and blocks triacylglycerol biosynthesis in mouse P388D1 macrophages. J Biol Chem. 1996 Dec 13;271:31937-41.

85.   Hazen SL, Zupan LA, Weiss RH, Getman DP, Gross RW. Suicide inhibition of canine myocardial cytosolic calcium-independent phospholipase A2. Mechanism-based discrimination between calcium-dependent and -independent phospholipases A2. J Biol Chem. 1991 Apr 15;266:7227-32.

86.   Lucas KK, Dennis EA. Distinguishing phospholipase A2 types in biological samples by employing group-specific assays in the presence of inhibitors. Prostaglandins Other Lipid Mediat. 2005 Sep;77:235-48.

87.   Balboa MA, Balsinde J, Dennis EA. Involvement of phosphatidate phosphohydrolase in arachidonic acid mobilization in human amnionic WISH cells. J Biol Chem. 1998 Mar 27;273:7684-90.

88.   Fuentes L, Perez R, Nieto ML, Balsinde J, Balboa MA. Bromoenol lactone promotes cell death by a mechanism involving phosphatidate phosphohydrolase-1 rather than calcium-independent phospholipase A2. J Biol Chem. 2003 Nov 7;278:44683-90.

89.   Ramanadham S, Hsu FF, Bohrer A, Ma Z, Turk J. Studies of the role of group VI phospholipase A2 in fatty acid incorporation, phospholipid remodeling, lysophosphatidylcholine generation, and secretagogue-induced arachidonic acid release in pancreatic islets and insulinoma cells. J Biol Chem. 1999 May 14;274:13915-27.

90.   Bao S, Bohrer A, Ramanadham S, Jin W, Zhang S, Turk J. Effects of stable suppression of Group VIA phospholipase A2 expression on phospholipid content and composition, insulin secretion, and proliferation of INS-1 insulinoma cells. J Biol Chem. 2006 Jan 6;281:187-98.

91.   Bao S, Miller DJ, Ma Z, Wohltmann M, Eng G, Ramanadham S, Moley K, Turk J. Male mice that do not express group VIA phospholipase A2 produce spermatozoa with impaired motility and have greatly reduced fertility. J Biol Chem. 2004 Sep 10;279:38194-200.

92.   Hill EE, Lands WE. Incorporation of long-chain and polyunsaturated acids into phosphatidate and phosphatidylcholine. Biochim Biophys Acta. 1968 May 1;152:645-8.

93.   Lands WE. Stories about acyl chains. Biochim Biophys Acta. 2000 Jan 3;1483:1-14.

94.   MacDonald JI, Sprecher H. Phospholipid fatty acid remodeling in mammalian cells. Biochim Biophys Acta. 1991 Jul 9;1084:105-21.

95.   Yamashita A, Sugiura T, Waku K. Acyltransferases and transacylases involved in fatty acid remodeling of phospholipids and metabolism of bioactive lipids in mammalian cells. J Biochem. 1997 Jul;122:1-16.

96.   Green JT, Orr SK, Bazinet RP. The emerging role of group VI calcium-independent phospholipase A2 in releasing docosahexaenoic acid from brain phospholipids. J Lipid Res. 2008 May;49:939-44.

97.   Smith WL, DeWitt DL, Garavito RM. Cyclooxygenases: structural, cellular, and molecular biology. Annu Rev Biochem. 2000;69:145-82.

98.   Wilkins WPr, Barbour SE. Group VI phospholipases A2: homeostatic phospholipases with significant potential as targets for novel therapeutics. Curr Drug Targets. 2008 Aug;9:683-97.

99.   Gross RW, Rudolph AE, Wang J, Sommers CD, Wolf MJ. Nitric oxide activates the glucose-dependent mobilization of arachidonic acid in a macrophage-like cell line (RAW 264.7) that is largely mediated by calcium-independent phospholipase A2. J Biol Chem. 1995 Jun 23;270:14855-8.

100.   Murakami M, Kambe T, Shimbara S, Kudo I. Functional coupling between various phospholipase A2s and cyclooxygenases in immediate and delayed prostanoid biosynthetic pathways. J Biol Chem. 1999 Jan 29;274:3103-15.

101.   Ma Z, Zhang S, Turk J, Ramanadham S, Ma Z, Zhang S, Turk J, Ramanadham S. Stimulation of insulin secretion and associated nuclear accumulation of iPLA(2)beta in INS-1 insulinoma cells. American Journal of Physiology - Endocrinology & Metabolism. 2002 Apr;282:E820-33.

102.	Ma Z, Turk J. The molecular biology of the group VIA Ca2+-independent phospholipase A2. Prog Nucleic Acid Res Mol Biol. 2001;67:1-33.

103.	Albert AP, Large WA. Store-operated Ca2+-permeable non-selective cation channels in smooth muscle cells. Cell Calcium. 2003 May-Jun;33:345-56.

104.	Wolf MJ, Wang J, Turk J, Gross RW. Depletion of intracellular calcium stores activates smooth muscle cell calcium-independent phospholipase A2. A novel mechanism underlying arachidonic acid mobilization. Journal of Biological Chemistry. 1997 Jan 17;272:1522-6.

105.	Smani T, Zakharov SI, Csutora P, Leno E, Trepakova ES, Bolotina VM. A novel mechanism for the store-operated calcium influx pathway. Nat Cell Biol. 2004 Feb;6:113-20.

106.	Csutora P, Zarayskiy V, Peter K, Monje F, Smani T, Zakharov SI, Litvinov D, Bolotina VM. Activation mechanism for CRAC current and store-operated Ca2+ entry: calcium influx factor and Ca2+-independent phospholipase A2beta-mediated pathway. J Biol Chem. 2006 Nov 17;281:34926-35.

107.	Singaravelu K, Lohr C, Deitmer JW. Regulation of store-operated calcium entry by calcium-independent phospholipase A2 in rat cerebellar astrocytes. J Neurosci. 2006 Sep 13;26:9579-92.

108.	Vanden Abeele F, Lemonnier L, Thebault S, Lepage G, Parys JB, Shuba Y, Skryma R, Prevarskaya N. Two types of store-operated Ca2+ channels with different activation modes and molecular origin in LNCaP human prostate cancer epithelial cells. J Biol Chem. 2004 Jul 16;279:30326-37.

109.	Andersson DA, Nash M, Bevan S. Modulation of the cold-activated channel TRPM8 by lysophospholipids and polyunsaturated fatty acids. J Neurosci. 2007 Mar 21;27:3347-55.

110.	Balboa MA, Saez Y, Balsinde J. Calcium-independent phospholipase A2 is required for lysozyme secretion in U937 promonocytes. J Immunol. 2003 May 15;170:5276-80.

111.	Ramanadham S, Gross RW, Han X, Turk J. Inhibition of arachidonate release by secretagogue-stimulated pancreatic islets suppresses both insulin secretion and the rise in beta-cell cytosolic calcium ion concentration. Biochemistry. 1993 Jan 12;32:337-46.

112.	Ma Z, Bohrer A, Wohltmann M, Ramanadham S, Hsu FF, Turk J. Studies of phospholipid metabolism, proliferation, and secretion of stably transfected insulinoma cells that overexpress group VIA phospholipase A2. Lipids. 2001 Jul;36:689-700.

113.	Takuma T, Ichida T. Role of Ca2+-independent phospholipase A2 in exocytosis of amylase from parotid acinar cells. J Biochem. 1997 Jun;121:1018-24.

114.   Andrei C, Margiocco P, Poggi A, Lotti LV, Torrisi MR, Rubartelli A. Phospholipases C and A2 control lysosome-mediated IL-1 beta secretion: Implications for inflammatory processes. Proc Natl Acad Sci U S A. 2004 Jun 29;101:9745-50.

115.   Bloch-Shilderman E, Abu-Raya S, Trembovler V, Boschwitz H, Gruzman A, Linial M, Lazarovici P. Pardaxin stimulation of phospholipases A2 and their involvement in exocytosis in PC-12 cells. J Pharmacol Exp Ther. 2002 Jun;301:953-62.

116.   Rastogi P, McHowat J. Inhibition of calcium-independent phospholipase A2 prevents inflammatory mediator production in pulmonary microvascular endothelium. Respir Physiol Neurobiol. 2009 Feb 28;165:167-74.

117.   Roshak AK, Capper EA, Stevenson C, Eichman C, Marshall LA. Human calcium-independent phospholipase A2 mediates lymphocyte proliferation. J Biol Chem. 2000 Nov 17;275:35692-8.

118.   Manguikian AD, Barbour SE. Cell cycle dependence of group VIA calcium-independent phospholipase A2 activity. J Biol Chem. 2004 Dec 17;279:52881-92.

119.   Atsumi G, Tajima M, Hadano A, Nakatani Y, Murakami M, Kudo I. Fas-induced arachidonic acid release is mediated by Ca2+-independent phospholipase A2 but not cytosolic phospholipase A2, which undergoes proteolytic inactivation. Journal of Biological Chemistry. 1998 May 29;273:13870-7.

120.   Atsumi G, Murakami M, Kojima K, Hadano A, Tajima M, Kudo I. Distinct roles of two intracellular phospholipase A2s in fatty acid release in the cell death pathway. Proteolytic fragment of type IVA cytosolic phospholipase A2alpha inhibits stimulus-induced arachidonate release, whereas that of type VI Ca2+-independent phospholipase A2 augments spontaneous fatty acid release. J Biol Chem. 2000 Jun 16;275:18248-58.

121.   Perez R, Matabosch X, Llebaria A, Balboa MA, Balsinde J. Blockade of arachidonic acid incorporation into phospholipids induces apoptosis in U937 promonocytic cells. J Lipid Res. 2006 Mar;47:484-91.

122.   Pruzanski W, Lambeau L, Lazdunsky M, Cho W, Kopilov J, Kuksis A. Differential hydrolysis of molecular species of lipoprotein phosphatidylcholine by groups IIA, V and X secretory phospholipases A2. Biochim Biophys Acta. 2005 Sep 5;1736:38-50.

123.   Boyanovsky BB, van der Westhuyzen DR, Webb NR. Group V secretory phospholipase A2-modified low density lipoprotein promotes foam cell formation by a SR-A- and CD36-independent process that involves cellular proteoglycans. J Biol Chem. 2005 Sep 23;280:32746-52.

124.   Mitsuishi M, Masuda S, Kudo I, Murakami M. Group V and X secretory phospholipase A2 prevents adenoviral infection in mammalian cells. Biochem J. 2006 Jan 1;393:97-106.

125.   Dessen A. Structure and mechanism of human cytosolic phospholipase A(2). Biochim Biophys Acta. 2000 Oct 31;1488:40-7.

126.   Moran JM, Buller RM, McHowat J, Turk J, Wohltmann M, Gross RW, Corbett JA. Genetic and pharmacologic evidence that calcium-independent phospholipase A2beta regulates virus-induced inducible nitric-oxide synthase expression by macrophages. J Biol Chem. 2005 Jul 29;280:28162-8.

127.   Mancuso DJ, Abendschein DR, Jenkins CM, Han X, Saffitz JE, Schuessler RB, Gross RW. Cardiac ischemia activates calcium-independent phospholipase A2beta, precipitating ventricular tachyarrhythmias in transgenic mice: rescue of the lethal electrophysiologic phenotype by mechanism-based inhibition. J Biol Chem. 2003 Jun 20;278:22231-6.

128.   McHowat J, Liu S, Creer MH. Selective hydrolysis of plasmalogen phospholipids by Ca2+-independent PLA2 in hypoxic ventricular myocytes. Am J Physiol. 1998 Jun;274:C1727-37.

129.   Ma Z, Ramanadham S, Wohltmann M, Bohrer A, Hsu FF, Turk J. Studies of insulin secretory responses and of arachidonic acid incorporation into phospholipids of stably transfected insulinoma cells that overexpress group VIA phospholipase A2 (iPLA2beta) indicate a signaling rather than a housekeeping role for iPLA2beta. J Biol Chem. 2001 Apr 20;276:13198-208.

130.   Gregoire FM, Smas CM, Sul HS. Understanding adipocyte differentiation. Physiol Rev. 1998 Jul;78:783-809.

131.   Mandrup S, Lane MD. Regulating adipogenesis. J Biol Chem. 1997 Feb 28;272:5367-70.

132.   Jenkins CM, Han X, Mancuso DJ, Gross RW. Identification of calcium-independent phospholipase A2 (iPLA2) beta, and not iPLA2gamma, as the mediator of arginine vasopressin-induced arachidonic acid release in A-10 smooth muscle cells. Enantioselective mechanism-based discrimination of mammalian iPLA2s. J Biol Chem. 2002 Sep 6;277:32807-14.

133.   Horton JD, Goldstein JL, Brown MS. SREBPs: activators of the complete program of cholesterol and fatty acid synthesis in the liver. Journal of Clinical Investigation. 2002 May;109:1125-31.

134.   Edwards PA, Tabor D, Kast HR, Venkateswaran A. Regulation of gene expression by SREBP and SCAP. Biochim Biophys Acta. 2000 Dec 15;1529:103-13.

135.   Yahagi N, Shimano H, Hasty AH, Amemiya-Kudo M, Okazaki H, Tamura Y, Iizuka Y, Shionoiri F, Ohashi K, et al. A crucial role of sterol regulatory element-binding protein-1 in the regulation of lipogenic gene expression by polyunsaturated fatty acids. J Biol Chem. 1999 Dec 10;274:35840-4.

136.   Sekiya M, Yahagi N, Matsuzaka T, Najima Y, Nakakuki M, Nagai R, Ishibashi S, Osuga J, Yamada N, Shimano H. Polyunsaturated fatty acids ameliorate hepatic steatosis in obese mice by SREBP-1 suppression. Hepatology. 2003 Dec;38:1529-39.

137.   Broekemeier KM, Iben JR, LeVan EG, Crouser ED, Pfeiffer DR. Pore formation and uncoupling initiate a Ca2+-independent degradation of mitochondrial phospholipids. Biochemistry. 2002 Jun 18;41:7771-80.

138.   Williams SD, Gottlieb RA. Inhibition of mitochondrial calcium-independent phospholipase A2 (iPLA2) attenuates mitochondrial phospholipid loss and is cardioprotective. Biochem J. 2002 Feb 15;362:23-32.

139.   Claros MG, Vincens P. Computational method to predict mitochondrially imported proteins and their targeting sequences. Eur J Biochem. 1996 Nov 1;241:779-86.

140.   Kinsey GR, McHowat J, Beckett CS, Schnellmann RG. Identification of calcium-independent phospholipase A2gamma in mitochondria and its role in mitochondrial oxidative stress. Am J Physiol Renal Physiol. 2007 Feb;292:F853-60.

141.   Kinsey GR, McHowat J, Patrick KS, Schnellmann RG. Role of Ca2+-independent phospholipase A2gamma in Ca2+-induced mitochondrial permeability transition. J Pharmacol Exp Ther. 2007 May;321:707-15.

142.   Khan AH, Pessin JE. Insulin regulation of glucose uptake: a complex interplay of intracellular signalling pathways. Diabetologia. 2002 Nov;45:1475-83.

143.   Kanzaki M, Pessin JE. Signal integration and the specificity of insulin action. Cell Biochem Biophys. 2001;35:191-209.

144.   Saltiel AR, Pessin JE, Saltiel AR, Pessin JE. Insulin signaling in microdomains of the plasma membrane. Traffic. 2003 Nov;4:711-6.

145.   Watson RT, Pessin JE, Watson RT, Pessin JE. GLUT4 translocation: the last 200 nanometers. Cellular Signalling. 2007 Nov;19:2209-17.

146.   Saltiel AR, Kahn CR. Insulin signalling and the regulation of glucose and lipid metabolism. Nature. 2001 Dec 13;414:799-806.

147.   Watson RT, Pessin JE, Watson RT, Pessin JE. Bridging the GAP between insulin signaling and GLUT4 translocation. Trends in Biochemical Sciences. 2006 Apr;31:215-22.

148.   Le Roith D, Zick Y. Recent advances in our understanding of insulin action and insulin resistance. Diabetes Care. 2001 Mar;24:588-97.

149.   Bandyopadhyay G, Standaert ML, Galloway L, Moscat J, Farese RV. Evidence for involvement of protein kinase C (PKC)-zeta and noninvolvement of diacylglycerol-

sensitive PKCs in insulin-stimulated glucose transport in L6 myotubes. Endocrinology. 1997 Nov;138:4721-31.

150.   Wang Q, Somwar R, Bilan PJ, Liu Z, Jin J, Woodgett JR, Klip A. Protein kinase B/Akt participates in GLUT4 translocation by insulin in L6 myoblasts. Mol Cell Biol. 1999 Jun;19:4008-18.

151.   Maslowska M, Legakis H, Assadi F, Cianflone K. Targeting the signaling pathway of acylation stimulating protein. J Lipid Res. 2006 Mar;47:643-52. Epub 2005 Dec 6.

152.   Zick Y. Ser/Thr phosphorylation of IRS proteins: a molecular basis for insulin resistance. Sci STKE. 2005 Jan 25;2005:pe4.

153.   Um SH, D'Alessio D, Thomas G. Nutrient overload, insulin resistance, and ribosomal protein S6 kinase 1, S6K1. Cell Metab. 2006 Jun;3:393-402.

154.   Whiteman EL, Cho H, Birnbaum MJ. Role of Akt/protein kinase B in metabolism. Trends Endocrinol Metab. 2002 Dec;13:444-51.

155.   Filippa N, Sable CL, Hemmings BA, Van Obberghen E. Effect of phosphoinositide-dependent kinase 1 on protein kinase B translocation and its subsequent activation. Mol Cell Biol. 2000 Aug;20:5712-21.

156.   Hresko RC, Murata H, Mueckler M. Phosphoinositide-dependent kinase-2 is a distinct protein kinase enriched in a novel cytoskeletal fraction associated with adipocyte plasma membranes. J Biol Chem. 2003 Jun 13;278:21615-22.

157.   Feng J, Park J, Cron P, Hess D, Hemmings BA. Identification of a PKB/Akt hydrophobic motif Ser-473 kinase as DNA-dependent protein kinase. J Biol Chem. 2004 Sep 24;279:41189-96.

158.   Dugo L, Collin M, Allen DA, Murch O, Foster SJ, Yaqoob MM, Thiemermann C. Insulin reduces the multiple organ injury and dysfunction caused by coadministration of lipopolysaccharide and peptidoglycan independently of blood glucose: role of glycogen synthase kinase-3beta inhibition. Crit Care Med. 2006 May;34:1489-96.

159.   Dugo L, Collin M, Thiemermann C. Glycogen synthase kinase 3beta as a target for the therapy of shock and inflammation. Shock. 2007 Feb;27:113-23.

160.   Sugita H, Kaneki M, Sugita M, Yasukawa T, Yasuhara S, Martyn JA. Burn injury impairs insulin-stimulated Akt/PKB activation in skeletal muscle. Am J Physiol Endocrinol Metab. 2005 Mar;288:E585-91.

161.   Franke TF, Kaplan DR, Cantley LC, Toker A. Direct regulation of the Akt proto-oncogene product by phosphatidylinositol-3,4-bisphosphate. Science. 1997 Jan 31;275:665-8.

162.   Datta SR, Brunet A, Greenberg ME. Cellular survival: a play in three Akts. Genes Dev. 1999 Nov 15;13:2905-27.

163.   Ahmed Z, Smith BJ, Pillay TS. The APS adapter protein couples the insulin receptor to the phosphorylation of c-Cbl and facilitates ligand-stimulated ubiquitination of the insulin receptor. FEBS Letters. 2000 Jun 9;475:31-4.

164.   Ribon V, Printen JA, Hoffman NG, Kay BK, Saltiel AR. A novel, multifuntional c-Cbl binding protein in insulin receptor signaling in 3T3-L1 adipocytes. Molecular & Cellular Biology. 1998 Feb;18:872-9.

165.   Moodie SA, Alleman-Sposeto J, Gustafson TA. Identification of the APS protein as a novel insulin receptor substrate. Journal of Biological Chemistry. 1999 Apr 16;274:11186-93.

166.   Thirone AC, Carvalheira JB, Hirata AE, Velloso LA, Saad MJ. Regulation of Cbl-associated protein/Cbl pathway in muscle and adipose tissues of two animal models of insulin resistance. Endocrinology. 2004 Jan;145:281-93.

167.   Chiang SH, Baumann CA, Kanzaki M, Thurmond DC, Watson RT, Neudauer CL, Macara IG, Pessin JE, Saltiel AR. Insulin-stimulated GLUT4 translocation requires the CAP-dependent activation of TC10. Nature. 2001 Apr 19;410:944-8.

168.   Baumann CA, Ribon V, Kanzaki M, Thurmond DC, Mora S, Shigematsu S, Bickel PE, Pessin JE, Saltiel AR. CAP defines a second signalling pathway required for insulin-stimulated glucose transport.[see comment]. Nature. 2000 Sep 14;407:202-7.

169.   Kanzaki M, Pessin JE. Caveolin-associated filamentous actin (Cav-actin) defines a novel F-actin structure in adipocytes. J Biol Chem. 2002 Jul 19;277:25867-9.

170.   Kanzaki M, Watson RT, Hou JC, Stamnes M, Saltiel AR, Pessin JE. Small GTP-binding protein TC10 differentially regulates two distinct populations of filamentous actin in 3T3L1 adipocytes. Mol Biol Cell. 2002 Jul;13:2334-46.

171.   Chunqiu Hou J, Pessin JE. Lipid Raft targeting of the TC10 amino terminal domain is responsible for disruption of adipocyte cortical actin. Mol Biol Cell. 2003 Sep;14:3578-91.

172.   Huang C, Thirone AC, Huang X, Klip A. Differential contribution of insulin receptor substrates 1 versus 2 to insulin signaling and glucose uptake in l6 myotubes. J Biol Chem. 2005 May 13;280:19426-35.

173.   Bandyopadhyay G, Kanoh Y, Sajan MP, Standaert ML, Farese RV. Effects of adenoviral gene transfer of wild-type, constitutively active, and kinase-defective protein kinase C-lambda on insulin-stimulated glucose transport in L6 myotubes. Endocrinology. 2000 Nov;141:4120-7.

174.   Maffucci T, Brancaccio A, Piccolo E, Stein RC, Falasca M. Insulin induces phosphatidylinositol-3-phosphate formation through TC10 activation. EMBO J. 2003 Aug 15;22:4178-89.

175.   Zheng CF, Guan KL. Properties of MEKs, the kinases that phosphorylate and activate the extracellular signal-regulated kinases. J Biol Chem. 1993 Nov 15;268:23933-9.

176.   Widegren U, Ryder JW, Zierath JR. Mitogen-activated protein kinase signal transduction in skeletal muscle: effects of exercise and muscle contraction. Acta Physiol Scand. 2001 Jul;172:227-38.

177.   Osman AA, Pendergrass M, Koval J, Maezono K, Cusi K, Pratipanawatr T, Mandarino LJ. Regulation of MAP kinase pathway activity in vivo in human skeletal muscle. Am J Physiol Endocrinol Metab. 2000 Jun;278:E992-9.

178.   Frodin M, Gammeltoft S. Role and regulation of 90 kDa ribosomal S6 kinase (RSK) in signal transduction. Mol Cell Endocrinol. 1999 May 25;151:65-77.

179.   Bryant NJ, Govers R, James DE. Regulated transport of the glucose transporter GLUT4. Nature Reviews Molecular Cell Biology. 2002 Apr;3:267-77.

180.   Cushman SW, Wardzala LJ, Simpson IA, Karnieli E, Hissin PJ, Wheeler TJ, Hinkle PC, Salans LB. Insulin-induced translocation of intracellular glucose transporters in the isolated rat adipose cell. Fed Proc. 1984 May 15;43:2251-5.

181.   Pascual JM, Wang D, Lecumberri B, Yang H, Mao X, Yang R, De Vivo DC. GLUT1 deficiency and other glucose transporter diseases. Eur. 2004 May;150:627-33.

182.   Watson RT, Kanzaki M, Pessin JE. Regulated membrane trafficking of the insulin-responsive glucose transporter 4 in adipocytes. Endocrine Reviews. 2004 Apr;25:177-204.

183.   Dugani CB, Klip A, Dugani CB, Klip A. Glucose transporter 4: cycling, compartments and controversies. EMBO Rep. 2005 Dec;6:1137-42.

184.   Giovannone B, Scaldaferri ML, Federici M, Porzio O, Lauro D, Fusco A, Sbraccia P, Borboni P, Lauro R, Sesti G. Insulin receptor substrate (IRS) transduction system: distinct and overlapping signaling potential. Diabetes Metab Res Rev. 2000 Nov-Dec;16:434-41.

185.   Katagiri H, Asano T, Ishihara H, Inukai K, Shibasaki Y, Kikuchi M, Yazaki Y, Oka Y. Overexpression of catalytic subunit p110alpha of phosphatidylinositol 3-kinase increases glucose transport activity with translocation of glucose transporters in 3T3-L1 adipocytes. J Biol Chem. 1996 Jul 19;271:16987-90.

186.   Tanti JF, Gremeaux T, Grillo S, Calleja V, Klippel A, Williams LT, Van Obberghen E, Le Marchand-Brustel Y. Overexpression of a constitutively active form of phosphatidylinositol 3-kinase is sufficient to promote Glut 4 translocation in adipocytes. J Biol Chem. 1996 Oct 11;271:25227-32.

187.   Okada T, Kawano Y, Sakakibara T, Hazeki O, Ui M. Essential role of phosphatidylinositol 3-kinase in insulin-induced glucose transport and antilipolysis in rat adipocytes. Studies with a selective inhibitor wortmannin. J Biol Chem. 1994 Feb 4;269:3568-73.

188.   Ishiki M, Randhawa VK, Poon V, Jebailey L, Klip A. Insulin regulates the membrane arrival, fusion, and C-terminal unmasking of glucose transporter-4 via distinct phosphoinositides. J Biol Chem. 2005 Aug 5;280:28792-802.

189.   Haruta T, Morris AJ, Rose DW, Nelson JG, Mueckler M, Olefsky JM. Insulin-stimulated GLUT4 translocation is mediated by a divergent intracellular signaling pathway. J Biol Chem. 1995 Nov 24;270:27991-4.

190.   Wang W, Hansen PA, Marshall BA, Holloszy JO, Mueckler M. Insulin unmasks a COOH-terminal Glut4 epitope and increases glucose transport across T-tubules in skeletal muscle. J Cell Biol. 1996 Oct;135:415-30.

191.   Thong FS, Dugani CB, Klip A, Thong FSL, Dugani CB, Klip A. Turning signals on and off: GLUT4 traffic in the insulin-signaling highway.[erratum appears in Physiology (Bethesda). 2005 Oct;20:table of contents]. Physiology (Bethesda). 2005 Aug;20:271-84.

192.   Barthel A, Kohn AD, Luo Y, Roth RA. A constitutively active version of the Ser/Thr kinase Akt induces production of the ob gene product, leptin, in 3T3-L1 adipocytes. Endocrinology. 1997 Aug;138:3559-62.

193.   Hill MM, Clark SF, Tucker DF, Birnbaum MJ, James DE, Macaulay SL. A role for protein kinase Bbeta/Akt2 in insulin-stimulated GLUT4 translocation in adipocytes. Mol Cell Biol. 1999 Nov;19:7771-81.

194.   Jiang ZY, Zhou QL, Coleman KA, Chouinard M, Boese Q, Czech MP. Insulin signaling through Akt/protein kinase B analyzed by small interfering RNA-mediated gene silencing. Proc Natl Acad Sci U S A. 2003 Jun 24;100:7569-74.

195.   Katome T, Obata T, Matsushima R, Masuyama N, Cantley LC, Gotoh Y, Kishi K, Shiota H, Ebina Y. Use of RNA interference-mediated gene silencing and adenoviral overexpression to elucidate the roles of AKT/protein kinase B isoforms in insulin actions. J Biol Chem. 2003 Jul 25;278:28312-23.

196.   Zhou QL, Park JG, Jiang ZY, Holik JJ, Mitra P, Semiz S, Guilherme A, Powelka AM, Tang X, et al. Analysis of insulin signalling by RNAi-based gene silencing. Biochem Soc Trans. 2004 Nov;32:817-21.

197.   Bandyopadhyay G, Standaert ML, Sajan MP, Kanoh Y, Miura A, Braun U, Kruse F, Leitges M, Farese RV. Protein kinase C-lambda knockout in embryonic stem cells and adipocytes impairs insulin-stimulated glucose transport. Mol Endocrinol. 2004 Feb;18:373-83.

198.   Kotani K, Ogawa W, Hashiramoto M, Onishi T, Ohno S, Kasuga M. Inhibition of insulin-induced glucose uptake by atypical protein kinase C isotype-specific interacting protein in 3T3-L1 adipocytes. J Biol Chem. 2000 Aug 25;275:26390-5.

199.   Etgen GJ, Valasek KM, Broderick CL, Miller AR. In vivo adenoviral delivery of recombinant human protein kinase C-zeta stimulates glucose transport activity in rat skeletal muscle. J Biol Chem. 1999 Aug 6;274:22139-42.

200.   Standaert ML, Bandyopadhyay G, Perez L, Price D, Galloway L, Poklepovic A, Sajan MP, Cenni V, Sirri A, et al. Insulin activates protein kinases C-zeta and C-lambda by an autophosphorylation-dependent mechanism and stimulates their translocation to GLUT4 vesicles and other membrane fractions in rat adipocytes. J Biol Chem. 1999 Sep 3;274:25308-16.

201.   Standaert ML, Bandyopadhyay G, Sajan MP, Cong L, Quon MJ, Farese RV. Okadaic acid activates atypical protein kinase C (zeta/lambda) in rat and 3T3/L1 adipocytes. An apparent requirement for activation of Glut4 translocation and glucose transport. J Biol Chem. 1999 May 14;274:14074-8.

202.   Mitra P, Zheng X, Czech MP. RNAi-based analysis of CAP, Cbl, and CrkII function in the regulation of GLUT4 by insulin. J Biol Chem. 2004 Sep 3;279:37431-5.

203.   Minami A, Iseki M, Kishi K, Wang M, Ogura M, Furukawa N, Hayashi S, Yamada M, Obata T, et al. Increased insulin sensitivity and hypoinsulinemia in APS knockout mice. Diabetes. 2003 Nov;52:2657-65.

204.   Liu YF, Herschkovitz A, Boura-Halfon S, Ronen D, Paz K, Leroith D, Zick Y. Serine phosphorylation proximal to its phosphotyrosine binding domain inhibits insulin receptor substrate 1 function and promotes insulin resistance. Mol Cell Biol. 2004 Nov;24:9668-81.

205.   Galic S, Hauser C, Kahn BB, Haj FG, Neel BG, Tonks NK, Tiganis T. Coordinated regulation of insulin signaling by the protein tyrosine phosphatases PTP1B and TCPTP. Mol Cell Biol. 2005 Jan;25:819-29.

206.   Seely BL, Staubs PA, Reichart DR, Berhanu P, Milarski KL, Saltiel AR, Kusari J, Olefsky JM. Protein tyrosine phosphatase 1B interacts with the activated insulin receptor. Diabetes. 1996 Oct;45:1379-85.

207.   Ugi S, Imamura T, Maegawa H, Egawa K, Yoshizaki T, Shi K, Obata T, Ebina Y, Kashiwagi A, Olefsky JM. Protein phosphatase 2A negatively regulates insulin's

metabolic signaling pathway by inhibiting Akt (protein kinase B) activity in 3T3-L1 adipocytes. Mol Cell Biol. 2004 Oct;24:8778-89.

208.   Nakashima N, Sharma PM, Imamura T, Bookstein R, Olefsky JM. The tumor suppressor PTEN negatively regulates insulin signaling in 3T3-L1 adipocytes. J Biol Chem. 2000 Apr 28;275:12889-95.

209.   Ono H, Katagiri H, Funaki M, Anai M, Inukai K, Fukushima Y, Sakoda H, Ogihara T, Onishi Y, et al. Regulation of phosphoinositide metabolism, Akt phosphorylation, and glucose transport by PTEN (phosphatase and tensin homolog deleted on chromosome 10) in 3T3-L1 adipocytes. Mol Endocrinol. 2001 Aug;15:1411-22.

210.   Sasaoka T, Wada T, Fukui K, Murakami S, Ishihara H, Suzuki R, Tobe K, Kadowaki T, Kobayashi M. SH2-containing inositol phosphatase 2 predominantly regulates Akt2, and not Akt1, phosphorylation at the plasma membrane in response to insulin in 3T3-L1 adipocytes. J Biol Chem. 2004 Apr 9;279:14835-43.

211.   Vollenweider P, Clodi M, Martin SS, Imamura T, Kavanaugh WM, Olefsky JM. An SH2 domain-containing 5' inositolphosphatase inhibits insulin-induced GLUT4 translocation and growth factor-induced actin filament rearrangement. Mol Cell Biol. 1999 Feb;19:1081-91.

212.   Wada T, Sasaoka T, Funaki M, Hori H, Murakami S, Ishiki M, Haruta T, Asano T, Ogawa W, et al. Overexpression of SH2-containing inositol phosphatase 2 results in negative regulation of insulin-induced metabolic actions in 3T3-L1 adipocytes via its 5'-phosphatase catalytic activity. Mol Cell Biol. 2001 Mar;21:1633-46.

213.   Gridley S, Lane WS, Garner CW, Lienhard GE. Novel insulin-elicited phosphoproteins in adipocytes. Cell Signal. 2005 Jan;17:59-66.

214.   Sano H, Kane S, Sano E, Miinea CP, Asara JM, Lane WS, Garner CW, Lienhard GE. Insulin-stimulated phosphorylation of a Rab GTPase-activating protein regulates GLUT4 translocation. J Biol Chem. 2003 Apr 25;278:14599-602.

215.   Behnia R, Munro S. Organelle identity and the signposts for membrane traffic. Nature. 2005 Dec 1;438:597-604.

216.   Zerial M, McBride H. Rab proteins as membrane organizers. Nat Rev Mol Cell Biol. 2001 Feb;2:107-17.

217.   Larance M, Ramm G, Stockli J, van Dam EM, Winata S, Wasinger V, Simpson F, Graham M, Junutula JR, et al. Characterization of the role of the Rab GTPase-activating protein AS160 in insulin-regulated GLUT4 trafficking. J Biol Chem. 2005 Nov 11;280:37803-13.

218.   Larance M, Ramm G, James DE, Larance M, Ramm G, James DE. The GLUT4 code. Molecular Endocrinology. 2008 Feb;22:226-33.

219.   Min J, Okada S, Kanzaki M, Elmendorf JS, Coker KJ, Ceresa BP, Syu LJ, Noda Y, Saltiel AR, Pessin JE. Synip: a novel insulin-regulated syntaxin 4-binding protein mediating GLUT4 translocation in adipocytes. Mol Cell. 1999 Jun;3:751-60.

220.   Omata W, Shibata H, Li L, Takata K, Kojima I. Actin filaments play a critical role in insulin-induced exocytotic recruitment but not in endocytosis of GLUT4 in isolated rat adipocytes. Biochem J. 2000 Mar 1;346 Pt 2:321-8.

221.   Furuta A, Tanaka M, Omata W, Nagasawa M, Kojima I, Shibata H. Microtubule disruption with BAPTA and dimethyl BAPTA by a calcium chelation-independent mechanism in 3T3-L1 adipocytes. Endocr J. 2009 Apr;56:235-43.

222.   Chen G, Raman P, Bhonagiri P, Strawbridge AB, Pattar GR, Elmendorf JS. Protective effect of phosphatidylinositol 4,5-bisphosphate against cortical filamentous actin loss and insulin resistance induced by sustained exposure of 3T3-L1 adipocytes to insulin. J Biol Chem. 2004 Sep 17;279:39705-9.

223.   Eyster CA, Duggins QS, Olson AL. Expression of constitutively active Akt/protein kinase B signals GLUT4 translocation in the absence of an intact actin cytoskeleton. J Biol Chem. 2005 May 6;280:17978-85.

224.   Kanzaki M, Pessin JE. Insulin-stimulated GLUT4 translocation in adipocytes is dependent upon cortical actin remodeling. J Biol Chem. 2001 Nov 9;276:42436-44.

225.   Kanzaki M, Watson RT, Khan AH, Pessin JE. Insulin stimulates actin comet tails on intracellular GLUT4-containing compartments in differentiated 3T3L1 adipocytes. J Biol Chem. 2001 Dec 28;276:49331-6.

226.   Tong P, Khayat ZA, Huang C, Patel N, Ueyama A, Klip A. Insulin-induced cortical actin remodeling promotes GLUT4 insertion at muscle cell membrane ruffles. Journal of Clinical Investigation. 2001 Aug;108:371-81.

227.   Lu PJ, Shieh WR, Rhee SG, Yin HL, Chen CS. Lipid products of phosphoinositide 3-kinase bind human profilin with high affinity. Biochemistry. 1996 Nov 5;35:14027-34.

228.   Brozinick JT, Jr., Hawkins ED, Strawbridge AB, Elmendorf JS. Disruption of cortical actin in skeletal muscle demonstrates an essential role of the cytoskeleton in glucose transporter 4 translocation in insulin-sensitive tissues. J Biol Chem. 2004 Sep 24;279:40699-706.

229.   Brozinick JT, Jr., Berkemeier BA, Elmendorf JS, Brozinick JT, Jr., Berkemeier BA, Elmendorf JS. "Actin"g on GLUT4: membrane & cytoskeletal components of insulin action. Curr Diabetes Rev. 2007 May;3:111-22.

230.   Lanner JT, Bruton JD, Katz A, Westerblad H. Ca(2+) and insulin-mediated glucose uptake. Curr Opin Pharmacol. 2008 Jun;8:339-45.

231.   Rizzuto R, Pozzan T. Microdomains of intracellular Ca2+: molecular determinants and functional consequences. Physiol Rev. 2006 Jan;86:369-408.

232.   Sudhof TC. Synaptotagmins: why so many? J Biol Chem. 2002 Mar 8;277:7629-32.

233.   Yoshihara M, Adolfsen B, Littleton JT. Is synaptotagmin the calcium sensor? Curr Opin Neurobiol. 2003 Jun;13:315-23.

234.   Whitehead JP, Molero JC, Clark S, Martin S, Meneilly G, James DE. The role of Ca2+ in insulin-stimulated glucose transport in 3T3-L1 cells. Journal of Biological Chemistry. 2001 Jul 27;276:27816-24.

235.   Shashkin P, Koshkin A, Langley D, Ren JM, Westerblad H, Katz A. Effects of CGS 9343B (a putative calmodulin antagonist) on isolated skeletal muscle. Dissociation of signaling pathways for insulin-mediated activation of glycogen synthase and hexose transport. J Biol Chem. 1995 Oct 27;270:25613-8.

236.   Brozinick JT, Jr., Reynolds TH, Dean D, Cartee G, Cushman SW. 1-[N, O-bis-(5-isoquinolinesulphonyl)-N-methyl-L-tyrosyl]-4- phenylpiperazine (KN-62), an inhibitor of calcium-dependent camodulin protein kinase II, inhibits both insulin- and hypoxia-stimulated glucose transport in skeletal muscle. Biochem J. 1999 May 1;339 (Pt 3):533-40.

237.   Bruton JD, Katz A, Westerblad H. Insulin increases near-membrane but not global Ca2+ in isolated skeletal muscle. Proc Natl Acad Sci U S A. 1999 Mar 16;96:3281-6.

238.   Bruton JD, Katz A, Westerblad H. The role of Ca2+ and calmodulin in insulin signalling in mammalian skeletal muscle. Acta Physiol Scand. 2001 Mar;171:259-65.

239.   Berridge MJ, Bootman MD, Roderick HL. Calcium signalling: dynamics, homeostasis and remodelling. Nat Rev Mol Cell Biol. 2003 Jul;4:517-29.

240.   Lanner JT, Katz A, Tavi P, Sandstrom ME, Zhang SJ, Wretman C, James S, Fauconnier J, Lannergren J, et al. The role of Ca2+ influx for insulin-mediated glucose uptake in skeletal muscle. Diabetes. 2006 Jul;55:2077-83.

241.   Li Y, Wang P, Xu J, Gorelick F, Yamazaki H, Andrews N, Desir GV. Regulation of insulin secretion and GLUT4 trafficking by the calcium sensor synaptotagmin VII. Biochem Biophys Res Commun. 2007 Oct 26;362:658-64.

242.   Bose A, Guilherme A, Robida SI, Nicoloro SM, Zhou QL, Jiang ZY, Pomerleau DP, Czech MP. Glucose transporter recycling in response to insulin is facilitated by myosin Myo1c. Nature. 2002 Dec 19-26;420:821-4.

243.   Chen XW, Leto D, Chiang SH, Wang Q, Saltiel AR. Activation of RalA is required for insulin-stimulated Glut4 trafficking to the plasma membrane via the exocyst and the motor protein Myo1c. Dev Cell. 2007 Sep;13:391-404.

244.   Bloom SR, Kuhajda FP, Laher I, Pi-Sunyer X, Ronnett GV, Tan TM, Weigle DS, Bloom SR, Kuhajda FP, et al. The obesity epidemic: pharmacological challenges. Molecular Interventions. 2008 Apr;8:82-98.

245.   Ogden CL, Carroll MD, Curtin LR, McDowell MA, Tabak CJ, Flegal KM. Prevalence of overweight and obesity in the United States, 1999-2004. JAMA. 2006 Apr 5;295:1549-55.

246.   Hossain P, Kawar B, El Nahas M. Obesity and diabetes in the developing world--a growing challenge. N Engl J Med. 2007 Jan 18;356:213-5.

247.   Wild S, Roglic G, Green A, Sicree R, King H. Global prevalence of diabetes: estimates for the year 2000 and projections for 2030. Diabetes Care. 2004 May;27:1047-53.

248.   Rocchini AP. Childhood obesity and a diabetes epidemic. N Engl J Med. 2002 Mar 14;346:854-5.

249.   Taslim S, Tai ES, Taslim S, Tai ES. The relevance of the metabolic syndrome. Annals of the Academy of Medicine, Singapore. 2009 Jan;38:29-5.

250.   Caballero AE, Caballero AE. Long-term benefits of insulin therapy and glycemic control in overweight and obese adults with type 2 diabetes. Journal of Diabetes & its Complications. 2009 Mar-Apr;23:143-52.

251.   Wellen KE, Hotamisligil GS. Inflammation, stress, and diabetes. Journal of Clinical Investigation. 2005 May;115:1111-9.

252.   LeRoith D, Novosyadlyy R, Gallagher EJ, Lann D, Vijayakumar A, Yakar S. Obesity and type 2 diabetes are associated with an increased risk of developing cancer and a worse prognosis; epidemiological and mechanistic evidence.[see comment]. Experimental & Clinical Endocrinology & Diabetes. 2008 Sep;116 Suppl 1:S4-6.

253.   Diabetes. 2009 [cited 2009 July, 01]; Available from: http://www.who.int/mediacentre/factsheets/fs312/en/index.html

254.   Hogan P, Dall T, Nikolov P. Economic costs of diabetes in the US in 2002. Diabetes Care. 2003 Mar;26:917-32.

255.   Kahn SE, Hull RL, Utzschneider KM. Mechanisms linking obesity to insulin resistance and type 2 diabetes. Nature. 2006 Dec 14;444:840-6.

256.   Boura-Halfon S, Zick Y. Phosphorylation of IRS proteins, insulin action, and insulin resistance. Am J Physiol Endocrinol Metab. 2009 Apr;296:E581-91.

257.   Draznin B. Molecular mechanisms of insulin resistance: serine phosphorylation of insulin receptor substrate-1 and increased expression of p85alpha: the two sides of a coin. Diabetes. 2006 Aug;55:2392-7.

258.   Yuan M, Konstantopoulos N, Lee J, Hansen L, Li ZW, Karin M, Shoelson SE. Reversal of obesity- and diet-induced insulin resistance with salicylates or targeted disruption of Ikkbeta. Science. 2001 Aug 31;293:1673-7.

259.   Aguirre V, Uchida T, Yenush L, Davis R, White MF. The c-Jun NH(2)-terminal kinase promotes insulin resistance during association with insulin receptor substrate-1 and phosphorylation of Ser(307). J Biol Chem. 2000 Mar 24;275:9047-54.

260.   Aguirre V, Werner ED, Giraud J, Lee YH, Shoelson SE, White MF. Phosphorylation of Ser307 in insulin receptor substrate-1 blocks interactions with the insulin receptor and inhibits insulin action. J Biol Chem. 2002 Jan 11;277:1531-7.

261.   Lee YH, Giraud J, Davis RJ, White MF. c-Jun N-terminal kinase (JNK) mediates feedback inhibition of the insulin signaling cascade. J Biol Chem. 2003 Jan 31;278:2896-902.

262.   Hirosumi J, Tuncman G, Chang L, Gorgun CZ, Uysal KT, Maeda K, Karin M, Hotamisligil GS. A central role for JNK in obesity and insulin resistance. Nature. 2002 Nov 21;420:333-6.

263.   Solinas G, Naugler W, Galimi F, Lee MS, Karin M. Saturated fatty acids inhibit induction of insulin gene transcription by JNK-mediated phosphorylation of insulin-receptor substrates. Proc Natl Acad Sci U S A. 2006 Oct 31;103:16454-9.

264.   Karin M. The beginning of the end: IkappaB kinase (IKK) and NF-kappaB activation. J Biol Chem. 1999 Sep 24;274:27339-42.

265.   Yin MJ, Yamamoto Y, Gaynor RB. The anti-inflammatory agents aspirin and salicylate inhibit the activity of I(kappa)B kinase-beta. Nature. 1998 Nov 5;396:77-80.

266.   Gao Z, Hwang D, Bataille F, Lefevre M, York D, Quon MJ, Ye J. Serine phosphorylation of insulin receptor substrate 1 by inhibitor kappa B kinase complex. J Biol Chem. 2002 Dec 13;277:48115-21.

267.   Kim JK, Kim YJ, Fillmore JJ, Chen Y, Moore I, Lee J, Yuan M, Li ZW, Karin M, et al. Prevention of fat-induced insulin resistance by salicylate. Journal of Clinical Investigation. 2001 Aug;108:437-46.

268.   Arkan MC, Hevener AL, Greten FR, Maeda S, Li ZW, Long JM, Wynshaw-Boris A, Poli G, Olefsky J, Karin M. IKK-beta links inflammation to obesity-induced insulin resistance. Nat Med. 2005 Feb;11:191-8.

269.   Nakamori Y, Emoto M, Fukuda N, Taguchi A, Okuya S, Tajiri M, Miyagishi M, Taira K, Wada Y, Tanizawa Y. Myosin motor Myo1c and its receptor NEMO/IKK-gamma promote TNF-alpha-induced serine307 phosphorylation of IRS-1. J Cell Biol. 2006 Jun 5;173:665-71.

270.   Griffin ME, Marcucci MJ, Cline GW, Bell K, Barucci N, Lee D, Goodyear LJ, Kraegen EW, White MF, Shulman GI. Free fatty acid-induced insulin resistance is associated with activation of protein kinase C theta and alterations in the insulin signaling cascade. Diabetes. 1999 Jun;48:1270-4.

271.   Yu C, Chen Y, Cline GW, Zhang D, Zong H, Wang Y, Bergeron R, Kim JK, Cushman SW, et al. Mechanism by which fatty acids inhibit insulin activation of insulin receptor substrate-1 (IRS-1)-associated phosphatidylinositol 3-kinase activity in muscle. J Biol Chem. 2002 Dec 27;277:50230-6.

272.   Kim JK, Fillmore JJ, Sunshine MJ, Albrecht B, Higashimori T, Kim DW, Liu ZX, Soos TJ, Cline GW, et al. PKC-theta knockout mice are protected from fat-induced insulin resistance. Journal of Clinical Investigation. 2004 Sep;114:823-7.

273.   Sun Z, Arendt CW, Ellmeier W, Schaeffer EM, Sunshine MJ, Gandhi L, Annes J, Petrzilka D, Kupfer A, et al. PKC-theta is required for TCR-induced NF-kappaB activation in mature but not immature T lymphocytes. Nature. 2000 Mar 23;404:402-7.

274.   Rabe K, Lehrke M, Parhofer KG, Broedl UC. Adipokines and insulin resistance. Mol Med. 2008 Nov-Dec;14:741-51.

275.   Catalan V, Gomez-Ambrosi J, Rodriguez A, Salvador J, Fruhbeck G, Catalan V, Gomez-Ambrosi J, Rodriguez A, Salvador J, Fruhbeck G. Adipokines in the treatment of diabetes mellitus and obesity. Expert Opinion on Pharmacotherapy. 2009 Feb;10:239-54.

276.   Boden G. Role of fatty acids in the pathogenesis of insulin resistance and NIDDM. Diabetes. 1997 Jan;46:3-10.

277.   Kelley DE, Mokan M, Simoneau JA, Mandarino LJ. Interaction between glucose and free fatty acid metabolism in human skeletal muscle. Journal of Clinical Investigation. 1993 Jul;92:91-8.

278.   Santomauro AT, Boden G, Silva ME, Rocha DM, Santos RF, Ursich MJ, Strassmann PG, Wajchenberg BL. Overnight lowering of free fatty acids with Acipimox improves insulin resistance and glucose tolerance in obese diabetic and nondiabetic subjects. Diabetes. 1999 Sep;48:1836-41.

279.	Jellema A, Plat J, Mensink RP. Weight reduction, but not a moderate intake of fish oil, lowers concentrations of inflammatory markers and PAI-1 antigen in obese men during the fasting and postprandial state. Eur J Clin Invest. 2004 Nov;34:766-73.

280.	Uysal KT, Wiesbrock SM, Marino MW, Hotamisligil GS. Protection from obesity-induced insulin resistance in mice lacking TNF-alpha function. Nature. 1997 Oct 9;389:610-4.

281.	Kern PA, Ranganathan S, Li C, Wood L, Ranganathan G. Adipose tissue tumor necrosis factor and interleukin-6 expression in human obesity and insulin resistance. Am J Physiol Endocrinol Metab. 2001 May;280:E745-51.

282.	Pickup JC, Mattock MB, Chusney GD, Burt D. NIDDM as a disease of the innate immune system: association of acute-phase reactants and interleukin-6 with metabolic syndrome X. Diabetologia. 1997 Nov;40:1286-92.

283.	Klover PJ, Zimmers TA, Koniaris LG, Mooney RA. Chronic exposure to interleukin-6 causes hepatic insulin resistance in mice. Diabetes. 2003 Nov;52:2784-9.

284.	Senn JJ, Klover PJ, Nowak IA, Mooney RA. Interleukin-6 induces cellular insulin resistance in hepatocytes. Diabetes. 2002 Dec;51:3391-9.

285.	Rotter V, Nagaev I, Smith U. Interleukin-6 (IL-6) induces insulin resistance in 3T3-L1 adipocytes and is, like IL-8 and tumor necrosis factor-alpha, overexpressed in human fat cells from insulin-resistant subjects. J Biol Chem. 2003 Nov 14;278:45777-84.

286.	Al-Khalili L, Bouzakri K, Glund S, Lonnqvist F, Koistinen HA, Krook A. Signaling specificity of interleukin-6 action on glucose and lipid metabolism in skeletal muscle. Mol Endocrinol. 2006 Dec;20:3364-75.

287.	Hotta K, Funahashi T, Bodkin NL, Ortmeyer HK, Arita Y, Hansen BC, Matsuzawa Y. Circulating concentrations of the adipocyte protein adiponectin are decreased in parallel with reduced insulin sensitivity during the progression to type 2 diabetes in rhesus monkeys. Diabetes. 2001 May;50:1126-33.

288.	Hu E, Liang P, Spiegelman BM. AdipoQ is a novel adipose-specific gene dysregulated in obesity. J Biol Chem. 1996 May 3;271:10697-703.

289.	Maeda N, Shimomura I, Kishida K, Nishizawa H, Matsuda M, Nagaretani H, Furuyama N, Kondo H, Takahashi M, et al. Diet-induced insulin resistance in mice lacking adiponectin/ACRP30. Nat Med. 2002 Jul;8:731-7.

290.	Berg AH, Combs TP, Du X, Brownlee M, Scherer PE. The adipocyte-secreted protein Acrp30 enhances hepatic insulin action. Nat Med. 2001 Aug;7:947-53.

291.   Yamauchi T, Kamon J, Waki H, Terauchi Y, Kubota N, Hara K, Mori Y, Ide T, Murakami K, et al. The fat-derived hormone adiponectin reverses insulin resistance associated with both lipoatrophy and obesity. Nat Med. 2001 Aug;7:941-6.

292.   Yamauchi T, Kamon J, Ito Y, Tsuchida A, Yokomizo T, Kita S, Sugiyama T, Miyagishi M, Hara K, et al. Cloning of adiponectin receptors that mediate antidiabetic metabolic effects. Nature. 2003 Jun 12;423:762-9.

293.   Tsuchida A, Yamauchi T, Ito Y, Hada Y, Maki T, Takekawa S, Kamon J, Kobayashi M, Suzuki R, et al. Insulin/Foxo1 pathway regulates expression levels of adiponectin receptors and adiponectin sensitivity. J Biol Chem. 2004 Jul 16;279:30817-22.

294.   Yamauchi T, Nio Y, Maki T, Kobayashi M, Takazawa T, Iwabu M, Okada-Iwabu M, Kawamoto S, Kubota N, et al. Targeted disruption of AdipoR1 and AdipoR2 causes abrogation of adiponectin binding and metabolic actions. Nat Med. 2007 Mar;13:332-9.

295.   Bjursell M, Ahnmark A, Bohlooly YM, William-Olsson L, Rhedin M, Peng XR, Ploj K, Gerdin AK, Arnerup G, et al. Opposing effects of adiponectin receptors 1 and 2 on energy metabolism. Diabetes. 2007 Mar;56:583-93.

296.   Liu Y, Michael MD, Kash S, Bensch WR, Monia BP, Murray SF, Otto KA, Syed SK, Bhanot S, et al. Deficiency of adiponectin receptor 2 reduces diet-induced insulin resistance but promotes type 2 diabetes. Endocrinology. 2007 Feb;148:683-92.

297.   Bluher M, Williams CJ, Kloting N, Hsi A, Ruschke K, Oberbach A, Fasshauer M, Berndt J, Schon MR, et al. Gene expression of adiponectin receptors in human visceral and subcutaneous adipose tissue is related to insulin resistance and metabolic parameters and is altered in response to physical training. Diabetes Care. 2007 Dec;30:3110-5.

298.   Yedgar S, Cohen Y, Shoseyov D. Control of phospholipase A2 activities for the treatment of inflammatory conditions. Biochim Biophys Acta. 2006 Nov;1761:1373-82.

299.   Derrickson BH, Mandel LJ. Parathyroid hormone inhibits Na(+)-K(+)-ATPase through Gq/G11 and the calcium-independent phospholipase A2. Am J Physiol. 1997 Jun;272:F781-8.

300.   Tithof PK, Olivero J, Ruehle K, Ganey PE. Activation of neutrophil calcium-dependent and -independent phospholipases A2 by organochlorine compounds. Toxicol Sci. 2000 Jan;53:40-7.

301.   Tithof PK, Peters-Golden M, Ganey PE. Distinct phospholipases A2 regulate the release of arachidonic acid for eicosanoid production and superoxide anion generation in neutrophils. J Immunol. 1998 Jan 15;160:953-60.

302.   Isenovic E, LaPointe MC. Role of Ca(2+)-independent phospholipase A(2) in the regulation of inducible nitric oxide synthase in cardiac myocytes. Hypertension. 2000 Jan;35:249-54.

303.   Turk J, Ramanadham S. The expression and function of a group VIA calcium-independent phospholipase A2 (iPLA2beta) in beta-cells. Can J Physiol Pharmacol. 2004 Oct;82:824-32.

304.   Bereziat G, Wolf C, Colard O, Polonovski J. Phospholipases of plasmic membranes of adipose tissue. Possible intermediaries for insulin action. Adv Exp Med Biol. 1978;101:191-9.

305.   Lakshmanan J, Elmendorf JS, Ozcan S. Analysis of insulin-stimulated glucose uptake in differentiated 3T3-L1 adipocytes. Methods Mol Med. 2003;83:97-103.

306.   Elmendorf JS. Fractionation analysis of the subcellular distribution of GLUT-4 in 3T3-L1 adipocytes. Methods Mol Med. 2003;83:105-11.

307.   Macdonald JL, Pike LJ. A simplified method for the preparation of detergent-free lipid rafts. J Lipid Res. 2005 May;46:1061-7.

308.   Malipa AC, Meintjes RA, Haag M. Arachidonic acid and glucose uptake by freshly isolated human adipocytes. Cell Biochem Funct. 2008 Mar-Apr;26:221-7.

309.   Nugent C, Prins JB, Whitehead JP, Wentworth JM, Chatterjee VK, O'Rahilly S. Arachidonic acid stimulates glucose uptake in 3T3-L1 adipocytes by increasing GLUT1 and GLUT4 levels at the plasma membrane. Evidence for involvement of lipoxygenase metabolites and peroxisome proliferator-activated receptor gamma. Journal of Biological Chemistry. 2001 Mar 23;276:9149-57.

310.   Malipa AC, Meintjes RA, Haag M, Malipa ACA, Meintjes RA, Haag M. Arachidonic acid and glucose uptake by freshly isolated human adipocytes. Cell Biochemistry & Function. 2008 Mar-Apr;26:221-7.

311.   Rodbell M. Metabolism of isolated fat cells. II. The similar effects of phospholipase C (Clostridium perfringens alpha toxin) and of insulin on glucose and amino acid metabolism. J Biol Chem. 1966 Jan 10;241:130-9.

312.   Blecher M. Effects of insulin and phospholipase A on glucose transport across the plasma membrane of free adipose cells. Biochim Biophys Acta. 1967 Jun 6;137:557-71.

313.   Loo RW, Conde-Frieboes K, Reynolds LJ, Dennis EA. Activation, inhibition, and regiospecificity of the lysophospholipase activity of the 85-kDa group IV cytosolic phospholipase A2. J Biol Chem. 1997 Aug 1;272:19214-9.

314.   Leslie CC. Properties and regulation of cytosolic phospholipase A2. J Biol Chem. 1997 Jul 4;272:16709-12.

315.   Yea K, Kim J, Lim S, Kwon T, Park HS, Park KS, Suh PG, Ryu SH. Lysophosphatidylserine regulates blood glucose by enhancing glucose transport in myotubes and adipocytes. Biochem Biophys Res Commun. 2009 Jan 23;378:783-8.

316.   Yea K, Kim J, Lim S, Park HS, Park KS, Suh PG, Ryu SH. Lysophosphatidic acid regulates blood glucose by stimulating myotube and adipocyte glucose uptake. J Mol Med. 2008 Feb;86:211-20.

317.   Inoue M, Chiang SH, Chang L, Chen XW, Saltiel AR. Compartmentalization of the exocyst complex in lipid rafts controls Glut4 vesicle tethering. Mol Biol Cell. 2006 May;17:2303-11.

318.   Kuwata H, Fujimoto C, Yoda E, Shimbara S, Nakatani Y, Hara S, Murakami M, Kudo I. A novel role of group VIB calcium-independent phospholipase A2 (iPLA2gamma) in the inducible expression of group IIA secretory PLA2 in rat fibroblastic cells. J Biol Chem. 2007 Jul 13;282:20124-32.

319.   Okada S, Mori M, Pessin JE. Introduction of DNA into 3T3-L1 adipocytes by electroporation. Methods Mol Med. 2003;83:93-6.

320.   Rangwala SM, Rhoades B, Shapiro JS, Rich AS, Kim JK, Shulman GI, Kaestner KH, Lazar MA. Genetic modulation of PPARgamma phosphorylation regulates insulin sensitivity. Dev Cell. 2003 Oct;5:657-63.

321.   Lanner JT, Bruton JD, Katz A, Westerblad H, Lanner JT, Bruton JD, Katz A, Westerblad H. Ca(2+) and insulin-mediated glucose uptake. Curr Opin Pharmacol. 2008 Jun;8:339-45.

322.   Worrall DS, Olefsky JM. The effects of intracellular calcium depletion on insulin signaling in 3T3-L1 adipocytes. Mol Endocrinol. 2002 Feb;16:378-89.

APPENDIX I

ABBREVIATIONS

2-APB, 2-Aminoethoxydiphenyl Borate

2-DOG, 2-Deoxyglucose

AA, Arachidonic Acid

AACOCF3, Arachidonyl Trifluoromethyl ketone (1,1,1-trifluoro-6Z, 9Z, 12Z, 15Z-heneicosatetraen-2-one)

AdipoR1, Adiponectin Receptor 1

AdipoR2, Adiponectin Receptor 2

AdPLA, Adipose PLA2

aPKC, Atypical Protein Kinase C

APS, Adapter Protein with Pleckstrin Homology and Src Homology Domains

ARDS, Adult Respiratory Distress Syndrome

ATP, Adenosine Triphosphate

BEL, Bromoenol Lactone ((E)-6-(bromomethylene)-3-(1-naphthalenyl)-2H-tetrahydropyran-2-one)

BMI, Body Mass Index

BSA, Bovine Serum Albumin

C/EBP, CCAAT/Enhancer-Binding Protein

C3G, Crk SH3-binding guanine nucleotide-releasing factor

cAMP, Cyclic Adenosine Monophosphate

CAP, Cbl-Associated Protein

CHO, Chinese Hamster Ovary

CIF, Calcium Influx Factor

COX, Cyclooxygenase

cPLA2, Cytosolic Ca2+-Dependent PLA2

CRAC, Calcium Release-Activated Channels

CREBP, cAMP-Response Element-Binding Protein

CrkII, Chicken Tumor Virus No.10 (CT10) Regulator of Kinase II

CT, Comparative Threshold

CYT, Cytosol

DMEM, Dulbecco's Modified Eagle's Medium

DMSO, Dimethyl sulfoxide

DNA, Deoxyribonucleic Acid

ER, Endoplasmic Reticulum

FBS, Fetal Bovine Serum

FCS, Fetal Calf Serum

FFA, Free Fatty Acids

Gab-1, Grb2-Associated Binder-1

GAP, GTPase Activating Protein

GLUT4, Glucose Transporter 4

Grb2, Growth Factor Receptor Bound 2

GS2, Gene Sequence 2

GSK-3β, Glycogen Synthase Kinase-3β

HDM, High Density Microsome

HEPES, 4-(2-Hydroxyethyl)-1-Piperazineethanesulfonic Acid

HES, HEPES-EDTA-Sucrose

HMIT, H+-Myo-Inositol Transporter

IBMX, 3-isobutyl-1-methylxanthine

IKKβ, IκB Kinase β

IL-1, Interleukin-1

IL-6, Interleukin-6

iNOS, Inductible Nitric Oxide Synthase

iPLA2, Cytosolic Ca2+-Independent PLA2

IR, Insulin Receptor

IRK, IR Tyrosine Kinase

IRS, Insulin Receptor Substrate

IκBα, Inhibitor of NFκB

JNK, c-Jun N-Terminal Kinase

KRPH, Kreb's Ringer Phosphate HEPES

LA, Linoleic Acid

LCPUFA, Long Chain Polyunsaturated Fatty Acid

LDL, Low-Density Lipoprotein

LDM, Low Density Microsome

LPA, Lysophosphatidic Acid

LPC, Lysophosphatidylcholine

LPLA2, Lysosomal PhosphoslipaseA2

LR, Lipid Raft

LT, Leukotriene

Lyso PL, Lysophospholipid

MAFP, Methyl Arachidonyl Fluorophosphonate (5Z, 8Z, 11Z, 14Z-eicosatetraenyl-phosphonofluoride, methyl ester)

MAPK, Mitrogen-Activated Protein Kinase

MN, Mitochondrial Nuclei

mTOR, Mammalian Target of Rapamycin

NEFA, Non-Esterified Fatty Acid

NEMO, Nuclear Factor κB Essential Modulator

NFκB, Nuclear Factor-κB

NR, Non-Raft

NTE, Neuropathy Target Esterase

N-WASP, Neuronal Wiskott-Aldrich Syndrome Protein

PAF, Platelet-Activating Factor

PAF-AH, Platelet-Activating Factor Acetylhydrolase

PAP-1, Mg2+-dependent phosphatidic acid phosphohydrolase (Lipin)

PBS, Phosphate-Buffered Saline

PC, Phosphatidylcholine

PDK, Phosphoinositide-Dependent Kinase

PG, Prostaglandin

PGE2, Prostaglandin E2

PI3K, Phosphatidylinositol 3-Kinase

PIP2, Phosphotidyl- 4, 5-Biphosphophate

PIP3, Phosphotidyl-3, 4, 5-Triphosphophate

PKB, Protein Kinase B(Akt)

PKC, Protein Kinase C

PL, Phospholipid

PLA2, Phospholipase A2

PM, Plasma Membrane

PP2A, Serine/Threonine Protein Phosphatase 2A

PPARα, Peroxisome Proliferator-Activated Receptor α

PPARγ , Peroxisome Proliferator-Activated Receptor γ

PTB, Phosphotyrosine Binding

PTEN, Phosphatase and Tensin Homolog Deleted on Chromosome 10

PTP1B, Protein Tyrosine Phosphatase 1B

PUFA, Polyunsaturated Fatty Acid

(R)-BEL, (R)-(E)-6-(bromomethylene)-3-(1-naphthalenyl)-2H-tetrahydropyran-2-one

RBP4, Retinol Binding Protein 4

RNA, Ribonucleic Acid

ROS, Reactive Oxygen Species

RSK2, p90 Ribosomal S6 Kinase

RT-PCR, Quantitative Teal-Time Reverse Transcriptase Polymerase Chain Reaction

S6K1, S6 Kinase 1

(S)-BEL, (S)-(E)-6-(bromomethylene)-3-(1-naphthalenyl)-2H-tetrahydropyran-2-one

SDS-PAGE, Sodium Dodecyl Sulfate-Polyacrylamide Gel

SH2, Src Homology 2

Shc, Src Homologous and Collagen

SHIP2, SH2-Containing Inositol Phosphatase 2

siRNA, Small Interfering RNA

SIRP, Signal-Regulated Protein

SNARE, Soluble N-ethylmaleimide-Sensitive Fusion protein (NSF) Attachment Protein Receptor

SOC, Store-Operated Ca2+ Channel

Sos, Son-of-Sevenless

sPLA2, Secreted PLA2

SREBP, Sterol Regulatory Element Binding Protein

STZ, Streptozotocin

TBS, Tris Buffered Saline

TNF-α, Tumor Necrosis Factor-α

TRP, Transient Receptor Potential

TRPM8, Transient Receptor Potential (Melastatin)-8

TTS-2.2, Transport Secretion Protein-2.2

VAMP, Vesicle-Associated Membrane Proteins

X-Gal, 5-Bromo-4-Chloro-3-Indoyl-β-D-Galactopyranoside

APPENDIX II

Protocol of Glucose Uptake Assay

The protocol is modified from the method described by Lakshmanan (305).

Reagents:

Serum Free DMEM

DMEM containing 5% D-glucose, 1% L-glutamine, 1% penicillin streptomycin and 0.1% BSA

KRPH Buffer

Final concentration	Stock solution	Volume (250 mL buffer)
136 mM NaCl	5.0 M NaCl	6.8 mL
20 mM HEPES	1.0 M HEPES	5.0 mL
5 mM sodium phosphate buffer (pH 7.4)	0.1 M sodium phosphate buffer (pH 7.4)	12.5 mL
4.7 mM KCl	1 M KCl	1.18 mL
1 mM $MgSO_4$	1 M $MgSO_4$	0.25 mL
1mM $CaCl_2$	1 M $CaCl_2$	0.25 mL

Add ddH_2O up to about 240 mL, adjust the pH to 7.4, and make up the volume to 250 mL with ddH_2O. Prepare fresh.

Cytochalasin B Stock and Working Solution

Stock: 10 mM (4.796 mg in 1 mL 95% EtOH); stored at -20°C.
Working: 20 µM in KRPH buffer (add 8 µL stock to 4 mL KRPH buffer). Prepare prior to use.

Insulin Stock and Working Solution

Stock: 335 µM (2 mg/mL insulin in 3 mM HCl); filter sterilized, and stored at 4 °C.
Working: 10 µM (dilute 100 µL stock with 3250 µL ddH_2O). Prepare prior to use.

KRPH-[^{3}H]-2-Deoxyglucose Label

Mix 25 µL of 100 mM 2-DOG stock, 45.5 µL of [^{3}H]-2-DOG and 2.442 mL KRPH. Prepare prior to use.

Procedure:

- For all incubation, the media volume added is depending on the cell culture dishes used for glucose assay: 1mL for 60 mm dish and 6-well plate, 500 μL for 12-well plate, and 300 μL for 24-well plate.
- The final concentrations of the inhibitor, DMSO, insulin, cytochalasin B, and radiolabeled 2-DOG are the same. The adding volume is adjusted according to the media volume in one dish (60 mm dish) or well (multiple-well plate).
- For the addition of each treatment (inhibitor, DMSO, insulin, cytochalasin B, orradiolabeled 2-DOG), the dishes or wells are treated in the same order and staggered at 1-minute intervals.
- To check the effect of treatment on insulin-stimulated glucose uptake. The cells are grouped into treatment group(s), control group, and non-specific uptake group. For each group, it is divided into two sub-groups treated with or without insulin to determine the basal and insulin-stimulated glucose uptake.
- 3T3-L1 adipocytes at 8-10 days post differentiation or L6-GLUT4^{myc} cells upon confluent are used for assays.
- For each group of cells, the glucose uptake values were denoted as "pmol radioactive 2-deoxyglucose taken up per minute and per mg protein", and the amount of [^{3}H]-2-deoxyglucose taken up was calculated according to the formula:

$$\frac{(\text{Observed cpm} - \text{cytochalasin B cpm}) \times 2/\text{total cpm} \times 25}{10 \times \text{mg protein per mL}}$$

Step1. Wash cells twice with PBS and incubate them in serum-free DMEM at 37 °C (2 hours for adipocytes, and 5 hours for L6-GLUT4^{myc} cells).

*Step2. If inhibitor treatment needed, change media to serum-free DMEM containing inhibitor with specific final concentration for dishes or wells in treatment group(s) and incubate at 37 °C for 30 minutes. Incubate cells in control and non-specific uptake groups in serum-free DMEM containing DMSO (The volume of DMSO is equal to the largest volume of inhibitor. For example, in experiment with both 10 μM and 50 μM BEL treatments, the control media contains DMSO with equal amount to BEL solution added to DMEM containing 50 μM BEL).

*Step3. Wash the inhibitor pretreated cells twice in KRPH buffer, and incubate them in KRPH buffer containing inhibitor with the treatment concentration for 15 minutes; wash and incubate cells in control and non-specific uptake groups with KRPH buffer containing DMSO.

* Step 2 and 3 can be skipped if no inhibitor treatment required. Wash and incubate serum-starved cells in KRPH buffer for 15 minutes.

Step4. At the last 5 minutes of KRPH incubation, change the buffer with premixed KRPH- cytochalasin B for non-specific uptake wells.

Step5. Add 100 µM insulin at a 1:100 dilution rate (final concentration as 100 nM) to all insulin stimulation dishes or wells and incubate for 30 minutes. For adipocytes, incubate at room temperature; for L6 myotubes, incubate at 37 °C.

Step6. Add KRPH-[^{3}H]-2-Deoxyglucose Label at a 1:20 dilution rate to all dishes or wells and incubate for 10 minutes at room temperature.

Step7. Wash the cells three times with ice-cold PBS buffer. Air-dry cells for 15 minutes at room temperature.

Step8. Solublize cells in 0.2N NaOH solution, mix cells by pipeting.

Step9. Use half of lysate for radiolabel counting. Mixed the lysate with 4 mL of scintillation cocktail to determine the total counts per minutes (cpm). Use equal volume of 0.2N NaOH solution mixed with 4 mL of scintillation cocktail as blank, and 1/25 volume of radiolabel added mixed with 4 mL of scintillation cocktail for the total cpm determination.

Step10. Use the rest of the lysate for protein assay.

APPENDIX III

Protocol of Lipid Rafts Separation

The protocol is following the method described by Pike and Macdonald (307).
All steps were carried out on ice. Centrifuge rotor and tubes, and gradient maker were pre-cold in 4ºC.

Reagents:

Base buffer

20 mM Tris-HCl, pH 7.8, 250 mM sucrose

50% Opti-Prep in base buffer containing 1 mM $CaCl_2$, 1 mM $MgCl_2$

20% OptiPrep in base buffer

5% OptiPrep in base buffer

Procedure:

Step1. Wash and scrape four 100-mm dishes of cells into base buffer containing 1 mM $CaCl_2$ and 1 mM $MgCl_2$;

Step2. Pellet cells by centrifugation for 2 min at 250g and resuspended in 1 mL of base buffer containing 1 mM $CaCl_2$, 1 mM $MgCl_2$, and protease inhibitor cocktail;

Step3. Lyse cells by passage through a 22 g×3" needle 20 times;

Step4. Centrifuge cell lysates were centrifuged at 1,000g for 10 minutes, and collect the resulting postnuclear supernatant. Transfer the supernatant to a separate tube.

Step5. Resuspend the pellet in 1 mL of base buffer containing 1 mM CaCl2, 1 mM MgCl2, and protease inhibitor cocktail, and lyse it again by sheering 20 times through a needle and syringe.

Step6. Centrifuge at 1,000g for 10 minutes, combined the second postnuclear supernatant with the first.

Step7. Add an equal volume (2 mL) 50% Opti-Prep in base buffer containing 1 mM $CaCl_2$, 1 mM $MgCl_2$ to the combined postnuclear supernatants (2 mL) and place the mixture at the bottom of a 12 ml centrifuge tube.

Step8. Layer an 8 mL continuous gradient of 5% to 20% OptiPrep in base buffer on the top of the lysate mixture (containing 25% of OptiPrep.)

*Step9. Centrifuge the gradients for 90 minutes at 52,000g, 4°C, using an SW-41 rotor in a Beckman ultracentrifuge.

*After centrifugation, cloudine**ss** could be seen throughout the gradient. A distinct white band was apparent at the top of gradients.

Step10. Fractionate gradients into 12 fractions (1mL/fraction).

Step11. Assess the distribution of various proteins by Western blotting, the total protein in each fraction by Bio-Rad BCA protein assay kit, and the total cholesterol in each fraction using the Wako CII Total Cholesterol assay kit.

Protocol of siRNA Transfection Using Electroporation

The protocol is modified from the method described by Okada (319).

Reagents:

Complete medium

DMEM containing 5% D-glucose, 10% FBS, 1% L-glutamine without antibiotics)

D-PBS Buffer

PBS buffer without Mg $^{2+}$ and Ca $^{2+}$)

SiRNA Stock and Working Solution

Stock: Disolve 5 nmol siRNA in 100 µL RNase-free H_2O (50µM)
Working: Dilute 5 µL siRNA stock with 20 µL RNase-free H_2O (10µM)

Procedure:

Step1. Add 2 mL/dish trysin-EDTA to four 100 mm dishes of 3T3-L1 adipocytes (at day 5 or 6 postdifferentiation) and swirl gently. Aspirate the trysin-EDTA solution and incubate the cells at 37°C for 10 minutes.

Step2. Resuspend all the trypsinized cells in 12 mL complete medium, and pipet up and down gently for 10 times in order to disperse the cell clumps. Transfer the cell solution to a 50 mL centrifuge tube.

Step3. Centrifuge the cell suspension for 5 minutes at 200 g and room temperature. Carefully remove the supernatant. Resuspend the pellet in 40 mL sterile D-PBS, disperse the cells by pipeting, and pellet the cells at 200 g and room temperature for 5 minutes. Repeat the wash in 40 mL sterile D-PBS for twice.

Step4. Suspend the cell pellet in 1.5-2 mL sterile D-PBS to achieve a final cell concentration approximately at 2×10^7 cells per mL.

Step5. Transfer 2.5 µL siRNA (10µM) into the bottom of an electroporation cuvet. Add 0.5 mL cell solution to the electroporation cuvet, and mix the cells and siRNA by gentle tapping.

Step6. Put the cuvet in the Bio-Rad Gene Pulse Xcell and electroporate the cells at the setting as 0.18 kV, and 950 µF capacitance.

Step7. Immediately after electroporation, add 1 mL fresh complete medium, and transfer the cell solution to a 15 mL centrifuge tube containing 1.5 mL fresh complete medium. Incubate for 10 minutes at room temperature.

Step8. Reseed the cells to 24- well plates (0.5 mL per well), and incubate the cells at 37 °C and 5% CO_2. Change the medium to normal growth medium 12 hours after electroporation.

Step9. Apply post-transfection assays after 48 hours post electroporation.